Proceeding
Of
3rd International Conference on Computer Science and Information Technology (ICCIT 2015),

3rd International Conference on Progress in Production, Mechanical and Automobile Engineering (ICPMAE-2015),

3rd International Conference on Innovations in Electrical and Electronics Engineering (ICIEEE 2015),

3rd International Conference on Biotechnology, Civil and Chemical Engineering (ICBCCE 2015)

Date: 8th February 2015
Gujarat

Editor-in-Chief

Prof. Tejinder Singh Saggu
Dept. of Electrical Engineering
PEC University of University,
Chandigarh

Organized by:

TECHNICAL RESEARCH ORGANISATION INDIA
Website: www.troindia.in

About Conference

Technical Research Organisation India (TROI) is pleased to organize the 3rd International Conference on Computer Science and Information Technology (ICCIT 2015), 3rd International Conference on Progress in Production, Mechanical and Automobile Engineering (ICPMAE-2015),3rd International Conference on Innovations in Electrical and Electronics Engineering (ICIEEE 2015) & 3rd International Conference on Biotechnology, Civil and Chemical Engineering (ICBCCE 2015).

ICCIT & ICPMAE is a comprehensive conference covering the various topics of Engineering & Technology such as Computer Science, Mechanical and IT. The aim of the conference is to gather scholars from all over the world to present advances in the aforementioned fields and to foster an environment conducive to exchanging ideas and information. This conference will also provide a golden opportunity to develop new collaborations and meet experts on the fundamentals, applications, and products of Computer science, IT and Mechanical. We believe inclusive and wide-ranging conferences such as ICIEEE can have significant impacts by bringing together experts from the different and often separated fields of Electrical & Electronics. It creating unique opportunities for collaborations and shaping new ideas for experts and researchers. This conference provide an opportunity for delegates to exchange new ideas and application experiences, we also publish their research achievements. ICIEEE & ICBCCE shall provide a plat form to present the strong methodological approach and application focus on Electrical, Electronics, civil & chemical engineering that will concentrate on various techniques and applications. The ICBCCE conference cover all new theoretical and experimental findings in the fields of Civil, Chemical and Biotechnology engineering or any closely related fields.

Topics of interest for submission include, but are not limited to:
 Computer Science & Engineering
 Information Technology
 Electrical Engineering
 Electronics Engineering
 Instrumentation Engineering
 Industrial Engineering
 Mechanical Engineering
 Chemical Engineering
 Aeronautical Engineering
 Environmental Engineering
 Nano-Technology,
Genetic Engineering
Materials and Metallurgical Engineering
Soft computing
Aeronautical Engineering
Agricultural engineering
Civil engineering
Engineering Science
Network Engineering
Software Engineering
Structural Engineering
Telecommunication Engineering
And many more….

Organizing Committee

Editor-in-Chief:
Prof. Tejinder Singh Saggu
Dept. of Electrical Engineering
PEC University of University,
Chandigarh

Programme Committee Members:

Dr. Dariusz Jacek Jakóbczak
Assistant Professor , Computer Science & Management .
Technical University of Koszalin, Poland

Prof. (Dr.) Arjun P. Ghatule
Director, Sinhgad Institute of Computer Sciences (MCA),Solapur(MS)

Dr. S.P.ANANDARAJ.,
M.Tech(Hon's),Ph.D.,
Sr.Assistant Professor In Cse Dept,
Srec, Warangal

Prof O. V. Krishnaiah Chetty
Dean, Mechanical Engineering
Sri Venkateswara College of Engineering and Technology
Chittoor- Tirupati

Dr. D.J. Ravi
Professor & HOD, Department of ECE
Vidyavardhaka College of Engineering, Mysore

Prof. Roshan Lal
PEC University of Technology/Civil Engineering Department,
Chandigarh, India
rlal_pec@yahoo.co.in

 Dr. Bhasker Gupta
Assistant Professor. Jaypee University of Information Technology, Himachal Pradesh

Dr. A. Lakshmi Devi,
Professor, department of electrical engineering,
SVU college of Engineering, Sri Venkateswara university, Tirupati

Prof. Shravani Badiganchala

Assistant professor, Shiridi sai institute of science and engineering

Prof. Surjan Balwinder Singh
Associate Professor in the Electrical Engineering Department,
PEC University of Technology, Chandigarh.

Dr. Shilpa Jindal ,
PEC University of Technology (Deemed University), Chandigarh
ji_shilpa@yahoo.co.in

Prof. S. V. Viraktamath
Dept. of E&CE S.D.M. College of Engg. & Technology Dhavalagiri, Dharwad

Subzar Ahmad Bhat
Assistant Professor, Gla University
Dr. G.Suresh Babu
 Professor,Dept. of EEE,CBIT, Hyderabad

Prof .Ramesh
Associate Professor in Mechanical Engineering,
St.Joseph's Institute of Technology

 Prof.Amit R. Wasnik
Sinhgad Institute of Technology, Pune, Maharashtra

IIT KHARAGPUR
Prof. Rajakumar R. V.
DEAN Acadedemic, rkumar @ ece.iitkgp.ernet.in
Prof. Datta D., ddatta @ ece.iitkgp.ernet.in
Prof. Pathak S S,r,ssp @ ece.iitkgp.ernet.in

Dr. Rajeev Agrawal
Assistant Professor,
Department of Production Engineering
Birla Institute of Technology
Ranchi, Jharkhand

Dr. Hansa Jeswani
Asso. Professor.,
Sardar Patel College of Engineering, Mumbai
Prof. Sunil agrawal

TABLE OF CONTENTS

SL NO	TOPIC	PAGE NO

Editor-in-Chief
Prof. Tejinder Singh Saggu

Editorial

The conference is designed to stimulate the young minds including Research Scholars, Academicians, and Practitioners to contribute their ideas, thoughts and nobility in these two integrated disciplines. Even a fraction of active participation deeply influences the magnanimity of this international event. I must acknowledge your response to this conference. I ought to convey that this conference is only a little step towards knowledge, network and relationship.

The conference is first of its kind and gets granted with lot of blessings. I wish all success to the paper presenters.

I congratulate the participants for getting selected at this conference. I extend heart full thanks to members of faculty from different institutions, research scholars, delegates, TROI Family members, members of the technical and organizing committee. Above all I note the salutation towards the almighty.

Editor-in-Chief:
Prof. Tejinder Singh Saggu
Dept. of Electrical Engineering
PEC University of University,
Chandigarh

VEHICULAR SPEED PATTERN ANALYSIS ON ACCESS CONTROLLED URBAN ROADWAY IN SURAT CITY

[1]Chauhan Boski P., [2]Dr. G.J Joshi, [3]Dr. Purnima Parida
[1]Ph.D. Scholar, CED, SVNIT, Surat, [2]Associate Professor, CED, SVNIT, Surat,
[3]Head, principal Scientist, Transportation planning Division, CRRI , Delhi
Email:[1]boski.chauhan@ckpcet.ac.in,[2]gjsvnit92@gmail.com,[3]punam31@gmail.com

Abstract— Driving cycle is depicted by a series of data points representing the speed of a vehicle versus time. The quality of a driving cycle is directly associated with the accuracy of any air quality analysis. The data collection of driving cycle comprises of selection of instrumentation, data collection technique, test route selection and days of collection technique. Performance Box is one of the instruments use for data collection. Data has been collected on Sardar Bridge at Adajan, Surat. Data analysis is done by statistical approach. One way ANOVA is used to compare effect of different mode of vehicles on driving cycle parameters.

Index Terms— ANOVA, Driving Cycle

I. INTRODUCTION

Driving cycles are used to assess the performance of vehicles in various ways and, as the most common example, to assess polluting emissions and fuel consumption in vehicle. Most of the macroscopic emission factors modeling systems have used the concept of driving cycles for the collection of their essential data. On the other hand, the microscopic emission models use driving cycles to transform instantaneous emissions into average emission factors.The driving cycle is a representative plot of driving behavior of a given city or a region and is characterized by speed and acceleration. Driving cycle data has been collected on working day (Monday), Saturday and Sunday. Data is collected by different modes of vehicles like bike, auto rickshaw and car. The effect of modes of vehicle on speed profile is analyzed with statistical approach.

Data analysis was done by SPSS software to find out driving cycle parameter (acceleration, deceleration, cruise speed and average speed)When compare means of more than two groups of variables, one way ANOVA can be used. ANOVA is used to find significant relation between various variables. One way ANOVA is used to find out effect of bike, car and auto rickshaw on vehicle speed.

II. CASE STUDY

Surat is Gujarat's second largest city with a population of 2.1 million at the 2001 census and 4.6 million at the 2011 census. Surat Municipal Corporation arises to improve road infrastructure of the city. Since last two decades most of the new development, including the most desirable

location for the city's middle and upper class, is the Adajan area. Sardar bridge of study area is the link between Adajan area and athwalines area. Fig. 1 shows morning pick hour traffic congestion at conflict point. Maximum vehicle speed fluctuation is observed at merging point during morning peak hour.

Fig. 1 Conflict point at Sardar Bridge, Surat

Performance Box is one of the instruments used for data collection at selected area. Performance Box is very easy to measure acceleration times, braking distances, quarter mile times and many more. There are a number of configurable screens that show specific test results such as 0-60, 0-100, 0-100-0, ½ mile and ¼ mile etc.

Performance Box is a very powerful tool for use in many different kinds of vehicle testing. Vehicle modification can be readily assessed and given specific improvement parameters – the perfect tool for any tuning enthusiast.

Performance Box is a self-contained GPS data logger and Performance Meter. A 10 Hz fully calibrated GPS engine is used to provide accuracy and precision and the data can be stored on a removable SD flash card. Real time results are displayed on the back-lit LCD display and a USB connection allows data to be downloaded to a laptop for further in-depth analysis.

III. DATA COLLECTION

Corridor selection basically depends on the type of study. The objective of the study is to observe the variation in driving parameters in different driving conditions and different modes of urban transport.

Data collection has been done at Sardar bridge, Adajan at merging conflict point. Traffic congestion is high at morning peak hour (9: 30

am to 10:30 am) from bhulka bhavan approach to Athwagate. Traffic from Gujrat Gas circle and Bhulka Bhavan merges at brige. Driving cycle data was collected with reference to the merging point of bridge, Fig. 3 indicates an uncontrolled intersection at a stretch of 200 m. Fig 2 shows data collection is done in car by V Box.

Fig. 2 Data collection by V- Box

Fig. 3 Section of Data collection

Table I Total no. of trips

Mode	Monday	Saturday	Sunday	Total
Bike	3	3	3	9
Car	3	3	3	9
Auto rickshaw	3	3	3	9

Base data contains 9 complete trips made on the bikes, cars and auto rickshaws. Total 9 trips are collected from the each day (Monday, Saturday and Sunday) as shown in Table I.

Driving cycle pattern

Driving cycle pattern of bike, car and auto rickshaw is collected for working day, Saturday and Sundays. Vehicle drives three times to get three driving cycle for each mode. Fig. 4, 5 and 6 show driving cycle pattern of each vehicle on

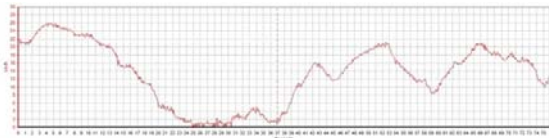Monday. Similarly it is collected for Saturday and Sunday.
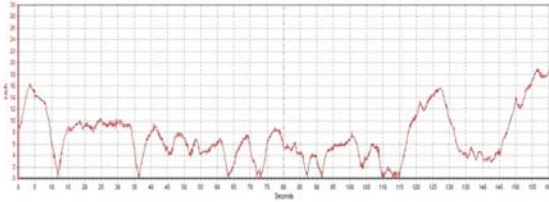

Fig. 4 Driving cycle pattern of Bike (Monday)

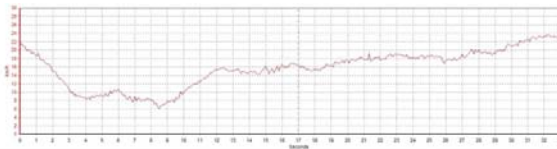Fig. 5 Driving cycle pattern of Car (Monday)

Fig. 6 Driving cycle pattern of Auto Rickshaw (Monday)

IV. DATA ANALYSIS

Speed and acceleration can be calculated from the V-box data, the parameters based on Speed and acceleration values which will set one of the important criteria for analysis. Total five driving parameters with their criteria are calculated according to following condition

1. Percentage acceleration in the base data (acceleration > 0.5 km/h /s)
2. Percentage deceleration in the base data (acceleration < -0.5 km/h /s)
3. Percentage cruise in the base data (speed > 5km/hr and acceleration < |0.5km/h/s|)
4. Percentage idle time (acceleration < |0.5 km/h/s| and speed < 5 km/h)
5. Average Speed

Data analysis has been done for driving cycle parameters by calculating percentage of acceleration, deceleration, cruise and idle phase for all modes of vehicle for different days. Statistically, all parameters are checked for standard deviation, mean and variance.

One way ANOVA is used to compare means of different population group. In present study one way ANOVA is used to compare driving cycle parameters with vehicle modes.
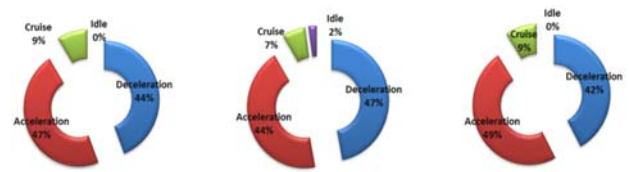
Fig. 7 Driving cycle parameters for Bike (Monday)
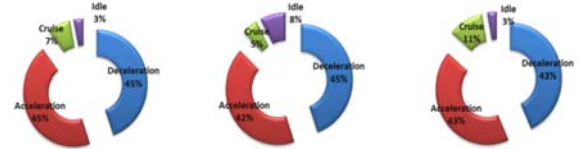
Fig. 8 Driving cycle parameters for car (Monday)
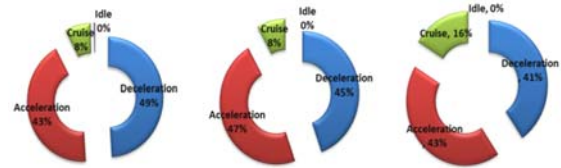
Fig. 9 Driving cycle parameter for Auto rickshaw (Monday)

Fig. 7,8 and 9 show the average value of percentage of driving parameters for working day for bike with 44 % deceleration , 47 % acceleration ,8 % cruise and 1 % idle , for car 44 % deceleration , 43% acceleration , 8 % cruise and 5 % idle and for auto rickshaw 45% deceleration , 45 % acceleration , 10% cruise with no idle period.

The average speed of all three cycles for bike is 14 kmph, for car 8 kmph and auto rickshaw 16 kmph as shown in Fig. 10. The average speed of car is less compared to bike and auto rickshaw.
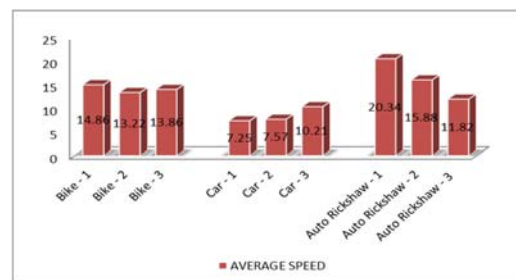
Fig. 10 Average speed of vehicle (Monday)

The average speed of all three cycles for bike is 20 kmph, for car 11 kmph and auto rickshaw 12 kmph as shown in Fig. 11. The average speed of car and auto rickshaw is less compared to bike.
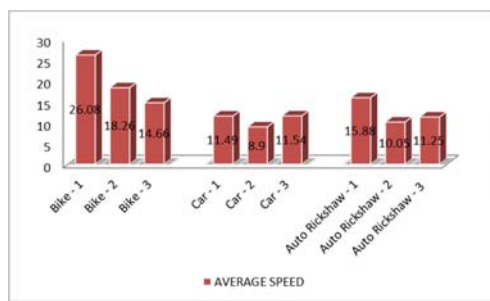
Fig. 11 Average speed of vehicle (Saturday)
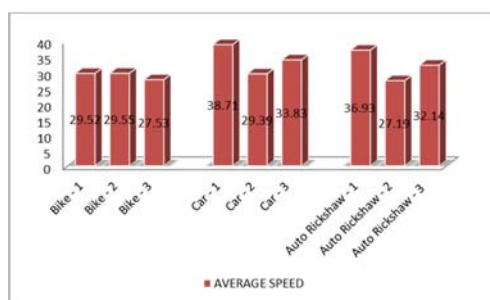
Fig. 12 Average speed of vehicles (Sunday)

The average speed of all three cycles for bike is 29 kmph, for car 34 kmph and auto rickshaw 32 kmph as shown in Fig.12.

One way ANOVA (ANalysis Of VAriance)

The ANOVA test is done with following assumptions

1. Population normality: data is numerical representing samples from normality distributed populations.
2. Homogeneity of variance : the variances of the groups are similar
3. The groups should be independent

ANOVA tests the null hypothesis that the means of the all groups being compared are equal, and produces a statistic called F. if the means of all the groups tested by ANOVA are equal.

Homogeneity of variance is one of the assumptions of ANOVA test, so not necessary to conduct it. Levene's test shows that homogeneity of variance is not significant (p > 0.05), one can

be confident that population variances for each group are approximately.

ANOVA table shows F test values along the degree of freedom and significance. If p > 5 % null hypothesis is accepted.

Table II Homogeneity of variance (Monday)

Levene's Statistic	df1	df2	Sig.
34.551	2	2624	.000

Table III ANOVA test result (Monday)

	Sum of Squares	Df	Mean Square	F	Sig.
Between Groups	42.585	2	21.292	.966	.381
Within Groups	57821.25	2624	22.036		
Total	57863.83	2626			

Table IV Homogeneity of variance (Saturday)

Levene's Statistic	df1	df2	Sig.
53.019	2	1472	.000

Table V ANOVA test result (Saturday)

	Sum of Squares	df	Mean Square	F	Sig.
Between Groups	26.025	2	13.01	.853	.426
Within Groups	22455.15	1472	15.25		
Total	22481.18	1474			

Table VI Homogeneity of variance (Sunday)

Levene's Statistic	df1	df2	Sig.
.064	2	1016	.938

Table VII ANOVA test result (Sunday)

	Sum of Squares	df	Mean Square	F	Sig.
Between Groups	3.798	2	1.899	.198	.820
Within Groups	9748.00	1016	9.594		
Total	9751.80	1018			

One way ANOVA is conducted for all driving cycles of Monday, Saturday and Sunday. Means of cycle 1- Bike, cycle 1 -Car and cycle 1- Auto rickshaw are compared within and between groups. Similarly for cycle 2 and cycle 3 of all days are compared. Null hypothesis is assumed that there is no significant difference of vehicle mode on driving parameter.

First assumption homogeneity of variance was performed, which has $p < 0.05$ for all groups of Monday, Saturday and Sunday. It indicates that null hypothesis is rejected and follow F test (ANOVA), which is shown in Table II, IV and VI. After Leven's F test, results are generated by one way ANOVA. Tables III, V and VI show the significance value of null hypothesis, which is more than 0.05, so null hypothesis is accepted. It interprets that there is no effect of vehicle type on driving parameter like acceleration, deceleration and cruise speed.

Distance – Time Relationship
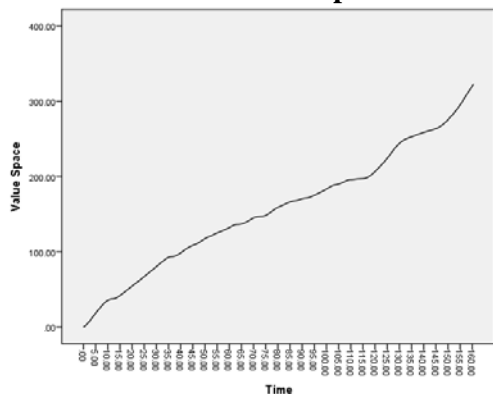
Fig. 13 Space – Time Trajectory (Monday)
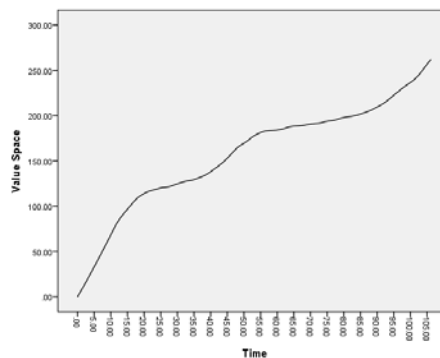
Fig. 14 Space – Time Trajectory (Saturday)
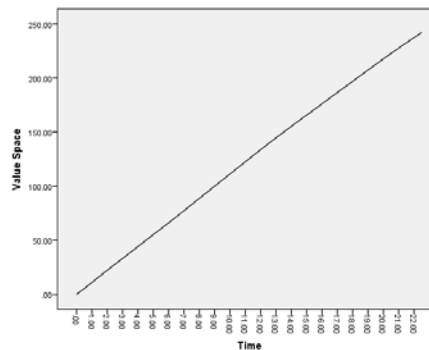
Fig. 15 Space – Time Trajectory (Sunday)

Speed Time trajectory is shown in Fig. 13, 14 and 15 for Monday, Saturday and Sunday respectively. From the space – time relation it is observed that the speed is constant on Sunday due to less traffic volume, whereas during week days speed fluctuation is observed significantly.

V. CONCLUSION

Driving cycle parameters have been calculated for three modes of vehicle for three days of week. The real world data was collected by V box and analysis was done. Analysis is based on five important parameter of speed – time profile; percentage acceleration, deceleration and cruise, idle and average speed.

Driving cycle parameters for working day and Saturday have percentage acceleration and deceleration approximate 45%, cruise 10% with idle time 4-5 % for all three modes, whereas on Sunday percentage acceleration and deceleration is approximate 40 %, cruise 15% with idle time 0 % for all three modes during morning peak hour. Traffic volume on working day and Saturday is higher than the Sunday, so cruise period is less on working day and Saturday with

idle period. Sunday all cycles have no idle period because of less traffic volume. The average speed of vehicles on Sunday is higher than Saturday and working day.

One way ANOVA is used for Statistical analysis. Analysis is done for driving cycle parameter with respect to modes of vehicle. By performing the test the p value is greater than more generally of the driving conditions on the emission. All the pollutants are sensitive to acceleration parameters (frequency of accelerations and strong accelerations, average acceleration, time spent at high acceleration)

5%, so null hypothesis is accepted for all cases and It is concluded that there is no effect of vehicle type on driving parameter.

The variations induced by the driving conditions can be more significant than the variation induced between the vehicles. This highlights well the importance of the driving cycle and

REFERENCES

[1] Andr, M., Rapone, M., Joumard, R., & Inrets-lte, R. (2006). Analysis of the cars pollutant emissions as regards driving cycles and kinematic parameters, Report INRETS – LTE 0607, March 2006

[2] Ricardo G. Sigua (1997), "Development of driving cycle for metro manila", Journal of Eastern Asia Society for Transportation Studies, vol. 2, No. 6, Autumn, 1997

[3] Dresser, C. (2011). "Project-Level Modeling in MOVES, Office of Transportation and air quality, U.S Environmental protection agency, 1–12.

[4] Fellendorf, M., & Vortisch, P. (2010). "Microscopic Traffic Flow Simulator VISSIM" International series in Operations research & Management Science 145,(pp. 63–94).

[5] Fotouhi, A. (2013). "Tehran driving cycle development using the k-means clustering method", Sharif University of Technology Scientia Iranica, 20(2), 286–293.

[6] Jie Lin, Debbie A. Niemeier, "Estimating Regional Air Quality Vehicle Emission Inventories: Constructing Robust Driving Cycles", Transportation Science INFORMS, Vol. 37, No. 3, August 2003, pp. 330–346

[7] Karabasoglu, O., & Michalek, J. (2013). "Influence of driving patterns on life cycle cost and emissions of hybrid and plug-in electric vehicle powertrains". Journal of Energy Policy, 1–17.

[8] Lei Yu. Ziqianli Wang,and Qinyi Shi, " PEMS- based approach to developing and evaluating driving cycle for air quality assessment, centre of transportation training and research , Texas southern university, April 2010

[9] Naghizadeh, M., Simulation, S., Cycle, D., & Economy, F. "Development of car drive cycle for simulation of emission and fuel economy", Proceeding 15th European simulation Symposium, SCS European Council/ SCS Europe BVBA, 2003 ISBN 3- 936150-28-1

VEHICULAR POLLUTION DISPERSION: CASE STUDY OF A TYPICAL STREET CANYON IN SURAT

[1]T.Banerjee, [2]R. A. Christian
[1]Ph. D. Scholar, CED, S.V.N.I.T,Surat, [2]Associate Professor, CED, S.V.N.I.T, Surat
Email:[1]tandara.banerjee@ckpcet.ac.in, [2]rac@ced.svnit.ac.in

Abstract— Vehicular pollutant dispersion in a typical street canyon in Surat city is analysed. For the street canyon under consideration the traffic volume count for a busy period of the day is measured along with the type of vehicle and average vehicular speed. Based on this count and using the emission data from CPCB, the total release in the 120 m long street is calculated. Based on this release data, calculations are carried out using OSPM to obtain the possible concentration level at the leeward and windward ground levels of the street. These calculations are then compared with 2D CFD simulations carried out for the road considering the source of release from the ground level.

Index Terms—**CFD, Dispersion, OSPM, Vehicular Pollution**

I. INTRODUCTION

Pollutant from vehicular exhaust constitutes a major fraction of total pollutant dispersion in atmosphere. These pollutants has direct impact on human health. Atmospheric air flow plays an important role in distribution of pollutants released from the vehicle into the air. Significant increase in computer power makes it now possible to use advanced numerical models for air pollution studies. But numerical analysis is also computationally expensive in terms of time. For urban street pollution monitoring, a simplified model which includes most of the complexities of real flow as well requires fewer calculation steps are preferable. The Operational Street Pollution Model (OSPM) [1] belongs to this category of parameterized models. This model is basically a semi-empirical one having few assumptions about flow and dispersion conditions. In this paper, calculations are first carried out using OSPM model for a sample street canyon in Surat city. The vehicular traffic flow and the air flow rate and direction of air flow are measured. The rate of emission from light and medium vehicles is calculated as per CPCB norms [2] according to the average speed of the vehicle.

Some of the assumptions of OSPM are very simplistic and hence result in gross inaccuracy of prediction of pollutant by this model. With the advent in Computational Fluid Dynamic (CFD) tools it is possible to rigorously check these simplistic assumptions and use the CFD simulation results to augment the model so that complex features of flow can be incorporated in these models. This is the aim of this research.

II. THE OPERATIONAL STREET POLLUTION MODEL (OSPM)

OSPM is based on similar principles as the CPB-model by Yamartino and Wiegand [3]. Concentrations of exhaust gases are calculated using a combination of a plume model for the direct contribution and a box model for the

recirculating part of the pollutants in the street (Fig. 1). OSPM makes use of a very simplified parameterization of flow and dispersion conditions in a street canyon. This parameterization was deduced from extensive analysis of experimental data and model tests [4].
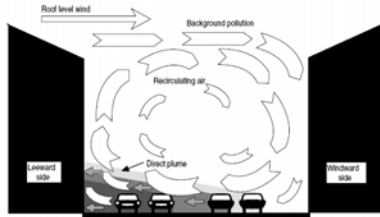

Fig. 1: Schematic of the basic principles in OSPM [1]

III DATA COLLECTION

A busy street of Surat city (near Bhagal Char Rasta) is selected as a case study (Fig. 2). The plan of the street is shown in Fig. 3.

Fig. 2: Bhagal Char Rasta

The street runs from east to west direction and the wind direction when measured was observed to be along north-west direction. The Street considered has the following dimensions and characteristics.

Width of street = 15.2 m

Height of the building = 15 m (approximate)

Length of street = 120 m

Ambient Temperature = 26.3^0 C

Average speed of vehicle = 10 km/hr =2.78 m/s

Wind direction = N-W

Angle of wind with reference to central line of the street is, $\Phi = 50^0$

Average roof top wind speed measured= 0.817 m/s
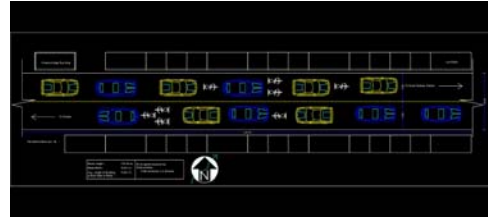
Fig. 3: Plan of the street under consideration

Measured vehicular traffic flow

Traffic volume count was carried out during peak traffic period. Table shows traffic count measured for 2-wheeler, 3-wheller and four wheelers in the street shown in fig. 3. This traffic count is used to generate the pollutant release in that period in the street under consideration. Based on this traffic count, the emission rate of Carbon monoxide (rate of release of CO) in the street is calculated as is discussed in the next section.

IV OSPM CALCULATIONS

Calculation of the emission rate of CO for the vehicular traffic

The emission factors for 2-wheeler, 3-wheeler, 4-wheeler vehicles are considered based on draft report. "Emission Factor development for Indian Vehicles" published by Central Pollution Control Board of India [5]. The values chosen are for Indian road conditions and considering the vehicle to have been manufactured after 2000. For 2-wheeler average emission factor is considered between scooter and motor cycle. For 3-wheeler average is taken between 2-stroke and 4-stroke engines of less than 200 cc capacity. Similarly for 4-wheelar average is considered between petrol, diesel and CNG driven vehicles. The average emission factors are shown in table II.

Calculation of dispersion of CO by Operational Street Pollution Model (OSPM)

The ground level concentration of pollutant established using OSPM as a sum of direct contribution (C_d), recirculation contribution (C_{rec}) and the background contribution (C_b) as shown below:

$$C = C_d + C_{rec} + C_b$$

Step 1: Calculation of direct contribution C_d

The direct contribution at any receptor point at the ground level is calculated as a sum total of

discrete contribution due individual source of emission and is expressed as:

where Q_i is the emission strength from the vehicles of the ith traffic lane in g/ms, x_i is the corresponding horizontal distance from the source to the receptor in m, σ_w is the mechanical turbulence created by wind and traffic in the street in m/s, u_b is the wind speed at the street level in m/s,

h_0 is the initial dispersion in the wakes of the vehicles assumed as approximately equal to 2m. Thus in order to obtain the direct contribution at any receptor point in the ground level located at a horizontal distance x_i from the source of strength Q_i, it is required to estimate the following:

(i) Calculation of emission strength, Q_i

Q_i= (No. of vehicles/sec)×(emssion factor in g/m)

The calculation is carried with the assumption is that there is a single lane along the center of the street.

ii) Calculation of street level wind speed, u_b

$$u_b = u_t \frac{\ln(h_0 / z_0)}{\ln(H / z_0)}[1 - 0.2.p.\sin(\Phi)]$$

where u_t = 0.817 m/s, h_0 = 2m, H = 15m, p = 1, Φ = 50^0 (wind angle with respect to street axis), Z_0 = 0.60m

(iii) Calculation of mechanical turbulence, σ_w

$$\sigma_w = \left[(\alpha u_b)^2 + \sigma_{w0}^2\right]^{1/2}$$

$$C_d = \sqrt{\frac{2}{\pi}} \frac{1}{u_b} \sum_i \frac{Q_i}{\left[h_0 + \left(\sigma_w/u_b\right)x_i\right]}$$

where α = 0.1, u_b = 0.258 m/s, σ_{w0} = traffic induced turbulence and is given by

$$\sigma_{w0} = b\left(\frac{N_{veh}.V.S^2}{W}\right)^{1/2}$$

where b = 0.3,
S^2 = horizontal area occupied by a single vehicle
$\qquad$ = 1.08 (2-Wheeler) [6]
$\qquad$ = 3.64 (3-Wheeler) [6]
$\qquad$ = 6.40 (4-Wheeler) [6]

(iv) Calculation of direct contribution, C_d

$$C_d = \sqrt{\frac{2}{\pi}} \frac{1}{u_b} \sum_i \frac{Q_i}{\left[h_0 + \left(\sigma_w/u_b\right)x_i\right]}$$

Thus the direct contribution is an inversely proportional to the distance of the source from the receptor.

Step 2: Calculation of recirculation contribution (C_{rec})

$$C_{rec} = \frac{Q.L_{rec}}{W\left(\sigma_{wt}L_t + u_t L_{s1} + u_b L_{s2}\right)}$$

Here Canyon ventilation,
$\sigma_{wt} = \left[(\lambda u_t)^2 + 0.4\sigma_{w0}^2\right]^{1/2}$;

$L_{rec} = \min\left(W, L_{vortex}.\sin(\Phi)\right)$ and L_{vortex} is taken equal to twice the height of the upwind building for u_t = 2 m/s. For u_t < 2 m/s, a linear decrease in L_{vortex} is observed.

Table I: Vehicular traffic flow for different types of vehicles

TIME (pm) / VEHICLE TYPE	2 WHEELER	3 WHEELER	4 WHEELER
06:05-06:10	287	154	24
06:10-06:15	348	194	18
06:15-06:20	335	141	29
06:20-06:25	317	202	20
06:25-06:30	319	198	27
06:30-06:35	293	204	36
06:35-06:40	303	197	27
06:40-06:45	329	207	21
06:45-06:50	315	205	15
06:50-06:55	274	187	24

06:55-07:00	342	209	19
07:00-07:05	322	199	14
07:05-07:10	307	215	23
TOTAL	4091	2512	297

Table II: Emissions factor for CO [5]

Type of vehicle	Total nos. of vehicle/hr	Emission factor[g/km]
2 wheeler	4091	1.205

| 3 wheeler | **2512** | **2.92** |
| 4 wheeler | 297 | 1.12 |

Length of recirculation zone, L_{rec} is taken as either equal to street width W or length of the vortex L_{vortex} whichever is smaller. When L_{vortex} > W and for an oblique wind angle, L_{rec} as shown in fig. 4 is given as $L_{rec} = \min(W, L_{vortex}.Sin(\Phi))$.
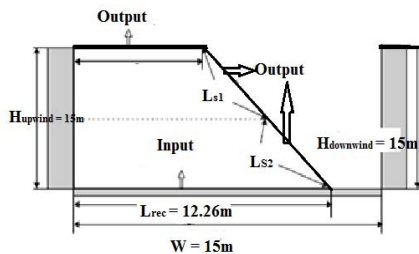
Fig. 4: Concept of top edge and slanting edge for escape of pollutant

The total concentration is made up of direct and the recirculation contributions. However, for a receptor on the leeward side, the direct contribution is calculated considering the emissions from traffic in the recirculation zone only. For a receptor on the windward side, only contributions from the emissions outside the recirculation zone are taken into account. If the recirculation zone extends through the whole canyon, no direct contribution s given for the receptor on the windward side. Thus the total concentration for the receptor on the leeward side is given as: $C_{Lee} = C_d + C_{rec}$

Since there is no source outside the recirculation zone in the present case, a receptor on windward side will only be influenced by the recirculation contribution.

The difference between the leeward and windward concentration is less in this case because the wind speed is very low which resembles the case of calm wind flow in the canyon. Only when the wind speed is more that 2m/s, there can be reasonable influence of wind. Thus a parametric variation of wind velocity is considered. The wind velocity is varied as 2m/s, 4m/s and 8m/s and the above calculations are repeated. Also the influences of wind angle for all these speed are calculated. The wind angle is varied from 0^0 (parallel to street axis) to 90^0 (perpendicular to street axis). These calculations are discussed below:

V PARAMETRIC INVESTIGATIONS

Fig. 5 Variation of leeward end ground level concentration as a function of wind angle and wind speed.

Fig. 5 shows the variation of leeward end ground level concentration as a function of wind angle and wind speed. It can be observed that the

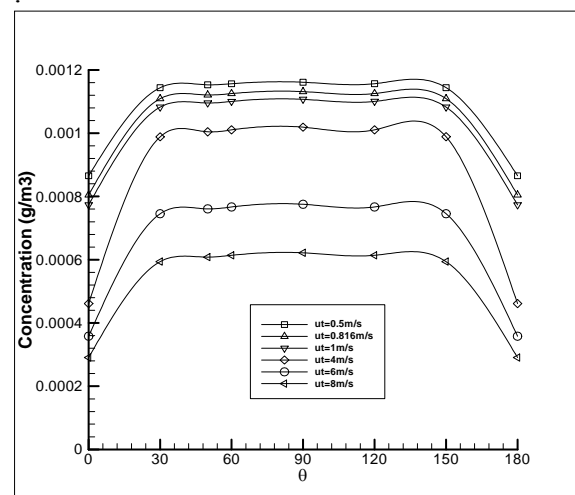leeward concentration decreases with increase in wind speed. This is because of the increase in recirculation vortex with wind speed which results in more ventilation of pollutant from the roof top level. The influence of wind angle is significant at lower wind angles. When the wind flow is parallel to the street axis the contribution to windward and leeward side is same and is equal to the direct contribution due to the plume.
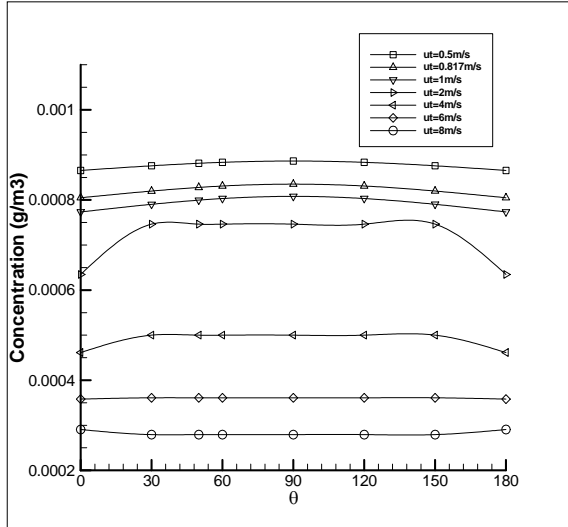

Fig. 6 Variation of windward end ground level concentration as a function of wind angle and wind speed.

Fig. 6 shows the variation of windward end ground level concentration as a function of wind angle and wind speed. For the windward side the direct contribution starts becoming important for wind speed less than 1m/s. For still lower wind speed the street vortex disappears and the wind direction dependence disappears too. Thus at vanishing ambient wind the concentration levels are solely determined by the traffic created turbulence. For higher wind speed the windward side concentration is due to recirculation component only.

VI CFD SIMULATION OF STREET CANYON

Two-dimensional simulations for flow inside the street canyon are developed by solving the Reynolds averaged Navier-Stokes (RANS) [7] equations with two equation k-ε model for turbulence being used as closure. The RANS equations are derived by Reynolds decomposition where the instantaneous flow variables are represented as sum of the mean value and the perturbations. The underlying assumption in the derivation of RANS equations are that the perturbation is velocity components do not significantly alter the average mass flow rate while the momentum equations are modified with extra stress terms called the Reynolds stresses. The Reynolds stresses in terms are represented in terms of eddy viscosity and gradient of mean velocity based on Boussinesq approximation. In k-ε model the eddy viscosity is obtained by solving the conservation equations of turbulent kinetic energy (k) and rate of decay of turbulent kinetic energy (ε) also called the eddy dissipation rate. The geometry of the canyon is generated in GAMBIT and is messed with structured rectangular grid structure. The mesh is then imported in FLUENT where the viscous model with standard k-ε option is enabled to solve the RANS equations. The convergence criteria for the mass, momentum, k and ε equations are kept as low as 10^{-5}. The pressure-velocity decoupling is solved using SIMPLE (Semi-Implicit Pressure Linked Equations) algorithm with first order upwind scheme being used for discretisation of advection terms. The results of simulations obtained for different wind speed at roof top level and different aspect ratio of the canyon are discussed here.

One of the most important feature of OSPM is the calculation of the recirculation component of the pollutant concentration. The calculation of the re-circulating component is based on the proposed length of the vortex in the street. The simplified linear approximation proposed in OSPM model may not be true. Also the OSPM model proposes that there is a single vortex responsible for recirculation in the street canyon for wind speed more than 2 m/s. However CFD simulations shows multiple vortices in the street particularly for deep streets with larger depth compared to the width of the canyon. Fig. 7 shows the vortex structure in street canyons for same aspect ratio for the three different wind speeds to highlight this feature.
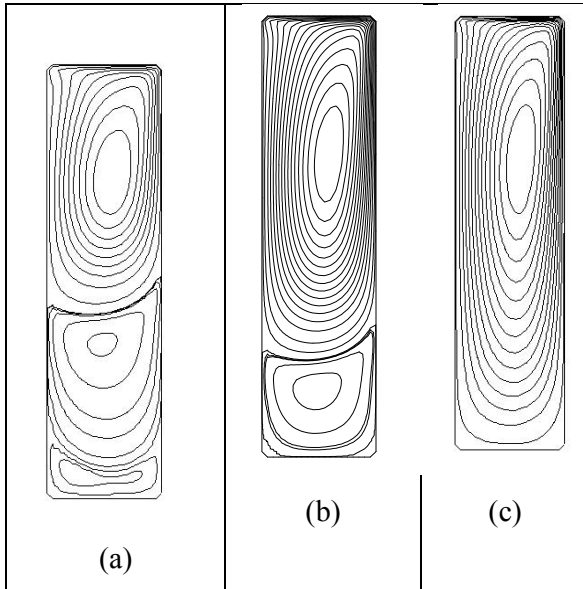
Fig 7 Vortex pattern in the street canyon for AR=0.25 and wind speed (a) 0.5 m/s (b) 1 m/s (c) 2 m/s

The other issue which needs to be addressed is the concept of vortex length for AR=1 as is demonstrated in Fig 8 It can be observed that the primary vortex occupies the entire street canyon even at wind velocities much lower than 2 m/s. However the OSPM predicts that the street will be completely occupied with the primary vortex only for wind speed above 2 m/s. and the length of the vortex as linearly decreases with the wind speed for values less than 2m/s. Accordingly the direct and recalculating components of pollutant distribution are calculated on the leeward and windward side. However if the CFD simulations are to be believed the windward side also receives the recirculating component of pollutant at much lower speeds than 2m/s.
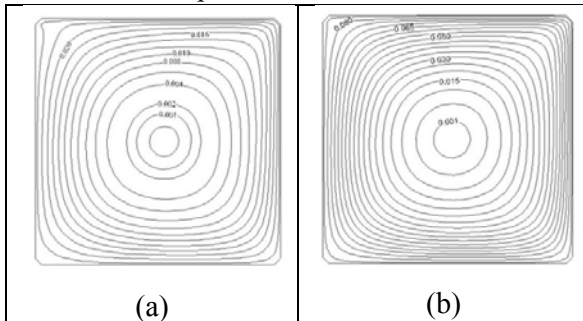
Fig 8 Vortex pattern in the street canyon for AR=1 and (a) wind speed =0.5 m/s (b) wind speed =2 m/s

Two dimensional CFD simulations of vehicular dispersion in street canyon

The multiphase model of FLUENT is enabled to generate the distribution of Carbon monoxide (CO) released from the vehicles in the street. The simulations shown in fig 9 are for AR=1 and wind speeds of 0.5 m/s and 1 m/s respectively. The volume fraction here represents the volume of CO per unit volume of air. It can be observed in both fig 9 (a) and (b) that the fluid current re-circulates the CO from the street level to the leeward wall and a part of this is flushed out from the rooftop level. A portion of this re-circulated concentration accumulates in the windward side as well. As the wind speed increases the amount of CO flushed out or ventilated from rooftop also increases thereby the deposition of the ground level concentration at both the leeward and windward level decreases.
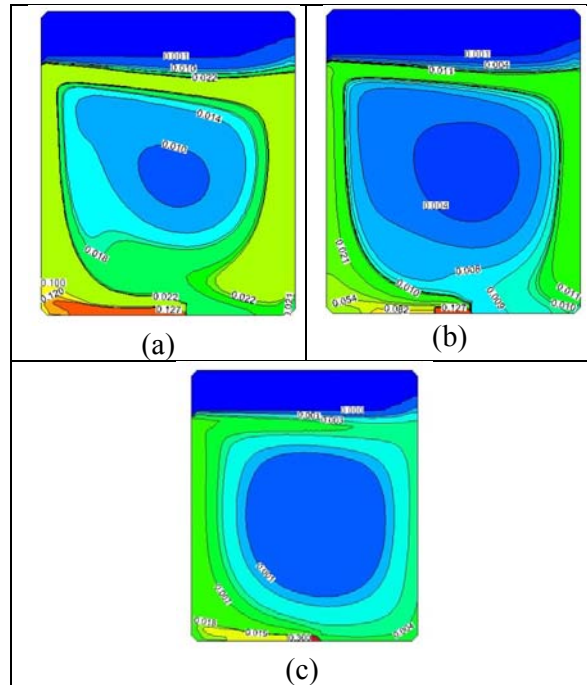
Fig. 9 Volume fraction distribution of CO in the street canyon for AR=1 and wind speed (a) 0.5 m/s (b) 1 m/s and (c) 2 m/s

Table III. Comparison of the ground level concentration predicted by CFD simulations with the OSPM calculations

Wind speed (m/s)	Leeward concentration obtained by OSPM	Leeward concentration obtained by CFD	Windward concentration obtained by OSPM	Windward concentration obtained by CFD
0.5	0.00122	0.001156	0.0002748	0.000421
0.817	0.001113	0.001101	0.0002963	0.000312
2	0.00143	0.001010	0.0007462	0.000674
4	0.00101	0.000912	0.0005000	0.000562
6	0.000777	0.000662	0.0003610	0.000284
8	0.000662	0.000521	0.0002793	

Table III shows the variation of ground level concentration at the leeward and windward end obtained by the OSPM and the CFD model for the street pollutant release conditions discussed in the previous chapter. It can be noted from the comparison that OSPM predicts larger deposition of concentration as compared to the results obtained by the CFD simulations. This is particularly true for higher wind speed. This is because the assumptions pertaining to OSPM allows reduced flush off from the roof top level as is calculated by the CFD simulations. Actually OSPM under predicts the strength of the recirculation vortex which is responsible for this flush out. The windward concentration predicted by the CFD model is slightly more than the OSPM calculation because of the re-circulating component which accumulated on the windward end for wind flow perpendicular to street axis.

REFERENCES

[1] Berkowicz R., OSPM-Aparametrised street pollution model, Environmental monitoring and assesment, 65, 323-331, 2000.

[2] CPCB, Status of the vehicular pollution control programme in India, New Delhi, March 2010.

[3] Yamartino R.J. and Wiegand G., Development and evaluation of simple models for the flow, turbulence and pollutant concentration fields within an urban street canyon, Atmospheric Environment, 20(11):2137–2156, 1986.

[4] Berkowicz R., OSPM-Aparametrised street pollution model, Environmental monitoring and assesment, 65, 323-331, 2000.

[5] CPCB/ MOEF, Draft report on "Emission Factor development for Indian Vehicles ,"Project Rep No.: AFL/2006-07/IOCL/Emission Factor Project/Final Rep dt. August 17, 2007One

[6] Joshi G, Sinha V, Patel J, Heterogeneous Traffic Characterisation and Flow Behaviour Modeling for Metropolitan Arterial in India, Journal of the Eastern Asia Society for Transportation Studies,Vol.9,2011

[7] Ferziger H J and Peric M, Computational Methods for Fluid Dynamics, Springer-Verlag, Berlin, 2002.

RISK MANAGEMENT IN CONSTRUCTION PROJECTS

[1]Mubin M. Shaikh
[1]Department of Civil Engineering, Maharashtra Institute of Technology, Pune
Email:[1]mubin_shaikh@rediffmail.com

Abstract— Construction industry is highly risk prone, with complex and dynamic project environments creating an atmosphere of high uncertainty and risk. The industry is vulnerable to various technical, sociopolitical and business risks. The track record to cope with these risks has not been very good in construction industry. As a result, the people working in the industry bear various failures, such as, failure of abiding by quality and operational requirements, cost overruns and uncertain delays in project completion. In light of this, it can be said that an effective systems of risk assessment and management for construction industry remains a challenging task for the industry practitioners. The aim of the this paper is to identify and evaluate current risks and uncertainties in the construction industry through extensive literature survey and aims to make a basis for future studies for development of a risk management framework to be adopted by prospective investors, developers and contractors.

Keywords- Project management; risk management; risk analysis; construction; contractors

I. INTRODUCTION

Risk can be defined as the event that negatively affects the project objectives such as time and schedule, cost, quality of work. Risk Management is the process of identifying the potential risk associated with risk and responding to those risks. Risk in any project is a choice rather than fate. According to the characteristic of the construction industry, which has high uncertainty, so it will occur many risks during the construction phase and or operational building. Risk in construction has been the object of attention because of time and cost over-runs associated with construction projects. Risk is present in all the activities in a project; it is only the amount which varies from one activity to another.

Risks and uncertainties inherent in the construction industry are more than other industries. The process of planning, executing and maintaining all project activities is complex and time-consuming. The whole process requires number of people with diverse skill sets and the coordination of a vast amount of complex and interrelated activities. The situation is made complex by many external factors. The track record of construction industry is very poor in terms of coping with risks, resulting in the failure of many projects to meet time schedules, targets of budget and sometimes even the scope of work. As a result, a lot of suffering is inflicted to the clients and contractors of such projects and also to the general public. Risk in the construction industry is perceived to be a combination of activities, which adversely affect the project objectives of time, cost, scope and quality. Some risks in construction processes can be easily predicted or readily identified; still some can be totally unforeseen. Construction risks can be related to

technical, management, logistical, or sociopolitical aspects or can be related to natural disasters. In the domain of project management, some of the critical effects of risks are failure to achieve operational requirements and the required quality, non completion of the project within stipulated time and estimated cost.

The current study is focused on concepts of risk management and will cover the related literature on the topic, development of a survey questionnaire and suggestions related to risk management practices in construction industry of Pakistan.

II. OBJECTIVES AND NEED OF STUDY

The development of infrastructure is one of the most important activities that can boost up the business of various industries, thereby increasing the gross domestic product (GDP) of a country. Due to this fact countries stress on infrastructure development and provide finances for the same in their short term and long term financial plans. The vastness of construction projects leaves a lot of scope for various environmental, socio- political and other unforeseen problems during conceptual phase, land expropriation, and execution leading to time and cost overruns in projects and compromise in quality. The cost overruns can be of huge magnitude in a project involving a large amount of money. The loss of services given by the project during the time in which the project overruns can be enormous if put into monetary terms. Hence, to reduce the losses, efficient management of a construction project is required. Application of various project management techniques have to be made from the conception to the completion stage, which include managing various risks associated with the project in its every stage. Risk management becomes an important part of project management. The construction industry, perhaps more than most of other industries, is overwhelmed by risks. If these risks are not dealt with satisfactorily then there is a maximum likelihood of cost overruns, time delays and low quality, resulting in dissatisfaction of clients and public. In India, like other developing countries less importance is given to this aspect of project management.

The basic aim of this paper is to identify and assess the current risks and uncertainties in the construction industry around the globe; and to evaluate the current state of risk management practices and make a basis for future studies for development of a framework for effective risk management which can be adopted by prospective foreign and local investors, developers and contractors in India.

III. METHODOLOGY

In this paper, general focus has been made on the general concepts of project risk management. A questionnaire was developed by going through literature on construction risk management. To achieve the objectives of this paper, questionnaires were deemed to be the most effective tool for gathering information. These questions helped identify any projects that should definitely not be undertaken by the parties and those which, although risky, should be examined further after a more rigorous examination of the potential sources of risk. The questionnaire was designed based on the knowledge of government, consultant, or contractor in large or infrastructure construction projects; the questions were meant to identify their method of risk identification and possible effects of those risks.

The general methodology of this study relies largely on the survey questionnaire which will be collected from the various multi project construction contractors and project manager of different sizes by mail or by personnel meeting. A thorough literature review was initially conducted to identify the risk factors that affect the performance of construction industry as a whole.

IV. CONCEPTS OF RISK ANALYSIS AND MANAGEMENT

The concept of risk is multi-dimensional. In the context of construction industry, the probability that a definite factor detrimental to the overall project occurs is always present. A lack of predictability related to the consequences of a planning situation and the associated uncertainty of estimated outcomes leads to the consequence that results can either be better than expected or can be worse. In addition to the different definitions of risks, risks can be categorized for different purposes

as well. The broad categories of construction risks are external risks and internal risks; while some other categories curtail risks as political, social and safety risk etc.

Project Risk: Risk management in a project encompasses the identification of influencing factors which could negatively impact the cost schedule or quality objectives of the project, quantification of the associated impact of the potential risk and implementation of measures to mitigate the potential impact of the risk. The riskier the activity is, the costlier will be the consequences in case a wrong decision is made. Proper evaluation and analysis of risks will help decide justification of costly measures to reduce the level of risk. Risks cannot be totally avoided but with proper management these can be minimized.

Determination of Risk: There are two methods to determine risks in a project, namely the qualitative and quantitative approach. The quantitative analysis relies on statistics to calculate the probability of occurrence of risk and the impact of the risk on the project. The most common way of employing quantitative analysis is to use decision tree analysis, which involves the application of probabilities to two or more outcomes. Another method is Monte Carlo simulation, which generates value from a probability distribution and other factors.

The qualitative approach relies on judgments and it uses criteria to determine outcome. A common qualitative approach is the precedence diagramming method, which uses ordinal numbers to determine priorities and outcomes. Another way of employing qualitative approach is to make a list of the processes of a project in descending order, calculate the risks associated with each process and list the controls that may exist for each risk.

V. FACTORS AFFECTING RISK:

Several factors expose projects to normal than higher risk.

a) History: Newer projects pose more risk because the process has not been refined with the passage of time. If a project of similar nature has been done many times before, then the likelihood of success with the current project is also enhanced.

b) Management Stability: Management stability means that the whole management team shares the same vision and direction, thereby leading successful achievement of goals. If the management is unstable then it can lead to unrealistic and impractical schedules for the project and inefficient use of resources.

c) Staff expertise and experience: In the event that the members of a project team lack the direct working knowledge and experience of the area, there is a likelihood of time delays, estimated cost upsets and poor quality.

d) Team Size: In case of large teams, the probability of problem occurrence increases due to the team size. One of the reasons can be the difficulty of communication due to the large team size.

e) Resource Availability: If the availability of resources is easy, the probability of responding to problems in real time also increases. For example, easy availability of money makes securing human, material and equipment resources easy on as needed basis. However, an abundance of resources does not provide quarantine against risks, all it does is to equip the project team with the tactics to respond to risks.

f) Time Compression: In case of highly compressed time schedule, the risks are magnified in the project. When more time is available, more flexibility is present in the project and there is an opportunity to mitigate and reduce the impact of occurring risks.

g) Complexity: In case of a highly complex or sophisticated project, the opportunity of a mistake or a problem is also enhanced.

VI. TYPES OF RISKS:

Risks can be associated to technical, operational or business aspects of projects. A technical risk is the inability to build a product that complies with the customer's requirement. An operational risk arises when the project team members are unable to work cohesively with the customer.

Risks can be either acceptable or unacceptable. An unacceptable risk is one which has a negative impact on the critical path of a project. Risks can either have short term or long term duration. In case of a short term risk, the impact is visible immediately, such as a

requirement change in a deliverable. The impact of a long term risk is visible in the distant future, such as a product released without adequate testing.

Risks can also be viewed as manageable and unmanageable. A manageable risk can be accommodated, example being a small change in project requirements. An unmanageable risk, on the other hand, cannot be accommodated, such as turnover of critical team members.

Finally, the risks can be characterized as internal or external. An internal risk is unique to a project and is caused by sources inherent in the project; example can be the inability of a product to function properly. Whereas, an external risk has origin in sources external to the project scope, such as cost cuts by senior management.

Risks associated with the construction industry can be broadly categorized into:

a) *Technical risks:*
- Inadequate site investigation
- Incomplete design
- Inadequate of specifications
- Uncertainty over the source and availability of materials
- Change in scope
- Construction procedures

b) *Logistical risks:*
- Availability of sufficient transportation facilities
- Availability of resources-particularly construction equipment spare parts, fuel and labor

c) *Management related risks:*
- Uncertain productivity of resources
- Industrial relations problems
- Contractual relation
- Contractors experience
- Attitude of participants
- communication

d) *Environmental risks:*
- Weather and seasonal implications
- Natural disasters

e) *Financial risks:*
- Availability and fluctuation in foreign exchange
- Delays in Payment
- Inflation
- Local taxes
- Improper estimation
- Low market demand

- Increase material costs

f) *Socio-political risks:*
- Change in laws and regulations
- Pollution and safety rules
- Bribery/ corruptions
- Language and cultural barrier
- Law and order
- War and civil disorders
- Requirement for permit then approval

g) *Physical Risks*
- Damage to structure
- Damage to equipment
- Labour injuries

h) *Construction risks:*
- Labour productivity
- Labour disputes
- Site conditions
- Equipment failure
- Design changes
- New technologies

VII. COMMON SOURCES OF RISK IN CONSTRUCTION PROJECTS:

The common sources of risks in construction industry are listed below:

- Changes in project scope and requirements
- Design errors and omissions
- Inadequately defined roles and responsibilities
- Insufficiently skilled staff
- Subcontractors
- Inadequate contractor experience
- Uncertainty about the fundamental relationships between project participants
- New technology
- Unfamiliarity with local conditions
- Force majeure

VIII. MAJOR PROCESSES OF PROJECT RISK MANAGEMENT:

Risk management involves four processes namely:

a. *Risk Identification:* Determination of most likely risks affecting the project and documentation of characteristics of each risk

b. *Risk quantification:* Assessment of risks

and the possible interactions of risks with project activities to evaluate the possible outcomes of the project

c. *Risk response development:* Definition of response steps for opportunities and threats associated with risks

d. *Risk response control:* Response to the changes implemented to remove risks throughout the project duration

IX. RISK IDENTIFICATION TECHNIQUES

The risk identification can be done by using following techniques

1. **Brainstorming:** This is one of the most popular techniques. Generally, it is used for idea generation; it is also very useful for risk identification. All relevant persons associated with project gather at one place. There is one facilitator who is briefing about various aspects with the participants and then after note down the factors. Before closing it the facilitator review the factors eliminate the unnecessary ones.

2. **Delphi Technique:** This technique is similar to brainstorming but the participants in this do not know each other and they are not at the same place. They will identify the factors without consulting other participants. The facilitator like in brainstorming sums up the identified factors.

3. **Interview/Expert Opinion:** Experts or personnel with sufficient experience in a project can be a great help in avoiding/solving similar problems over and over again. All the participants or the relevant persons in the project can be interviewed for the identification of factors affecting risk.

4. **Past Experience:** Past experience from the same kind of project, the analogy can be formed for identification of the factors. When comparing the characteristics of projects will provide insight about the common factors.

5. **Checklists:** These are simple but very useful predetermined lists of factors that are possible for the project. The check

list which contains a list of the risks identified in projects undertaken in the past and the responses to those risks provides a head start in risk identification.

X. RISK CONTROL

Risk control is the final step of the process. After we have implemented response actions, we must track and record their effectiveness and any changes to the project risk profile. Did the response actions have a positive or negative effect on achieving project objectives? Responses taken in risks should also be documented for future reference and project plans.

XI. ADVANTAGES OF RISK MANAGEMENT:

Following are advantages of risk management:

a) Achievement of objectives
b) Shareholders reliability
c) Reduction of capital cost
d) Less uncertainty
e) Creation of value

XII. LIMITATIONS OF RISK MANAGEMENT:

In the event of improper assessment of risks, important time can be wasted in dealing with risk losses which are unlikely to occur. If too much time is spent on the assessment and management of unlikely risks, then important resources can be diverted which otherwise could have been very profitable. Unlikely events can occur, but if the likelihood of the risk occurrence is too low, then it is better to retain the risk and deal with the result if the risk in fact occurs.

XII. CONCLUSION

Formal risk analysis and management techniques are rarely employed by construction industry owing to the lack of experience and knowledge in the area. The industry also holds disbelief that these techniques are suitable to be employed in construction projects, much in the same manner as employed in other industries. The perception of risk by contractors and

consultants is mostly based on their intuition and experience. The most utilized risk response measures are risk elimination and risk transfer. However, the respondents have revealed that these practices cause the problems of delays, low quality and low productivity in projects.

XIII. REFRENCES

1. Akintoye, A.S. and MacLeod, M.J.; "Risk analysis and management in construction"; International Journal of Project Management (1997)
2. Baker, S., Ponniah, D., and Smith, S.,; Risk response techniques employed currently for major projects, Construction Management & Economics (1999)
3. Dariusz Skorupka,; "Risk management in building projects"; AACE International Transactions (2003)
4. Dilesh Pardhi AnandKumar Patil,; "Risk Management In BOT Projects",; Thesis (2008)
5. Dr. M. J. Kolhatkar, Er. Amit Bijon Dutta,; "Study of Risk in Construction Projects", ;GRA (2013)
6. Ekaterina Osipova,;"Risk management in construction projects: a comparative study of the different procurement options in Sweden",; Thesis (2008)
7. F. Y. Y. Ling and L. Hoi,; "Risks faced by Singapore firms when taking construction projects in India," (2006)
8. Kinnaresh Patel M.E. (C.E.M.)*,; A study on risk assessment and its management in India,; AJCE (2013)
9. Mehmood Alam, Dr. Nadeem Ehsan, Ebtisam Mirza, Azam Ishaque,;"Risk Management in construction industry",;(2010)
10. A Study of Risk Management Techniques for Construction Projects in Developing Countries 142
11. Prof. Shakil S. Malek, Nazneen I. Pathan, Haaris Mal,; "Risk Management in Construction Industry",; IJAR (2013)
12. S. Q. Wang and M. F. Dulami,; "Risk management frame work for construction projects in developing countries," (2004)
13. Smith, N.J., Tony, M., and Jobling, P.,; Managing risk in construction projects, 2th ed: Blackwell Publishing (2006)
14. Soon Kim; Deepak Bejaj,; Risk management in construction: An approach for contractors in South Korea,; (2000)
15. Tsung-ChiehTsai, Min-LanYang,; "Risk assessment of Design-Bid-Build and Design-Build Building projects"; Journal of the Operations Research Society of Japan (2010)
16. Uher, T. E. & Toakley, A. R.; Risk management in the conceptual phase of a project.International Journal of Project Management (1999).
17. Zenghua Kuang,; "Risk Management in Construction Projects"; (2011)

IMPROVEMENT IN QUALITY OF DVR MANUFACTURING IN MATRIX COMSEC THROUGH ROOT CAUSE ANALYSIS

[1]Edward Bernard, [2]Gajanan S. Patange
[1]M.Tech Student, [2]Assistant Professor
Email:[1]Edwardbernard001@gmail.com, [2]gajananpatange.me@charusat.ac.in

Abstract— Making high quality and improving productivity has become increasingly critical role in industry and has been the focus of study by the researchers. From a practical perspective, how to measure quality and productivity suitably is important for a firm to determine whether the desired target is achieved. Here quality of Hard disk in video surveillance organisation has been improved using root causes analysis. Measuring quality and productivity improvement in an appropriate way has received widespread attention due to the vital role the customer satisfaction plays in gaining competitive advantages. Since quality and productivity improvement directly correlates with customer satisfaction, measuring quality and productivity that attempts to asses validity is a concern for many firms. A systematic procedure has to be developed for designing a framework for improvement of quality and productivity. This paper focus on a procedure is to improve the quality and productivity by establishing control procedures to ensure that the performance level does not fell below the desired level.

Index Terms — Productivity, Quality, Root causes analysis, Video surveillance.

I. INTRODUCTION

The pressure from globalization has made manufacturing organizations moving towards three major competitive arenas: quality, cost, and responsiveness. Quality is a universal value and has become a global issue. In order to survive and be able to provide customers with good products, manufacturing organizations are required to ensure that their processes are continuously monitored and product qualities are improved. Manufacturing Organization applies various quality control techniques to improve the quality of the process by reducing its variability. The main objective of this paper is to use quality tools to improve the level of quality management in an industry in the installation phase. First a diagnostic of quality management functions is made to identify priority areas for quality improvement, later quality tools are used to carry out effective actions to improve quality.

The surveillance industry continues to transition from analog to digital. This transition is taking place on two fronts — how the images are captured and how they are stored. The way surveillance images are stored has also changed from analog-based recording solutions — like VHS tapes and film — to digital storage on hard drives. As a result, most surveillance systems in place today make use of hard disks to store surveillance images digitally. With hard drive capacity doubling approximately every two

years and the cost per unit shrinking by 50% surveillance storage is less expensive, more efficient and progressively powerful.

Root causes Analysis (RCA) is a method of problem solving that tries to identify the root causes of faults or problems. A root cause is a cause that once removed from the problem fault sequence, prevents the final undesirable event from recurring. A causal factor is a factor that affects an event's outcome, but is not a root cause. Though removing a causal factor can benefit an outcome, it does not prevent its recurrence for certain.

II. ROOT CAUSES ANALYSIS IN MANUFACTURING

Root Cause Analysis (RCA) is a popular and often-used technique that helps people answer the question of why the problem occurred in the first place.
RCA seeks to identify the origin of a problem. It uses a specific set of steps, with associated tools, to find the primary cause of the problem, so that you can:

1. Determine what happened.
2. Determine why it happened.
3. Figure out what to do to reduce the likelihood that it will happen again.

RCA assumes that systems and events are interrelated. An action in one area triggers an action in another, and another, and so on. By tracing back these actions, you can discover where the problem started and how it grew into the symptom you're now facing.
You'll usually find three basic types of causes:

1. **Physical causes** – Tangible, material items failed in some way (for example, a car's brakes stopped working).
2. **Human causes** – People did something wrong, or did not do something that was needed. Human causes typically lead to physical causes (for example, no one filled the brake fluid, which led to the brakes failing).
3. **Organizational causes** – A system, process, or policy that people use to make decisions or do their work is faulty (for example, no one person was responsible for vehicle maintenance, and everyone assumed someone else had filled the brake fluid).

RCA looks at all three types of causes. It involves investigating the patterns of negative effects, finding hidden flaws in the system, and discovering specific actions that contributed to the problem. This often means that RCA reveals more than one root cause.
You can apply RCA to almost any situation. Determining how far to go in your investigation requires good judgment and common sense. Theoretically, you could continue to trace root causes back to the Stone Age, but the effort would serve no useful purpose. Be careful to understand when you've found a significant cause that can, in fact, be changed.
The Root Cause Analysis Process RCA has five identifiable steps.

A. *Step One: Define the Problem*

- What do you see happening?
- What are the specific symptoms?

B. *Step Two: Collect Data*

- What proof do you have that the problem exists?
- How long has the problem existed?
- What is the impact of the problem?

You need to analyze a situation fully before you can move on to look at factors that contributed to the problem. To maximize the effectiveness of your RCA, get together everyone – experts and front line staff – who understands the situation. People who are most familiar with the problem can help lead you to a better understanding of the issues.
A helpful tool at this stage is CATWOE . With this process, you look at the same situation from different perspectives: the Customers, the people (Actors) who implement the solutions, the Transformation process that's affected, the World view, the process Owner, and Environmental constraints.

C. *Step Three: Identify Possible Causal factors*

- What sequence of events leads to the problem?
- What conditions allow the problem to occur?
- What other problems surround the occurrence of the central problem?

During this stage, identify as many causal factors as possible. Too often, people identify one or

two factors and then stop, but that's not sufficient. With RCA, you don't want to simply treat the most obvious causes – you want to dig deeper.

Use these tools to help identify causal factors:

- Appreciation – Use the facts and ask "So what?" to determine all the possible consequences of a fact.
- **5** Whys – Ask "Why?" until you get to the root of the problem?
- Drill Down – Break down a problem into small, detailed parts to better understand the big picture.
- Cause and Effect Diagrams – Create a chart of all of the possible causal factors, to see where the trouble may have begun.

D. Step Four: Identify the Root cause (s)

- Why does the causal factor exist?
- What is the real reason the problem occurred?

Use the same tools you used to identify the causal factors (in Step Three) to look at the roots of each factor. These tools are designed to encourage you to dig deeper at each level of cause and effect.

E. Step Five: *Recommend and Implement Solutions*

- What can you do to prevent the problem from happening again?
- How will the solution be implemented?
- Who will be responsible for it?
- What are the risks of implementing the solution?

Analyze your cause-and-effect process, and identify the changes needed for various systems. It's also important that you plan ahead to predict the effects of your solution. This way, you can spot potential failures before they happen.

One way of doing this is to use Failure Mode and Effects Analysis (FMEA). This tool builds on the idea of risk analysis to identify points where a solution could fail. FMEA is also a great system to implement across your organization; the more systems and processes that use FMEA at the start; the less likely you are to have problems that need RCA in the future. Fig 1 :
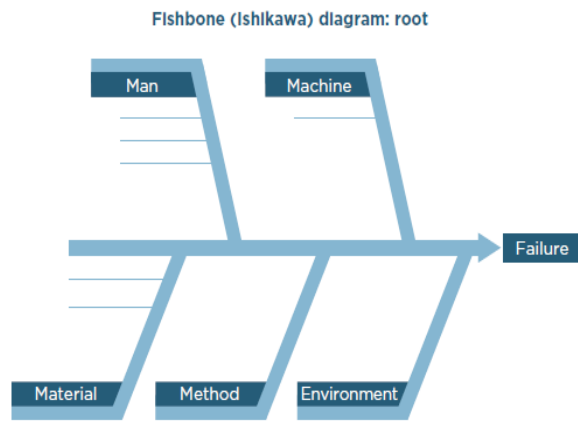

Fig. 1 The fishbone (Ishikawa) diagram is a tool for brainstorming root causes. (Source)

III. PROBLEM DEFINATION & METHODOLOGY

However, efficient and hard work by matrix comsec Private limited still there some issue arises. In their security sector specialize in SATATYA (video surveillance) facing some problem in hard disk failure issue. This paper focuses the work is to go through the problem and identify the more efficient way to solve the problem using quality control tools like root causes analysis and failure mode effect analysis.

Fig. 2 Camera of matrix comsec.

Hard disk plays an important role in video surveillance because if recording were properly not safe then it will become a big problem. So organization must provide an efficient tool so that this issue not rises on regularly bases.

I had visited the production unit of matrix comsec located in GIDC Wagodia Vadodara. I got the opportunity to talk the production manager and Quality manager. I had asked them some present quality level questionnaires and quality standards on which they do work.

A. Digital Video Recorder

DVR stand for Digital Video Recorder. Key function of a DVR is recording data into digital format within the mass storage drive.

DVR support Analog Camera recording with different functions such as Real-time recording/ Playback/ Backup/ Remote access Motion Detection/ Video Blind/ Video Loss/ PTZ HDD Management/ User Management.

Fig. 3 Interfacing Diagram.

B. Methodology

As in video surveillance, recording or CCTV footage is crucial for customer or consumer so below mention points are covered during this case study.

4.4.1 Symptoms

1. Device is restarting in regularly interval i.e. 2-3 times in a day. So recording is missing of that particular time.

2. Device is not getting up while we are providing proper power supply.

4.4.2 Root causes analysis

For 1st symptoms we do following analysis;

Take out hard disk and diagnose the hard disk log. So during diagnoses status of the hard disk shows "Error" and on that particular date and time event, system shows a restart event. So such type of error happens 2-3 times in a day we can conclude hard disk may be faulty or due to hard disk fault.

For 2nd symptoms we do following analysis;

Device is not getting up; we first remove the hard disk from the system and again start the system. After removing the hard disk if system gets starts then there are two check points that we need to check before any conclusion:

1. Hard disk: - If we use same power cable & different hard disk in the system and still system is not getting up then we can conclude that there is a problem in the hard disk.

2. Power cable: - If we use same hard disk & different power cable in the system and still system is not getting up then we can conclude that there is a problem in the power cable.
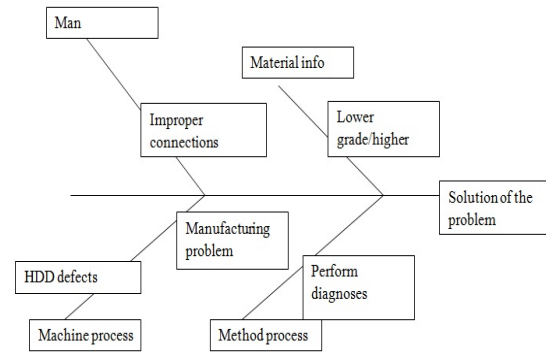

Fig. 4 using fishbone technique in Root causes analysis solution.

C. Conclusion

This study was started with the purpose of throwing light on the Importance of Quality in electronics manufacturing industry and implementation of Root causes analysis. This led to the concept that Root causes analysis is a quality-oriented approach and has effects on quality performance that are supported by leading studies. In this study it enables us to identify defects and generate the solution in easier way.

IV. RECOMMENDATION

After implementing Root causes analysis we have suggested the following points to the company so that they improve their product and get customer trust and satisfaction:-

1. Use special surveillance based hard disks which have high RPM range from 4200-7200

2 use special type of software to reduce HDD failure while writing the data into it.

3. Use better quality of power and SATA cable for hard disk (RJ-6),

4. If HDD fails then use data recovery software in order to get CCTV footage back from HDD.

Some products provide best solution for storage purpose. As company name Veracity has

developed a range of storage systems designed specifically for video surveillance. They are aimed particularly at storage of mega-pixel video and long-archive time applications.

The radical sequential storage approach of COLDSTORE produces amazing benefits including 90% power savings, increased disk reliability, reduced disk costs, simplicity, and even removable, playable disks. Designed specifically for long retention requirements.

Fig. 5 Surveillance storage systems

V. REFERENCES

[1]. ISO 9001:2008, Quality management systems Requirements, ISO, 2008.

[2]. K. Ishikawa, Guide to Quality Control. NY: Quality Resources, 1968.

[3]. J. Tarí, and V. Sabater, "Quality tools and techniques: Are they necessary for quality management?"Int. J. Production Economics, Volume 92, pp. 267–280, 2004.

[4]. G. Paliska, D. Pavletic and M. Sokovic, "Quality Tools - Systematic use in process industry", Journal of Achievements in Materials and Manufacturing Engineering, November 25(1), pp. 79–82, 2007.

[5]. Hundy Brian, A Brief History of Quality, Manufacturing Engineering Magazine, September, UK, p.p 48-52, 1991.

[6]. Lucas Manufacturing Systems Engineering Handbook, Lucas Engineering & Systems, Mini Guide, UK, 1988.

[7]. S. B. Merriam, Qualitative research and case study applications in education. San Francisco: Jossey-Bass, 1998.

[8]. H. Teixeira, I.S. Lopes and S. D. Sousa, "A methodology for quality problems diagnosis in SMEs", in proceedings of ICIESM 2012: Int Conf on Industrial Engineering and Systems Management, Paris, France, pp. 794–799,2012.

[9]. S. D. Sousa, E. M. Aspinwall, P. Sampaio and A. G. Rodrigues, "Performance measures and Quality Tools in Portuguese small and medium enterprises: survey results", Total Quality Management and Business Excellence, vol. 16, no. 2, pp. 277–307, 2005.

[10]. Antony, J. & Kaye, M. (1995). Experimental quality. Manufacturing Engineer, 74(4), pp.178- 181.

[11]. Chung, W.W.C., K.C.M. Wong & Soon, P.T.K. An ANN-based DSS system for quality assurance in production network. Journal of Manufacturing Technology Management. 18(7), pp. 836-857, 2007.

[12]. Tzu-Liang (Bill) Tseng, M.C. Jothi shankar, Tong (Teresa)Wu. Quality Control Problem in Printed Circuit Board Manufacturing, An Extended Rough Set Theory approach, Journal of manufacturing system vol23/1 2004.

[13]. Nipa S. Ouppara and Maria Victoria U. Sy. Quality of Work Life Practices in a Multinational Company in Sydney, Australia, Procedia- Social and Behavioral Sciences 40, 116 – 121, 2012.

[14]. Gulser Koksal, Inci Batmaz, Murat Caner Testik T. A review of data mining applications for quality improvement in manufacturing industry. Expert Systems with Applications 38, pp. 13448–13467, 2011.

COMPARISON OF TCP AND CBR IN AOMDV ROUTING PROTOCOL OVER MANET

[1]Abhilash Menon, [2]Meet Patel, [3]Krunal Patel, [4]Prof. Payal Mahida
Computer Science & Engineering department, Shri S`ad Vidya Mandal Institute of Technology
Email:[1]menonabhilash69@yahoo.co.in, [2]meet4226@yahoo.com, [3]patelkru06@gmail.com,
[4]payal_mahida@yahoo.co.in

Abstract

A MANET is a self-configuring network of mobile devices connected without wires. Routing protocols have a significant role in managing the transmission of data across these networks. In ,this paper we have evaluated the performance of AOMDV routing protocol which is a multipath distance vector routing protocol .This protocol has been selected due to its significant edge over other protocols in terms of delay, overhead etc. The assessment of AOMDV is done by obtaining the Packet Delivery Ratio, routing overhead and end to end delay for 10,20,30,40 and 50 node simulations using TCP as well as CBR with 10 distinct configurations for covering all possible conditions. The simulation has been done using NS-2.35.

Keywords: MANET, unipath, multipath, AOMDV, CBR, TCP, PDR, DELAY

1. Introduction

1.1 Mobile Ad hoc Networks

A MANET is a self configuring network of mobile devices connected without wires. It doesn't need much tangible infrastructure like routers, servers, cables etc. Each mobile machine functions as a node as well as a router. MANETs characteristics are distributed operation, multihop routing, autonomous terminal, dynamic topology, light weight terminals, shared physical medium and the applications range from high-performance military communication equipment for soldiers to PDA and Personal Area Networks.

1.2 Routing Protocols

A routing protocol specifies how routers communicate with each other, broadcasting information that enables them to select routes between any two nodes on a network. In ad hoc networks, nodes are not aware of the topology of their networks. Instead, they have to discover it. More importantly route construction is to be done with minimum resources i.e less overhead and bandwidth consumption. Basically the MANET routing protocols are classified into two major parts namely multipath and unipath[1].

1.2.1 Unipath Routing Protocols

The unipath routing protocols save a single route for a pair of source and destination. A route discovery is required in case of every route break which leads to high overhead and latency. The two parts of unipath routing protocols are i) Route Discovery: finding a route between a source and destination. ii) Route Maintenance: when routes are broken or new route is to be registered for the pair of source and destination in case of route failure. Some of the most popular unipath routing protocols are Ad Hoc On-demand Distance Vector (AODV), Dynamic

Source Routing (DSR), and Destination Sequenced Distance Vector (DSDV).

1.2.2 Multipath Routing Protocols

The multipath routing protocols discover multiple routes between a source and destination in order to satisfy Quality of Service (QoS) requirements. The three main parts of multipath routing protocols are *i) Route Discovery:* finding multiple routes which are node disjoint, link disjoint, or non-disjoint between a source and destination. *ii) Traffic Allocation:* Once the route discovery is done, the source will have selected a set of paths to the destination and then starts sending data to the destination along the paths. *iii) Path*

Maintenance: regeneration of paths after original path discovery in order to avoid link failures that happen over time and node mobility. The advantages of the multipath routing protocols are i) Fault tolerance: As redundant Information is routed to the destination via alternative paths, it reduces the chances of the disruption in transmission in case of link failures, ii) Load Balancing: selecting multiple traffic through different paths in order to avoid congestion in links, iii) Bandwidth aggregation: Splitting the data into various streams and then each of it is routed through a unique path to the same destination and iv) Reduced delay: In the unipath routing protocols, the path discovery procedure needs to be initiated to find a new route in the interest of avoiding a route failure and this leads to route discovery delay. This delay is reduced in multipath routing protocols as multiple routes have already been discovered and registered in the initial route discovery process. Currently the most popular multipath algorithms are Temporarily-Ordered Routing Algorithm (TORA) , Split Multipath Routing (SMR) , Multipath Dynamic Source Routing (MP-DSR) , Ad hoc On-demand Distance Vector-Backup Routing (AODVBR) and Ad Hoc On-Demand Multipath Distance Vector Routing (AOMDV)[1].

2. Traffic Patterns

CBR

The CBR service category is employed for connections that transport traffic at a constant bit rate. There is an inherent dependence on time synchronization between the traffic source and destination.

The characteristics of Constant Bit Rate (CBR) traffic pattern i) unreliable: as it has no connection establishment phase, there is no guarantee that the data will reach the destination, ii) unidirectional: there is no acknowledgment or conformation from the destination regarding the transmitted data and iii) predictable: it has fixed packet size, intervals and stream duration[2].

TCP

The characteristics of Transmission Control Protocol (TCP) are i) reliable: since connection is established before transmitting data, there is a guarantee that the data will be transmitted to the destination, ii) bi-directional: each packet that is transmitted by the source will be acknowledged by the destination upon arrival of the data iii) conformity: there is flow control of data to avoid overloading the destination and congestion control mechanism exists to shape the traffic in order to conform it to the available network capacity. Today most of the Internet Protocol traffic is carried out through TCP[2].

3. AOMDV Routing Protocol

AOMDV is similar to AODV in many ways. It is based on the distance vector routing concept and uses hop-by-hop approach. Moreover, AOMDV

also finds routes on demand. The main difference between AODV and AOMDV lies in the number of routes found in each route discovery[1]. In AOMDV,

RREQ propagation from the source to the destination creates multiple reverse paths at intermediate nodes and the destination. Multiple RREPs traverse these reverse paths back in order to form many forward paths to the destination at the source as well as intermediate nodes.

AOMDV also provides alternate paths to intermediate nodes as they are useful in reducing route discovery frequency.

The distinguishing feature of the AOMDV protocol lies in making sure that multiple paths discovered are loop-free and disjoint, and in finding such paths using a flood-based route discovery. AOMDV route update rules which are applied locally at each node, play a significant role in maintaining loop-freedom as well as disjointness [1]. AOMDV relies mostly on the routing information already accessible in the underlying AODV protocol, thereby limiting the overhead caused due to multiple path discovery. In particular, it does not use any special control packets. In fact, extra RRERs and RREPs for multipath discovery and maintenance and a few extra fields in routing control packets (i.e., RRER,RREQs, and RREPs) are the only additional overhead in AOMDV compared to AODV.

4. Simulation Parameters
Table 1

Parameter	Value
Simulator	NS-2.35
Mac Type	802.11
Simulation time	60 seconds
Channel Type	Wireless
Routing Protocol	AOMDV
Antenna Model	Omni
Simulation Area	800m X 800m
Traffic Type	tcp, cbr
Interface Queue Length	50
Interface Queue Type	Droptail/priqueue
Number of Nodes	10,20,30,40,50

5. Performance Metrics

Performance Metrics are measures that are used to evaluate MANET routing protocols and to understand their functionality at a deeper level by obtaining their performance values. We have considered the following four metrics in order to evaluate AOMDV with two traffic types CBR and TCP.

5.1 Packet delivery fraction(PDR)

The ratio of the number of data packets delivered to the destination to the number of data packets sent is known as the Packet Delivery Ratio(PDR)

Packet Delivery Ratio= (no. of packets received/number of packets sent) X 100.

5.2 Average Throughput

Average Throughput is the number of bytes received successfully at the destination

Average Throughput = (number of bytes received X 8/simulation time X 1000) kbps

5.3 Routing Overhead

Routing Overhead is the number of control packets generated by the router during simulation.

Routing Overhead = number of control packets

5.4 Average End to End Delay

End to End delay is the average time taken by a packet to arrive at the destination including all kinds of delay caused like the route discovery delay and the queued packet delay. Only the packets that have reached thee destination are counted.

Average End to end delay = $\sum$ (arrive time – send time) / $\sum$ Number of connections

6. Results and Discussion
6.1 Packet Delivery Ratio
Table 2

PACKET DELIVERY RATIO		
Number of nodes	TCP	CBR
10	97.486	62.446
20	95.261	60.666
30	96.098	65.200
40	90.032	60.860
50	97.320	58.190

Table 2 shows the average readings of all five node configurations and we can clearly see that using TCP traffic a better Packet Delivery Ratio can be achieved.
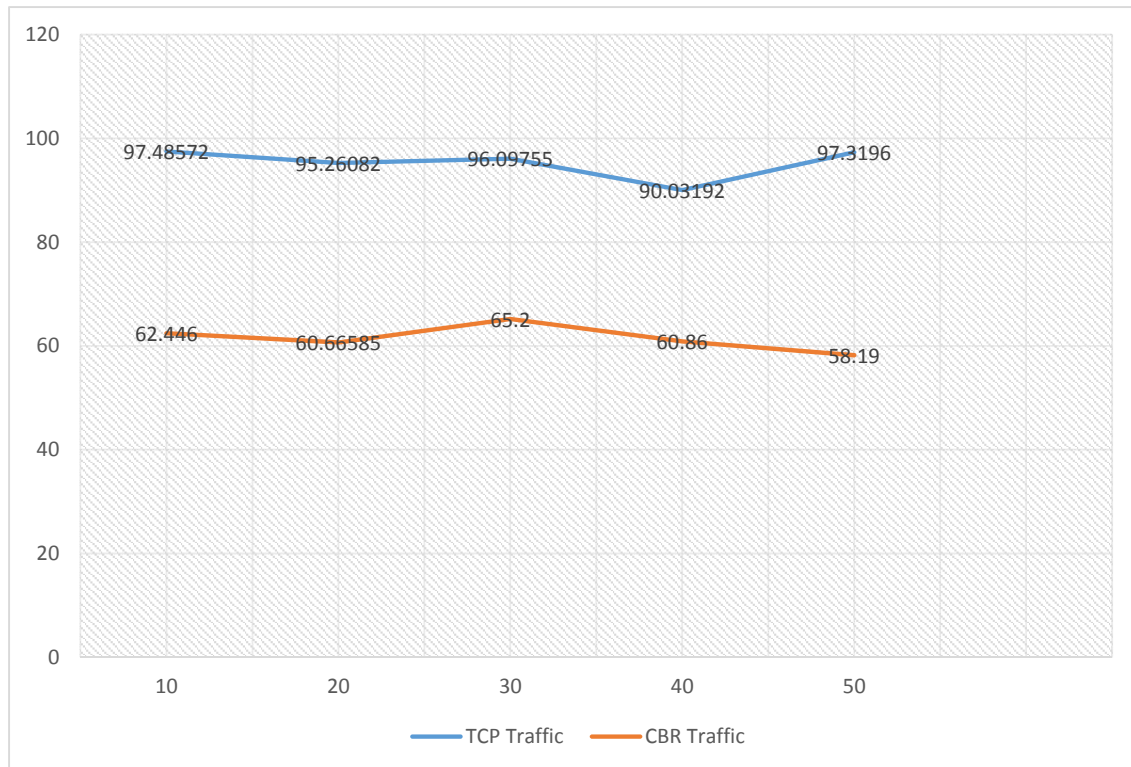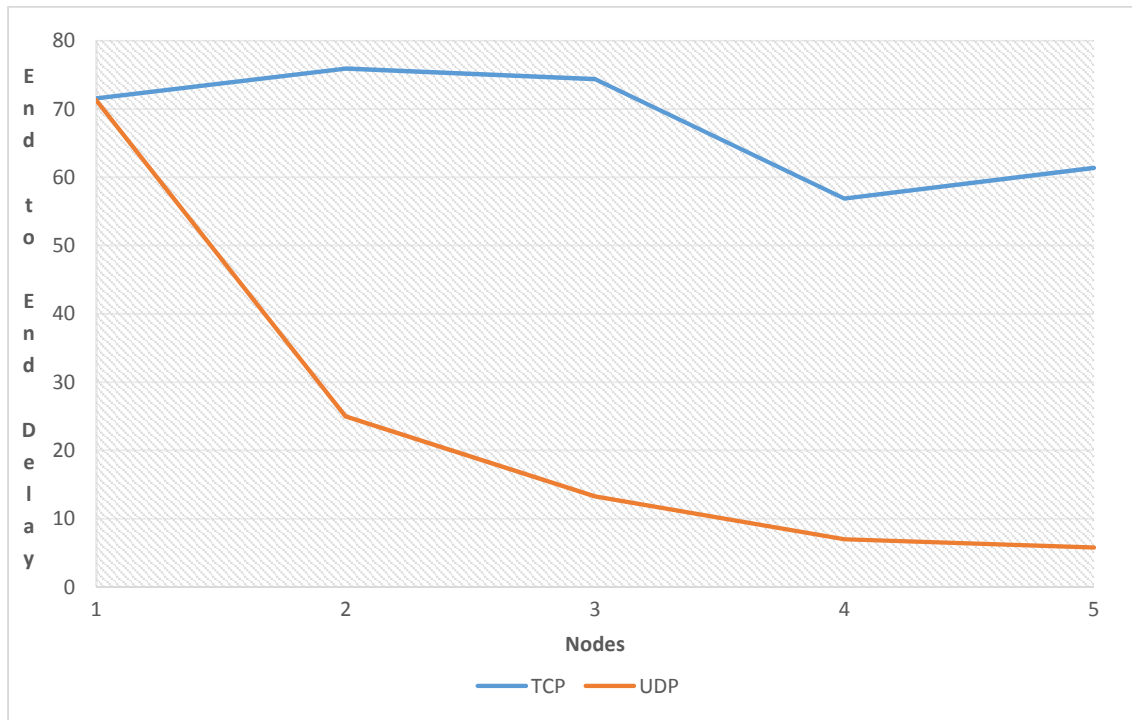

### 6.4 Average End to End Delay

Table 3

Average End to End Delay		
Number of nodes	**TCP**	**CBR**
10	71.561	71.284
20	75.930	24.972
30	74.385	13.266
40	56.880	6.981
50	61.373	5.771

Table 3 highlights the advantage of cbr traffic as lower delay is achieved and this helps in faster data transmission which is a necessary aspect for certain networks.
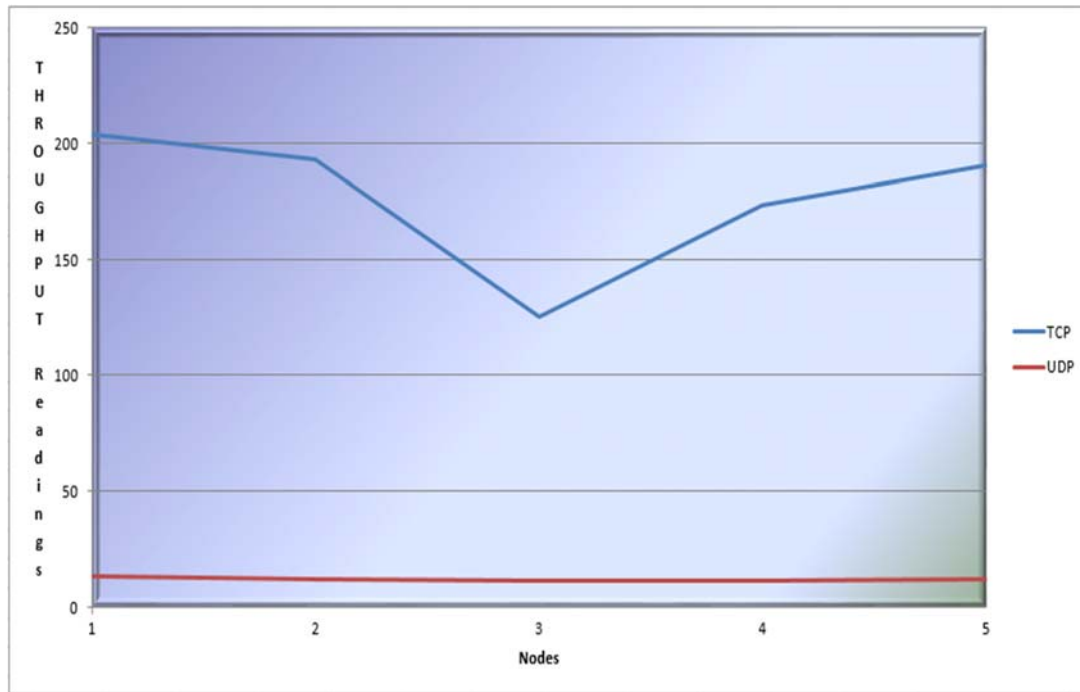
6.5 Routing Overhead

Average Overhead		
Number of nodes	**TCP**	**CBR**
10	3.512	11.835
20	21.524	49.689
30	28.795	116.199
40	1687.386	234.390
50	31.4772	333.490
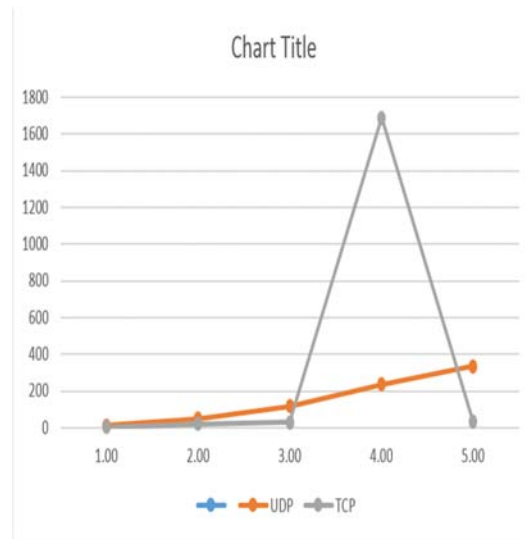
6.6 Throughput

Average Throughput		
Number of nodes	**TCP**	**CBR**
10	204.192	13.81
20	193.056	12.536
30	125.318	11.389
40	173.545	11.68
50	191.011	12.332

References

[1] Ad hoc on-demand multipath distance vector routing. Mahesh K. Marina1 and Samir R. Das2

[2] Performance evaluation of AOMDV based on various traffic patterns and scenarios. Neetika Bhardwaj and Rajdeep Singh

COMPUTATION OF POWER FOR A NEW CITY

[1]Neha Srivastava, [2]Dr.B.R. Parekh, [3]Keval Velani
[1]M.E. Student, BVM Engineering College,
[2]HOD, BVM Engineering College,
[3]Design Engineer, Takalkar Power Engineers Consultancy & Ltd.
Email:[1]er.neha00510@gmail.com, [2]brp_bvm@yahoo.co.in, [3]keval.velani@tpec.in

Abstract— This paper describes the Electrical Power Computation of a new city. A model for Computation of power demand has been presented here based on the available data of average power consumption or demand of various categories of consumers at already existing city. The area under study is Dholera located in Gujarat, India. The load demand has been calculated based on the type of various categories of load divided as per the town planning scheme of the city considering the load factor and diversity factor. Also, Weighted Arithmetic Mean (WAM) methodology has been incorporated in the calculations for the power computation of mixed plots. Based on this model, the power demand of TP2E of Dholera city would be 960.77MVA which would be supplied with a 400kVMRSS and three 220kV Substations through H.T cables.

Index Terms— Diversity factor, Dholera (TP2E), Load Prediction, Load demand, Load Factor, Power computation, WAM (Weighted Arithmetic Mean).

I. INTRODUCTION

Electrical Load Prediction is the estimation for future load by an electrical utility. Prediction of load is an important and central process in the planning of transmission and distribution system. Load forecasting is vitally important for the electric utilities in the deregulated economy. It involves the accurate prediction of both the magnitudes and geographical locations of electric load over the different periods of the planning time [1]. Accurate power demand prediction holds a great saving potential for electric utility corporations. The accuracy of load prediction has a significant effect on power system operations, as economy of operations and control of power systems may be quite sensitive to errors due to load prediction. The present scenario of various cities power demand is raising an alarming issue. The inaccurate load prediction is leading to many problems [2]. Some of them are:

- Overloading
- Instability in the system
- Power cuts and power shortage
- Power theft
- High dependency on Conventional sources of Energy
- Increased amount of CO_2 in the atmosphere due to losses in distribution system
- Poor reliability and safety issues

These are just few to be listed out. All these result in load shedding and blackouts. So there is need of proper estimation of load demand so that even if the demand increases in the nearby future the city doesn't fail to supply the same or cope up with it.

II. STUDY AREA

The study area is a part of Dholera Special Investment Region (DSIR) which will be a new Industrial hub located around 100km south of Ahmedabad and around 130km from

Gandhinagar. The DSIR covers an area of about 920sq.km.and contains 19 villages of Dhandhuka Taluka and 3 villages of 3 Barwala Taluka; total 22 villages of Ahmedabad district, making it the largest investment nodes proposed so far in the Delhi-Mumbai Industrial Corridor (DMIC) influential area. The site is strategically situated between the main industrial centres of Surat, Vadodara, Ahmedabad, Bhavnagar and Rajkot. It is linked to the major ports of Gujarat by State Highways but yet has no direct rail connection [12].

The study area of this project, however, is Town Planning 2East [TP2E]. The figure shows the area of TP2E. It covers an area of about 57sq.km.

Fig.1 TP2E Area (Study area)

Now Dholera is being named under the "Smart City" of India. So it will require bulk amount of power for its infrastructure and development. So load prediction for this city needs to be computed considering the increase in power demand in the nearby future with all the smart technologies and smart appliances being used. Thus a proper system for power computation is required for such a city that not only fulfils the present power demand but also of future thus taking a sustainable development approach.

Thus, the main objective of the paper is to compute the load demand or do the load forecasting of the city in a way that it not only meets the present demand of the system but also its future demand without compromising the needs of future expansion. The system designed on such a basis will be reliable and healthy so that during any contingency it will be able to supply the same required power without any failure.

III. POWER COMPUTATION

A. *Various categories of plots as per usage according to the town planning*

The town planning map provides clues to the establishments which are planned in a given area. The total plots involved in TP2E are classified in various categories [12]:

- Residential
- High Access Corridor
- Industrial
- Recreation, Sports and entertainment.
- Strategic Infrastructure
- Roads
- Public Facility Zone
- Tourism and Resorts
- Village Buffer
- Original Village (Gamtal)
- River/Water Body
- Coastal Region Zone

Again, as these individual categories have mixed type of usage (i.e. total area of every type of plot is subdivided under different land use) defined as under.

Residential

Residential plots consist of Residential, Commercial office/Retail, Leisure and hospitality, Public/Community facility, Local Public open space, local roads, utilities and Information Communication Technology Devices usage.

High Access Corridor

High Access corridor plots consist of Residential, Commercial office/Retail, Leisure and hospitality, Public/Community facility, Local Public open space, local roads, utilities and Information Communication Technology Devices usage.

Industrial

Total Industrial plots are primarily divided into actual industry type as per Development Plan (DP) report [12]. The bifurcation is as follows.

Table I Different types of industries considered in industrial load prediction

Sr.no.	Types of Industries	% of plot
1	General manufacturing	5.37
2	Electronics	16.59
3	Automobile	24.27
4	Agro & Food processing	4.15
5	Heavy Engineering	27.44
6	Metal & Metallurgical Products	5.85
7	Pharmaceutical & Biotechnology	13.66
8	Logistics	2.67

Again, industrial plots consist of Industrial, Public/Community facility, Local Public open space, local roads and Information Communication Technologies Devices usage.

Recreation, Sports and Entertainment

Recreation Sports and Entertainment plots consist of Leisure and hospitality, Local Public open space, Recreation Sports & Entertainment, local roads, Utilities and Information Communication Technology Devices usage.

Strategic Infrastructure

Strategic Infrastructure plots consist of residential, commercial office/Retail, Industry, Leisure and hospitality, Public/Community facility, Recreation Sports and Entertainment, Utilities and Information Communication Technology Devices usage.

Roads

Roads consist of Residential, Commercial offices/Retails, Leisure and hospitality, Public/ Community facilities, Local Public open space, local roads, Utilities and Information Communication Technology Devices usage.

As per the categories of usages or plots, the power consumption for different purposes like lightning load, power load, workstation load, HVAC load, lifts load and load for common

area/parking are calculated. The power consumption for different usage is then calculated using individual load factor for each type of usage [3]-[17]. The data used here is of Vadodara city using the confidential data collected from various places and MGVCL (Madhya Gujarat Vij. Company Limited).

Table II- Load demand of various categories of load considering load factor

Type of usage	Power consumption (watt/sq.m)
Residential	46.10
Commercial Offices/Retail	124.80
Leisure/Hospitality	83.80
Light Service Industry	31.40
Industry	151.90
Education	50.00
Public Facility/ Community Facility	20.00
Local Public Open Space	3.00
Recreation Sports & Entertainment	40.30
Roads	2.00
Utilities	2.00

IV. COMPUTATION OF POWER FOR MIXED PLOTS

Next step was calculation of power consumption of mixed plots. Mixed plot means an area covered by two or more types of plots. For example a plot shared by residential as well as public facility zone is computed under mixed plot. The percentage of mixed plotting is as per the town planning scheme.

Built up area (BUA) of each plot was calculated baesd on the town planning scheme and same is calculated based on Floor Space Index (FSI) norms. It is uncertain that particular plot will be dedicated for the specific purpose at the stage of load forecasting. Hence, it is difficult to calculate the Wattage per square meter based on specific use of individual plot. It is better to calculate the Wattage per Square meter on the

basis of mixed plot usage and same can be arrived by working a methodology of Weighted Arithmetic Mean. The method used here is Weighted Arithmetic Mean (WAM).For example assume a Residential zone which is allotted for 54% residential, 2% commercial offices, 1 % leisure & hospitality, 10% community, 10% local public open space, 22% local roads, 1% utilities. Let the total sq.m area under residential be denoted by "Y".

Uniform Watt/sq.m by means of Weighted Arithmetic Mean (WAM) =

(54%*Y*46.1+2%*Y*124.8+1%*Y*83.8+ 10%*Y*20+10%*Y*2+22%*Y*2+1%*Y*2)/Y

Same way the power consumption for every other plot is calculated and has been summarized in the table below

Table III Load demand after considering mixed type of plots

Type of usage	Power demand (watt/sq.m.)
Residential	30.89
High access corridor	32.75
Industrial	120.96
Recreation Sports and Entertainment	43.13
Strategic Infrastructure	32.95
Roads	2.00
Public facility zone	26.68
Tourism & resorts	58.27
Village buffer	26.45
Gamtal	46.10
River / water body	2.00
Coastal region zone	0.16

The power consumption varies at day and night time. It depends on the type of usage system and the amount of power consumed. For example, a public facility area may need power from morning till evening whereas an industry will need power for the whole day round. For this purpose, diversity factor was used to calculate the total power consumption of the whole area. The Power consumption was calculated as:

$$\text{Total Power Demand (MW)} = \frac{\text{Diversity Factor} \times \text{Power Demand obtained from mixed plots}}{\text{Total area covered by that usage} \times \text{land use factor}}$$

Thus the total power consumption of TP2E considering the diversity factor is as shown in the Table 5 below.

Table IV Total Power Consumption without Considering Diversity Factor

Areas	Power Demand (MW)
Residential Zone	86.92
High Access Corridor	6.13
Industrial Zone	293.61
Recreation, Sports & Entertainment	200.91
Strategic Infrastructure	1.32
Public facility zone	2.82
Tourism & Resorts	115.81
Village buffer	9.31
River / Water Body	0.30
Coastal Region Zone	0.25
Total Wattage (MW)	717.38
METRO Rail & Other Miscellaneous Power Consumption (MW)	25.00

V. TOTAL POWER DEMAND USING DIVERSITY FACTOR

Table 5 Total load demand of TP2E after considering diversity factor

12 -- 8	8 -- 11	11 -- 6	6 -- 12	12 -- 8	8 -- 11	11 -- 6	6 – 12
Group Diversity Factor Considered				**Demand After Considering Group Diversity Factor**			
0.6	0.8	0.7	0.8	52.15	69.54	60.84	69.54
0.5	0.6	0.6	0.8	3.06	3.68	3.68	4.90
0.5	0.9	0.9	0.6	146.80	264.25	264.25	176.17
0.2	0.6	0.4	0.8	40.18	120.55	80.37	160.73
0.6	0.8	0.8	0.6	0.08	0.11	0.11	0.08
0.2	0.9	0.9	0.6	0.56	2.54	2.54	1.69
0.3	0.9	0.4	0.8	34.74	104.23	46.33	92.65
0.3	0.5	0.6	0.5	2.79	4.66	5.59	4.66
0.6	0.4	0.4	0.6	0.18	0.12	0.12	0.18
0.8	0.6	0.6	0.9	0.20	0.15	0.15	0.22
Total				280.76	569.81	463.96	510.82

Thus, the total maximum demand after considering diversity factor is 569.81 or 570MW.

The total load demand in MVA considering 0.85 power factor and taking load 10% higher than of that of actual (742.38MW) is computed as **960.77MVA**

VI. DISTRIBUTION PLANNING AS PER THE LOAD DEMAND

So according to the calculated load demand, a 400kV Main Receiving Substation (MRSS) will be required. As per the load demand and the major roads connecting the various plots, the whole area has been divided into clusters. There were 24 clusters that were formed as per the major roads connecting the plots.
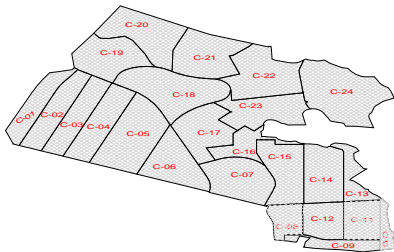

Fig.2 Cluster distribution of TP2E

The power consumption of each cluster is as shown below:

Table VI Power Consumption of Various Clusters

Cluster number	Power consumption in MVA (@ 10% rise)
1	48.418
2	61.78
3	36.27
4	68.78
5	111.21
6	61.99
7	44.52
8	16.31
9	12.17
10	6.01
11	24.19
12	25.19
13	11.65
14	34.79
15	37.12
16	12.73
17	30.29
18	60.24
19	18.15
20	25.09
21	27.06
22	47.62
23	38.07

24	68.88
25 (Metro)	32.35
Total	**960.77**

The power computation of each cluster has been done and these clusters were merged to form zones. Each zone will be requiring 220/66kV substation. Cable lines will be required to supply the same power through 400/220/66/11kV substation.
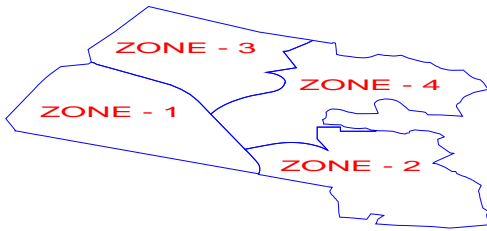

Fig.3 Zone distribution after merging various clusters

Table VII Zone Wise Power Consumption

Zone number	Power consumption in MVA (@ 10% rise)
1	388.25
2	212
3	130.56
4	197.61
Total	(928.41+32.35)=**960.77**

All the 220/66kV substations will be interconnected to form a Ring Main. The industrial load will be fed through 66/11kV feeders depending upon the predicted load of the plots.

VII. CONCLUSIONS

It is concluded that based on demand supply matrix of various categories of consumers in existing cities, the comprehensive planning of power infrastructure for a new upcoming city may be computed. A model for such computation for upcoming city at Dholera is presented. The load demand has been computed taking ten percent higher margin as it would be prudent keeping in view of increase in future demand. Based on this model, the power demand of TP2E of Dholera city would be 960.77MVA which would be supplied with a 400kVMRSS and three 220kV Substations through H.T cables.

REFERENCES

1) H.L.Willis, "Distribution load forecasting", IEEE Tutorial course on power distribution planning, EHO 361-6-PWR, 1992.
2) Andrew P. Douglas, Arthur M. Breipohl, "Risk Due To Load Forecast Uncertainty in Short Term Power System Planning" IEEE Transactions on Power Systems, Vol. 13 No. 4, November, 1998.
3) Energy Audit Report, Dec 2010 , by: Tracy Willcoxon; CEM, CEA, CIAQP, LEED AP Office of Energy Services and Sustainability (ESS)

4) The Ohio State University Facilities Operation and Development

5) Improving industrial audit analyses by Barney L. Capeha,Lynne C. Capehart, University of Florida EADC /IAC

6) Energy Management in Hospitality: a Study of the Thessaloniki1 Hotels by Soultana(Tania)Kapiki at Economics And Organization Of Future Enterprise 1/2010

7) Energy systems optimization of a Shopping mall by Aristotelis Giannopoulos ,26/09/08

8) Reduction of total energy consumption in hospitals by Trond Thorgeir Harsem in June 2010

9) Energy Consumption In Non-Domestic Buildings: A Review of Schools Richard A.R. Kilpatrick,*, Phillip FG. Banfill1 1 Heriot-Watt University, Edinburgh, Scotland ,EEE.8-11 may 2011

10) Energy Efficiency Solutions Energy audit of the hotel

11) Energy Conservation in Commercial Complexes by Electrical India Vol. 47 No. 10 October 2007

12) Energy cost & consumption in a Large Acute Hospital byS.C. Hu, J.D. Chen and Y.K. Chuah Department of Air-Conditioning and Refrigeration Engineering, National Taipei University of Technology Taiwan International Journal on Architectural Science, Volume 5, Number 1, p.11-19, 2004

13) Draft Development Plan Report-DSIRDA, September 2012Abdel-Moamen M. A., IEEE Member

14) https://www.electricireland.ie/ei/residential-energy-services

15) http://www.torrentpower.com

16) https://www.sldcguj.com/

17) http://www.fypower.org/com/bpg/view.html?b=hotels&m=Planning_an_Energy_Program&s=Energy_Audits

18) http://www.pge.com/mybusiness/energysavingsrebates/analyzer/

BER PERFORMANCE ANALYSIS OF MIMO-OFDM SYSTEM USING EQUALIZER

Rohini S. Shiranal[1,]Sudhirkumar.S.Dhotre[2]
[1] P.G.Student [2]Associate Professor,
NageshkarajgiOrchid College of Engineering & Technology, Solapur. Maharashtra.
Email:[1]rohini.b84@gmail.com

ABSTRACT: MIMO-OFDM (multiple input and multiple output orthogonal frequency division multiplexing) system is a new wireless broadband technology which has gained great popularity for its capability of high rate transmission and its robustness against multipath fading. Fading effects are the major effects to be considered at the receiver. Fading effects must be mitigated at the receiver before demodulation by using equalization techniques. Equalizer is used to allow recovery of the transmit symbols, which
.

is the major factor responsible for the Bit Error Rate (BER). In this paper Zero Forcing equalization and Minimum Mean Square Error equalization techniques are presented for reduction in bit error rate for the BPSK modulation technique. The performance is evaluated in terms of BER versus SNR. The performance of MIMO-OFDM system is evaluated by using different equalizers.
Key words: MIMO, OFDM, BER, ZF and MMSE EQUALIZERS

1. INTRODUCTION: In wireless communication technology the main objective is to provide high quality of data. Orthogonal frequency division multiplexing (OFDM) has become a more popular technique for transmission of signals over wireless channels. In OFDM, signals are transmitted in sub-channel of different frequency in parallel fashion. The frequency of sub-channel are so selected that these frequencies are orthogonal to each other and therefore do not interfere with each other. This phenomenon makes it possible to transmit the data in overlapping frequency and hence reduces the bandwidth requirement considerably. OFDM is beneficial in many aspects such as high spectral efficiency, robustness, low computational complexity, frequency selective fading, and easy to implementation using IFFT/FFT [1]. In wireless communication systems the data bits are transmitted in radio space, channels are typically multipath fading channels, which causes inter

symbol interference (ISI) in the received signal. ISI is undesirable and it increases bit error rate. ISI causes due to multipath propagation and band limited channels. Whenever the modulation bandwidth exceeds the radio channel coherence bandwidth, ISI is produced. To eliminate ISI from the signal, strong equalizers are used, which requires channel impulse response (CIR) [2]. Equalizer compensate the inter symbol interference means it works in such a way that BER should be low and SNR should be high [3]. Equalization techniques have importance to design of high data rate wireless

systems. Most of the wireless receivers are equipped with the equalizer which gives good result. The quality of wireless communication depends upon the three parameters i.e. rate, range and reliability of transmission. These parameters are related with each other. Simultaneous improvement in all three parameters can be accomplished with the help of

new technique called MIMO assisted OFDM system. Now a day's integration of OFDM technique with MIMO system has been an area of interesting in the field of broad band wireless communication. MIMO is a frequency-selective technique. OFDM can be used to convert such a frequency-selective channel into set of parallel frequency-flat sub channels. MIMO-OFDM system can achieve reliable high data rate transmission over broad band wireless channel [4]. BPSK modulation technique is used in MIMO-OFDM system to evaluate the BER performance.

2. System model
A). OFDM System Model:
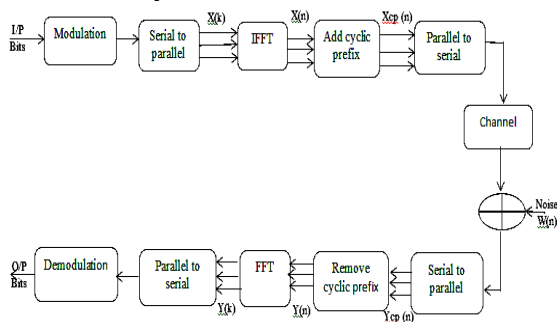
Fig. 1. Block Diagram of a Baseband OFDM transceiver System

Figure. 1 represents the basic block diagram of OFDM [5][6] system. It consist of transmitter and receiver sections, named OFDM transceiver system. The data bits inserted from the source are firstly mapped with BPSK modulation technique and after that converted from serial to parallel through convertor. Now N subcarriers are there and each sub-carrier consists of data symbol X(k) (k=0,1,….,N-1), where k shows the sub-carrier index. These N subcarriers are provided to inverse fast Fourier transform (IFFT) block. After transformation, the time domain OFDM signal at the output of the IFFT [6][7] can be written as:

$$x(n) = \sum_{k=0}^{N-1} X(k)\exp(\frac{j2\pi kn}{N}) \quad ………..……(1)$$

where, n is the time domain sample index of an OFDM signal. After that, Cyclic Prefix (CP) [8] is added to mitigate the ISI effect. We get signal $\mathbf{x}_{cp}$ (n), which is sent to parallel to serial convertor again and then, this signal is sent to frequency selective multi-path fading channels [6][9] and a noisy channel with independent and identically distributed (i.i.d.) AWGN noise. The received signal can be given by

$$y_g(n) = x_g(n)*h(n)+w(n), \quad …………\;(2)$$
$$0 \quad \leq \quad n \quad \leq \quad N\text{-}1$$

W(n) i.i.d. additive white Gaussian noise sample and h (n)is the discrete time channel impulse response (CIR).

At the receiver, firstly serial to parallel conversion occurs and cyclic prefix removed. After removing the CP, the received samples are sent to a fast Fourier transform (FFT)block to de-multiplex the multi-carrier signals. Then the output of the FFT [6] in frequency domain signal on the kth receiving subcarrier can be expressed as:

$$y(k) = \frac{1}{N}\sum_{n=0}^{N-1} y(n)\exp(\frac{-j2\pi kn}{N})$$
$$= X(k)H(k)+W(k)\;0 \leq k \leq \text{N-1}……(3)$$

where, W(k) is noise in time domain and H(k) is the channel frequency response.

B). MIMO system model: Multiple antennas can be used at the transmitter and receiver. This arrangement is called a multiple input multiple output (MIMO) system. In MIMO system there is a channel/path between each of the transmitters and each of the receiver antennas [10].Uncorrelated received signal can achieved by keeping well spacing between the transmitter and receiver. In this paper 2×2 MIMO system is used.
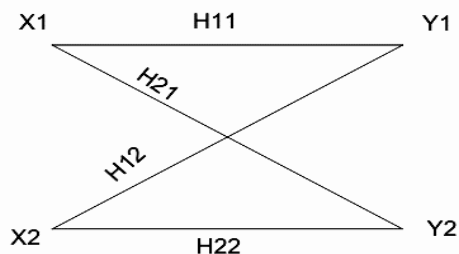

Fig.2 Channel matrix

The channel matrix is given by

$$[H] = \begin{bmatrix} H_{11} & H_{12} \\ H_{21} & H_{22} \end{bmatrix}$$

If X represents the transmitted signal from transmitted antenna and R represents the received signal, then the transmitted samples go through the multipath channel and would reach at the receiver. This could represented as,

$$R = HX + n$$

Where n is the noise.

3. CHANNELDESCRIPTION:-

Rayleigh fading channel is used in this paper.

Rayleigh fading is a statistical model for the effect of a propagation environment on a radio signal, such as that used by wireless devices. Rayleigh fading models assume that the magnitude of a signal that has passed through such a transmission medium (also called a communications channel) will vary randomly, or fade, according to a Rayleigh distribution. Rayleigh fading is the effect of heavily built-up urban environments on radio signals.[12][13] Rayleigh fading is most applicable when there is no dominant propagation along a line of sight between the transmitter and receiver. If there is a dominant line of sight, Rician fading may be more applicable. The Rayleigh distribution is basically the magnitude of the sum of two equal independent orthogonal Gaussian random variables and the probability density function(pdf) is given by:

$$p(z) = \frac{z}{\sigma^2} e^{\frac{-z^2}{2\sigma^2}}, z \geq 0 \quad \ldots\ldots\ldots\ldots(4)$$

Where σ^2 is the time-average power of the received signal and eq. (4) is called Probability density function.

4. SIGNAL DETECTION OF MIMO-OFDM SYSTEM

MIMO-OFDM detection methods consist of linear and nonlinear detection methods. We are using only linear detection methods in this paper

A) Zero Forcing Equalizer: -

This is a linear equalization algorithm used in communication systems, which inverts the frequency response of the channel at the receiver to restore the signal before the channel [11]. ZF algorithm considers as the signal of each transmitting antenna output as the desired signal, and consider the remaining part as a disturbance, so the mutual interference between the different transmitting antennas can be completely neglected. ZF equalizers ignore the additive noise and may considerably amplify noise for channels with spectral nulls.

Mathematical expression of sub-channel in the MIMO-OFDM system is as follows:

$$R(K) = H(K).X(K)+ n(k)\ldots\ldots\ldots\ldots.(5)$$

Where, $R(k)$, $X(k)$ and $n(k)$ respectively expresses output signal, the input signal and noise vector of the (k) sub-channels in MIMO-OFDM system. The relation between input $X(k)$ and output signal $R(k)$ as in eq. (5) exploits that this is a linear equalizer. A ZF detection algorithm for MIMO OFDM is the most simple and basic algorithm, and the basic idea of ZF algorithm is kept of MIMO-channel interference by multiplying received signal and the inverse matrix of channel matrix. Zero- Forcing solution of MIMO-OFDM system is as follows:

$$X_{ZF} = H^{-1}R = x + H^{-1}n \quad \ldots\ldots\ldots\ldots.(6)$$

in which H^{-1} is the channel matrix for the generalized inverse matrix.

B) Minimum Mean Square Equalizer: - MMSE equalizer is a more balanced linear equalizer that does not eliminate ISI entirely but minimizes total noise power and ISI components in the output. In wireless communications, MMSE equalizer approach minimizes the mean square error (MSE), which is a common measure of estimator quality. Let X is an unknown random variable, and let Y is a known random variable. An estimator $\breve{X}_y$ is any function of the measurement Y, and its MSE is given by

$$MSE = E\{(\breve{X} - X)^2\} \quad \ldots\ldots\ldots\ldots(7)$$

where, the expectation is taken over both X and Y. When it is not possible to determine a closed form for the MMSE equalizer then minimize the MSE within a particular class, such as the class of linear equalizers. Assuming the case where two symbols are interfered with each other. In the first time slot, the received signal on the first receive antenna is,

$$y_1 = h_{1,1}x_1 + h_{1,2}x_2 + n_1 = [h_{1,1}\, h_{1,2}]\begin{bmatrix} x_1 \\ x_2 \end{bmatrix} + n_1$$

$$y_2 = h_{2,1}x_1 + h_{2,2}x_2 + n_2 = [h_{2,1}\, h_{2,2}]\begin{bmatrix} x_1 \\ x_2 \end{bmatrix} + n_2$$

In matrix form, the above equation can be expressed as:

$$\begin{bmatrix} y_1 \\ y_2 \end{bmatrix} = \begin{bmatrix} h_{1,1}\, h_{1,2} \\ h_{2,1}\, h_{2,2} \end{bmatrix} \begin{bmatrix} x_1 \\ x_2 \end{bmatrix} + \begin{bmatrix} n_1 \\ n_2 \end{bmatrix}$$

The above wireless channel is modulated by the theorem $Y = H x + n$. The MMSE approach tries to find a coefficient W which minimizes the criterion,

$$E\{[W_{y-x}][W_{y-x}]^H\}$$

To solve X we need to find a matrix W which satisfies WH =1. The MMSE equalizer for satisfying this constraint is given by,

$$W = [H^H H + N_0 I]^{-1} H^H \qquad \text{--------- (8)}$$

Where, W- equalization matrix and H- channel matrix.

5. BIT ERROR RATE (BER):- In digital transmission, the number of bit errors is the number of received bits of a data stream over a communication channel that have been altered due to noise, interference, distortion or bit synchronization errors. The bit error rate or bit error ratio (BER) is the number of bit errors divided by the total number of transferred bits during a studied time interval.

The bit error rate or bit error ratio (BER) is defined as the rate at which errors occur in a transmission system during a studied time interval. BER is a unit less quantity.

6. SIGNAL TO NOISE RATIO (SNR):- There are a number of ways in which the noise performance, and hence the sensitivity of a radio receiver can be measured. The most obvious method is to compare the signal and noise levels for a known signal level, i.e. the signal to noise (S/N) ratio or SNR. Obviously the greater the difference between the signal and the unwanted noise, i.e. the greater the S/N ratio or SNR, the better the radio receiver sensitivity performance.

$$SNR = \frac{P_{signal}}{P_{noise}}$$

7. RESULTS AND DISCUSSION

The parameters used in the experiment are as shown in below table 1.

Parameters	Value
Modulation	BPSK
Channel model	AWGN, Rayleigh
Noise model	AWGN
FFT & IFFT Point	64
Sub-carrier Number	52

Table 1.

On the basis of experiment performed,it is found that when binary phase shift keying signal is fed in a 2 input and 2 output receiver system, bit error rate differs drastically for the ZF and MMSE equalizer.
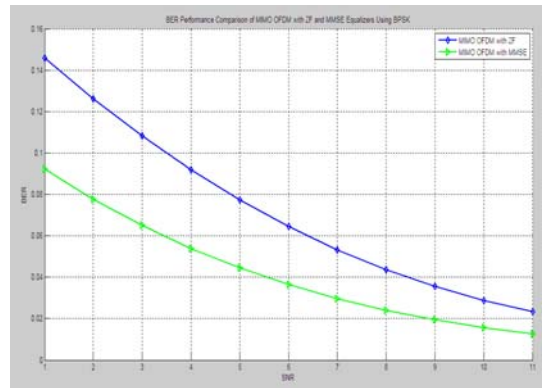

Fig.4 BER for MIMO-OFDM using MMSE equalizer for Rayleigh channel

Fig.3 and fig.4 represents the BER values as a function of SNR for the MIMO-OFDM system for ZF and MMSE equalizers respectively with Rayleigh channel. By analyzing these two graphs it is observed that BPSK modulation gives the least bit error rate in MMSE equalizer than the ZF equalizer.

8. CONCLUSION

In this paper the BER performance is evaluated for BPSK modulation and Rayleigh fading channel. It is found that MMSE equalizer performs better as compared to ZF equalizer.

Further work can be extended with using different modulation techniques and using other equalizers.

REFERENCES

1. G.L. Stuber, J.R. Barry, S.W. McLaughlin, Ye Li, M.A. Ingram and T.G. Pratt, *"Broadband MIMO-OFDM wireless communications,"* Proceed-ings of the IEEE, vol. 92, No. 2, pp. 271-294, February. 2004.

2. *DIG-COMM-BARRY LEEMESSERSCHMITT]*,DigitalCommunication:Third Edition, by John R. Barry, Edward A. Lee, David G. Messerschmitt.

3. ShaileshShankhi, K.Satya Prasad, *"Performance Analysis of Channel*

Estimation Based on MMSE Equalizer in OFDM System", International Journal of Advanced Innovative Research, Vol. 2 Issue 8, ISSN: 2278-7844, pp. no.-155-159.

4. Kala Praveen Bagadi, Prof. Susmita Das, *MIMOOFDM Channel Estimation using Pilot Carries*, International Journal of Computer Applications, ISSN No.- 0975 – 8887, Volume 2 – No.3, pp 81-88, May 2010.

5. Kuixi Chen, Jihua Lu, Bo Yang, Zhilun Li and Zibin Zhang, "*Performance Analysis of an OFDM Transmission System Based on IEEE802.11a"* IEEE Communications Letters, pp. 1-6, Oct. 2011.

6. Tian-Ming Ma, Yu-Song Shi, and Ying-Guan Wang, *"A Low Complexity MMSE for OFDM Systems over Frequency-Selective Fading Channels"*, IEEE Communications Letters, vol.-16, no.-3, March 2012

7. Allert van Zelst and Tim C. W. Schenk, *"Implementation of a MIMO OFDM-Based Wireless LAN System,"* IEEE Transaction on Signal Processing, vol.-52, Issue 2, pp. 483-494, February 2004

8. MitaleeAgrawal and YudhishthirRaut, *"BER Analysis of MIMO OFDM System for AWGN & Rayleigh Fading Channel"*, International Journal of Computer Applications, vol.-34, no.-9, November 2011..

9. T. S. Rappaport, *Wireless Communications, Principles and Practice* 2nd ed., Pearson Edu., vol.-1, pp. 356–376, 2002.

10. Kai Yu and Bjorn Ottersten, *"Models for MIMO Propagation Channels, A Review"*, in Special Issue on *"Adaptive Antennas and MIMO Systems", Wiley Journal on Wireless Comm. and Mobile Computing,* vol.-2, Issue 7, pp. 653-666, November 2002.

11. Jin-Sung Kim, Sung-Hyun Moon, and Inkyu Lee, *"A New Reduced Complexity ML Detection Scheme for MIMO Systems"* IEEE Journals and Magazines, vol.-58, Issue 4, pp. 1302 – 1310, April 2010.

12. John G. Proakis (1995). *Digital Communications (3rd ed.). Singapore*: McGraw–Hill Book Co. pp. 767–768. ISBN 0-07-113814-5.

13. Bernard Sklar (July 1997). *"Rayleigh Fading Channels in Mobile Digital Communication Systems Part I:*

*Characterization". IEEE Communications Magazine*35(7):90–100. doi:10.1109/35.601747+ISSN+0163-6804

ANALYSIS OF MICROCONTROLLER BASED FOUR QUADRANT SPEED CONTROL SYSTEM FOR A DC MOTOR

[1]K.Dhivya Dharshini, [2]S.Arockia Edwin Xavier
[1,2]Electrical and Electronic Engineering , Thiagarajar College of Engineering , Madurai
(Tamil Nadu)
Email:[1]dhivya606@gmail.com ,[2]saexee@tce.edu

Abstract --- **In this paper a four quadrant speed control system for DC motor has been designed, constructed and tested. The main advantage in using a DC motor is that the Speed-Torque relationship can be varied to almost any useful form. To achieve the speed control, an electronic technique called Pulse Width Modulation is used which generates High and Low pulses. These pulses vary the speed in the motor. For the generation of these pulses a microcontroller is used. As a microcontroller is used setting the speed ranges as per the requirement is easy which is done by changing the duty cycles time period in the program. Different speed grades and the direction are depended on different buttons. Experiment have proved that this system is of higher performance.**

Keywords--- AT89S51; DC motor; PWM

I. INTRODUCTION

In recent years, with scientific and technological progress and social development, the electronic technology is developing rapidly, to achieve the portability and low cost and energy efficient, and the noise limit, a DC motor is used widely, so, the study of DC motor speed adjustable is more practical significance. The motor is operated in four quadrants i.e. clockwise; counter clock-wise,

forward brake and reverse brake. It also has a feature of speed control. The four quadrant operation of the dc motor is best suited for industries where motors are used and as per requirement as they can rotate in clockwise, counter-clockwise and also apply brakes immediately in both the directions. In case of a specific operation in industrial environment, the motor needs to be stopped immediately. In such scenario, this proposed system is very apt as forward brake and reverse brake are its integral features. Instantaneous brake in both the directions happens as a result of applying a reverse voltage across the running motor for a brief period and the speed control of the motor can be achieved with the PWM pulses generated by the microcontroller.

II. METHODOLOGY

The traditional method of control speed was that the resistance is strung in the rotor circuit or adjust the voltage of electrical machinery circuit, the two methods is easy, but they exist some shortcomings: The smooth character is bad and the characteristic is soft in low speed, The motor speed will be changed larger when the load is changed; The motor speed is very hard to get a low when the load is light

;The larger the I resistance are, the greater its losses are,

the Efficiency reduce noticeably. Therefore, a new kind of speed control method is called PWM (pulse width modulation) speed regulating system has been widely used in the motor control speed.

With the wide use of PWM technological, the power energy can make full use of and the circuit efficient is very high. This paper utilizes the timing of the microcontroller timer function, outputs analog PWM signal at the P1.0 pin, to adjust the duty cycle according to the number of different pulse high, thus to achieve the governor's role.

A. System Overview

The design was broken down into different modules to simplify the circuit design. Figure1 describes the overall system design for the four quadrant speed control of dc motor.
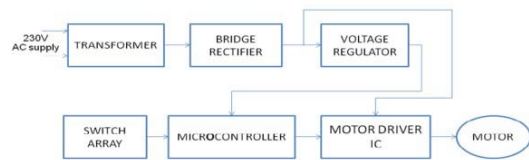
Figure1. Block diagram of the system

The circuit uses standarad power supply comprising of a step down transformer from 230V to 12V and the four diodes forming a bridge rectifier that delivers pulsating dc which is unregulated is regulated to constant 5V dc. The output of the power supply which is 5V is connected to the 40pin of microcontroller and ground is connected to 20pin. Pin no 1 to 7 of port 1 are connected to switches.Pin no 21,22,23 of microcontroller are connected to input 1,2, enable pins of motor driver L293D.Pin 3 and 6 are connected to motor terminals. *B. Four quadrant operation of DC motor*

There are four possible modes or quadrants of operation using a DC Motor which is depicted in Figure2 When DC motor is operating in the first and third quadrant, the supplied voltage is greater than the back emf which is Forward motoring and reverse motoring modes respectively, but the direction of current

flow differs. When the motor operates in the second and fourth quadrant the value of the back emf generated by the motor should be greater than the supplied voltage which are the forward braking and reverse braking modes of operation respectively, here again the direction of current flow is reversed
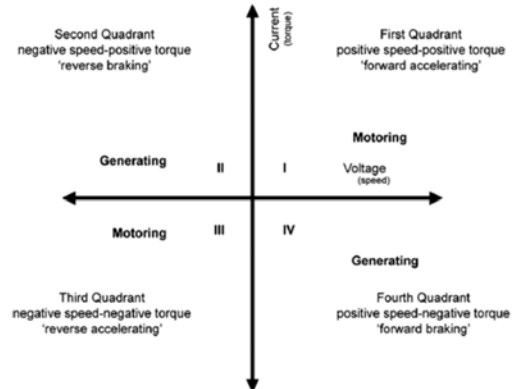

Figure 2. Four quadrants of operation

C.Pulse Width Modulation

Pulse-width modulation (PWM) is a commonly used technique for controlling power to an electrical device, made practical by modern electronic power switches. The average value of voltage (and current) fed to the load is controlled by turning the switch between supply and load on and off at a fast pace. The longer the switch is on compared to the off periods, the higher the power supplied to the load is. The term duty cycle describes the proportion of on time to the regular interval or period of time; a low duty cycle corresponds to low power, because the power is off for most of the time. Duty cycle is expressed in percent, 100% being fully on.

The main advantage of PWM is that power loss in the switching devices is very low. When a switch is off there is practically no current, and when it is on, there is almost no voltage drop across the switch. Power loss, being the product of voltage and current, is thus in both cases close to zero. PWM works also well with digital controls, which, because of their on/off nature, can easily set the needed duty cycle. PWM has also been used in certain communication systems where its duty cycle has been used to convey information over a

communications channel. The duty cycle determines the speed of the motor. The desired speed can be obtained by changing the duty

The PWM pulses generated from the microcontroller are viewed for various duty cycles in the simulation done in proteous software.
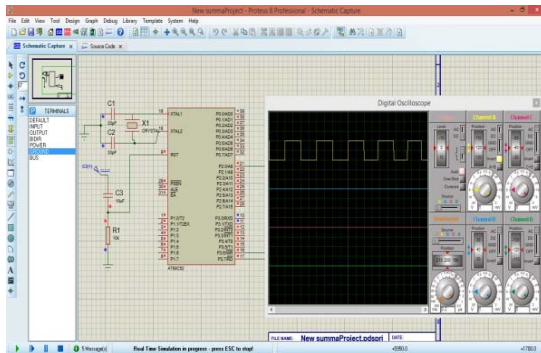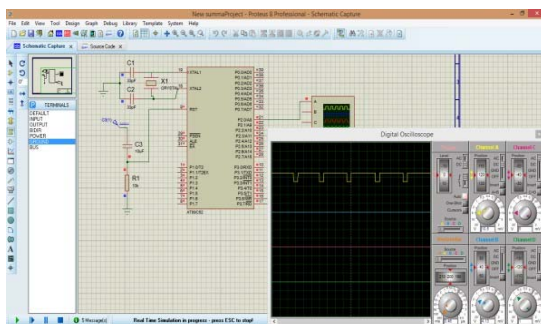

Figure 3. For 50% duty cycle

Figure 4. For 80% duty cycle

D. Motor driver IC

L293D is a dual H-bridge motor driver integrated circuit (IC). Motor drivers act as current amplifiers since they take a low-current control signal and provide a higher-current signal. This higher current signal is used to drive the motors.
L293D contains two inbuilt H-bridge driver circuits. In its common mode of operation, two DC motors can be driven simultaneously, both in forward and reverse direction. The motor operations of two motors can be controlled by input logic at pins 2 & 7 and 10 & 15. Input logic 00 or 11 will stop the corresponding motor. Logic 01 and 10 will rotate it in clockwise and anticlockwise directions, respectively. Enable pins 1 and 9 (corresponding to the two motors) must be high

cycle. The PWM in microcontroller is used to control the duty cycle of DC motor.

Average voltage = D * Vin

for motors to start operating. When an enable input is high, the associated driver gets enabled. As a result, the outputs become active and work in phase with their inputs. Similarly, when the enable input is low, that driver is disabled, and their outputs are off and in the high-impedance state.

III. COMPLETE DRIVE SYSTEM

The overall block of the system is implemented in the proteous software and the response and the operation of the motor is viewed as in figure 5.
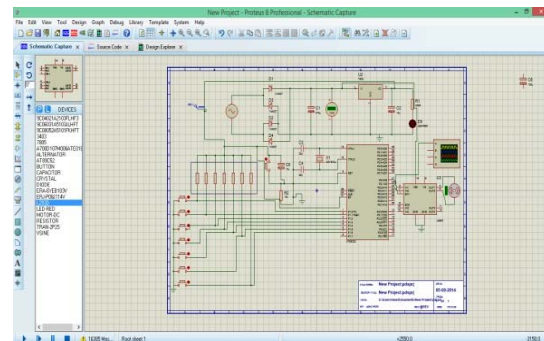

Figure 5. System tested in software

The response of the motor connected can be seen visually according to the program fed into the microcontroller and the operations are carried accordingly. It is the easiest way to check whether the hardware will get the desired output. The changes can be made to get the desired output and the operation can be carried out accordingly.

IV. HARDWARE DESCRIPTION

The following procedures are carried out for the for the four quadrant DC motor speed control operation using microcontroller. Here seven switches are interfaced to MC to control the speed of motor in four quadrants. When start switch is pressed the motor starts rotating in full speed being driven by a motor driver IC L293D that receives control signal continuously from the microcontroller. When clockwise switch is pressed the motor rotates in forward direction as per the logic provided by the program from the microcontroller to the motor driver IC.

While forward brake is pressed a reverse voltage is applied to the motor by the motor driver IC by sensing reverse logic sent by the microcontroller for a short time period due to

and reverse brake switch is pressed the microcontroller delivers a logic to the motor driver IC that develops for very small time a reverse voltage across the running motor due to which instantaneous brake situation happens to the motor.PWM switch is used to rotate the motor at varying speed by delivering from the microcontroller a varying duty cycle to the enable pin of the motor driver IC. It starts from 100% duty cycle and reduces in steps of 10% when it is pressed again and finally reaches to 10% duty cycle and the process repeats. Stop button is used to switch OFF the motor by driving the enable pin to ground from the microcontroller command accordingly.

III. PRACTICAL IMPLEMENTATION

The practical implementation of the four quadrant control of the DC motor is shown in figure 6. The hardware is designed and the operation has been done based upon the program written in the microcontroller for the four quadrant operation of the DC motor and the speed is also controlled by
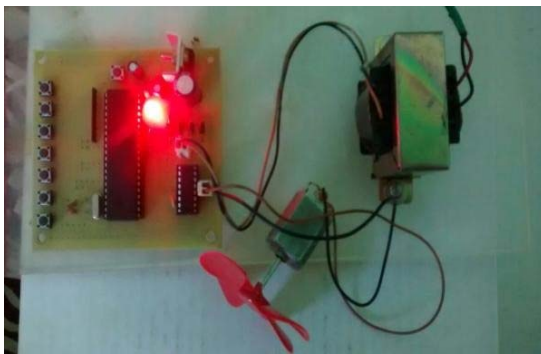using PWM technique

Figure 6. Practical Implementation

which instantaneous brake situation is applied to the motor. Similarly when motor is rotating in anti-clockwise direction by appropriate logic from the microcontroller to the motor driver IC
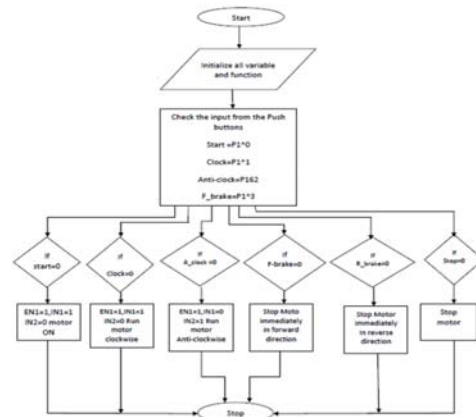

Figure 7. Flow chart for operation of DC motor

VI . CONCLUSION

The hardware for four quadrant dc motor speed control using microcontroller is designed. It is proved to be operated so simple. It is practical and highly feasible in economic point of view and has an advantage of running motors of higher ratings. It gives a reliable, durable, accurate and efficient way of speed control of a DC motor. The program is found to be efficient and the results with the designed hardware are promising. The developed control and power circuit functions properly and satisfies the application requirements. The motor is able to operate in all the four quadrants successfully. Regenerative braking is also achieved. Simulation and experimental results tally with each other and justify effectively the developed system. Further this four quadrant speed control system of a DC motor will be implemented in dSPACE in real time and its responses will be viewed.

REFERENCES

[1] "DS1103 PPC Controller Board", Germany: dSPACE, July 2008. Janice Gillispie Mazidi. "Books on Microcontroller: The
8051 microcontroller and embedded systems"

[2] Maiocchi.G., "Books on DC motors: Driving DC Motors
"BL.Theraja. "DC Motors and drives "

[3] ValterQuercioli., "Books on PWM technique: Pulse Width
Modulated Power supplies".

EFFICACY OF DIGITAL IMAGE PROCESSING TECHNIQUES IN INTRA ORAL DENTISTRY

[1]Kavindra R. Jain, [2]Narendra C. Chauhan,
[1]PhD Scholar, RK UNIVERSITY,Rajkot,
[2]HOD, IT Deptt.,ADIT,New V.V.Nagar,Anand, India,s
Email:[1]kavindrajain@gcet.ac.in, [2]narendracchauhan@gmail.com

Abstract— **Medical image processing is essential in many fields of medical research and clinical practices because it greatly facilitates early detection and diagnosis of diseases. This paper surveys an add-on approach in the area of medical image analysis for diagnosis of diseases in oral radiology using dental Xrays in dentistry. In case of medical images human involvement and perception is of prime importance. It is indeed a difficult task to interpret fine features in various contrast situations. The raw data obtained directly from X-ray acquisition device may yield a comparatively poor image quality representation. Because of the role of a human (dentist) interpretation based on his knowledge, experience and perception which may differ from doctor to doctor; there are chances of error in deciding the right medical treatment. Software developers along with domain experts have designed various standardized and scientific tools to minimize the human error in the case of deciding the right treatment on the basis of visual perception. One of the aims of this paper is to focus on the extracted part of the tooth from digital dental X-ray, finding the required information in the form of features and helping the dentist in the form of pre-diagnosis suggestions at an early stage.**

Keywords- Dental radiograph (X-ray), dentistry, image enhancement, segmentation, feature extraction, software's for dentistry.

1. INTRODUCTION

The importance of the medical imaging in healthcare is constantly growing, making health care more effective and patient friendly. With innovative imaging technologies diseases can be detected at an early stage and with more accuracy. They can be treated more specifically and are less invasive hence the therapeutic result can be closely monitored. Image post-processing of digital dental radiographs are used commonly in dental practices. Digital radiography has been available in dentistry for more than 25 years and its use by dental practitioners is steadily increasing. Digital acquisition of radiographs enables computer-based image post-processing to enhance image quality and increase the accuracy of interpretation. Image post-processing applications can easily be practiced in dental office by a computer and image processing program.

1.1 Digital Dental Radiograph (X-rays)

Dental Radiographs (X-rays) are a type of picture of the teeth and mouth. X-rays are a form of electromagnetic radiation, just like visible light. They are of higher energy and can penetrate the body to form an image on film. Structures that are dense (such as silver fillings or metal restoration) block most of the photons and appear white on developed film. Structures containing air appear as black on film while teeth, tissue, and fluid appear as shades of gray. Dental X-rays help to find problems with the teeth, mouth, and jaw. Dental X-ray pictures can show cavities,

hidden dental structures (such as wisdom teeth), and bone loss that cannot be seen during a visual examination. They are very useful in detecting the early stages of decay between teeth.

Compared to traditional X-rays, only half the dosage of radiation is needed for obtaining a dental X-rays of comparable quality. They do not require time for film development, so dentists need to wait for only a few seconds before the acquired image is displayed. Dentists can take another image instantly if the acquired image is not of good quality, so in general digital dental X-rays in a patient's record have better image quality than conventional dental X-rays. Mainly due to their advantages in speed, storage, and image quality, digital dental X-rays are now routinely used.

1.2 Types of Dental Radiographs: - There are four types of dental radiographs (X-rays) [4]:

➢ **Bitewing**: - The bitewing type of X-ray is when the patient bites on a paper tab and shows the crown portions of the top and bottom teeth together as shown in Figure 1(a). This type of X-ray shows the upper and lower back teeth and how the teeth touch each other in a single view [4]. These X-rays are used to check for decay between the teeth and how well the upper and lower teeth line up. They also show bone loss when severe gum disease or a dental infection is present. The planes of the detector and the cone are aligned parallel in bitewing X-rays. This arrangement makes bitewing X-rays give exact view of the internal structure of the teeth

➢ **Periapical**: - The periapical type of X-ray shows one or two complete teeth from crown to root as shown in Figure 1(b).
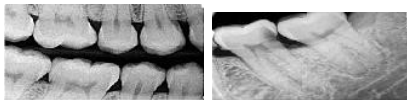

(a) Bitewing Dental X-ray   (b) Periapical Dental X-ray

Figure 1 Various types of dental X-rays

{Courtesy: Dr. Ronak Panchal}

➢ **Palatal (also called occlusal)**:- This type of X-ray captures all the upper and lower teeth in one shot while the film rests on the biting surface of the teeth as shown in Figure 1(c).

➢ **Panoramic**: - A panoramic type of X-ray requires a special machine that rotates around the head. The X-ray captures the entire jaws and teeth in one shot as shown in Figure 1(d).
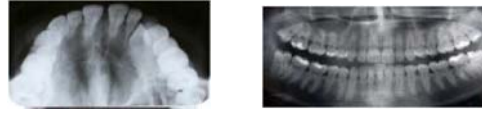
(c) Palatal Dental X-ray (d) Panaromic Dental

X-ray Figure 1 Various types of dental X-rays

{Courtesy: Dr.Ronak Panchal}

These X-rays do not find cavities. They are used for dental implants, to check for impacted wisdom teeth, and to detect jaw problems. A panoramic X-ray is not good for detecting cavities, unless the decay is very advanced and deep. These X-rays show problems such as *impacted teeth, bone abnormalities, cysts, solid growths (tumors) , infections, and fractures*. With the development of digital imaging technology, digital X-ray machines are becoming popular in dental clinics [2].

Dentist manipulates the indicator cone behind the teeth where area of diagnosis is required. The indicator cone is operated from outside the position and orientation of the film adjusted inside the mouth to get exact projection.

The paper is organized as follows: Section 2 comprises of basic background related to oral radiology and tooth structure. Section 3 is divided into three parts. First part of this section provides a literature review on image enhancement in dental X- ray images. Second part of the survey section is literature review on image segmentation, feature extraction and involvement of dental X-ray images on forensic sciences. Major work done in this domain is concentrated towards human identification [4], [5], and [6]. Last sub section comprise of comparative analysis of software's available in the market that helps dentists to analyze based on dental radiographs.

2. BACKGROUND

2.1 Basics of Tooth Structure

Dental anatomy is a field of anatomy dedicated to the study of human tooth structures. The development, appearance, and classification of teeth fall within its purview. Tooth formation begins before birth, and teeth's eventual

morphology is detected during this time. This basis tooth structure is shown in Figure 2.

Dental anatomy is also a taxonomical science: it is concerned with the naming of teeth and the structures of which they are made, this information serves a practical purpose in dental treatment. Usually, there are 20 primary ("baby") teeth and 28 to 32 permanent teeth, the last four being third molars or "wisdom teeth", each of which may or may not grow.
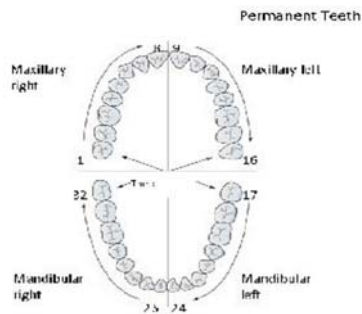

Figure 2 Dental Anatomy { Courtesy: Dr. Ronak Panchal }

Among primary teeth, 10 usually are found in the maxilla (upper jaw) and the other10 in the mandible (lower jaw). Among permanent teeth, 16 are found in the maxilla and the other 16 in the mandible. Most of the teeth have distinguishing features. Figure 3 refers to a healthy tooth cut in half lengthways showing the layers of the tooth and its internal structure, as well as how the tooth relates to the gum and surrounding jaw bone.
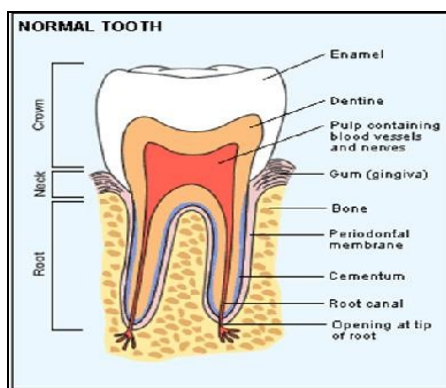

Figure 3 Tooth Structure [Courtesy by Dr. Ronak Panchal]

• **Crown.** It is the part of the tooth that is visible above the **gum (gingiva)** and is covered with enamel which protects the underlying dentine [7].

• **Neck.** It is the region of the tooth that is at the gum line, between the root and the crown.

• **Root.** It is the region of the tooth that is below the gum. Some teeth have only one roots, for example, incisors and canine ('eye') teeth, whereas molars and premolar shave 4 roots per tooth.

• **Enamel.** It is the hardest substance in the human body, harder even than bone. It gains its hardness from tightly packed rows of calcium and phosphorus crystals within a protein matrix structure. Once the enamel has been formed during tooth development, there is little turnover of its minerals during life. Mature enamel is not considered to be a 'living' tissue [9].

• **Dentine.** The major component of the inside of the tooth is **dentine**. This substance is slightly softer than enamel, with a structure more like bone. It is elastic and compressible in contrast to the brittle nature of enamel. Dentine is sensitive. It contains tiny tubules throughout its structure that connect with the central nerve of the tooth within the pulp. Dentine is a 'live' tissue.

• **Pulp.** The **pulp** forms the central chamber of the tooth. The pulp is made of soft tissue and contains **blood vessels** to supply nutrients to the tooth, and **nerves** to enable the tooth to sense heat and cold. It also contains small lymph vessels which carry white blood cells to the tooth to help fight bacteria.

3. REVIEW

The overall survey is presented into three subsections. The first subsection presents review of image enhancement methods for dental X-ray images. The second subsection focuses on review of various techniques used for image segmentation and feature extraction. This subsection also discusses the use of dental X-rays in forensic applications. The last subsection covers a brief review on the software's used by the dentists to analyze X-rays based on various parameters.

3.1 Review in Dental X Ray images based on image enhancement

Bardia Youseif et.al. [2] Developed a technique for image enhancement of digital dental X-ray using the wavelet image fusion and Bayesian classifier. One of the bases of such systems was generating better concepts of location of teeth

and canals in dentistry applications such as Root Canal Treatment (RCT). For this purpose, the Laplacian transform was applied to the image, and then structure element along with morphological operation was used. Afterward, the obtained image was fused by using wavelet transform with input image and the next step was Bayesian classifier which classified teeth and canals from achieved image. Finally, the outcome image was fused second time to original image by wavelet image fusion technique. Figure 4 infers to two such resultant images.
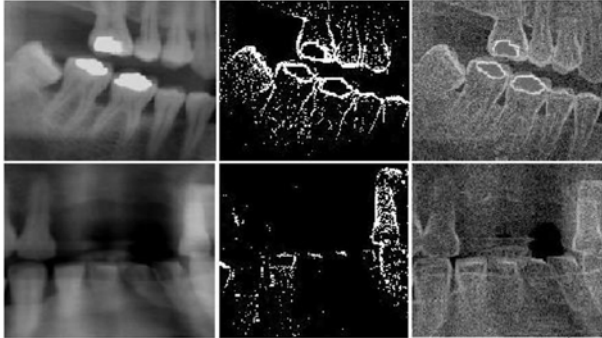

Figure 4 Two different samples of digital dental X-ray and the resultant images using the Bayesian classifier and wavelet fusion [2]

This approach was applied to the 30 dental radiographs. However the limitation of the suggested approach was that the number of teeth having the same intensity as the background cannot be detected. The classification accuracy was highly affected and fine particles of gum area were not visible for analysis purpose.

In 2008, Stefan Opera et.al. Proposed a method [3] showing how image processing techniques help to check the dental X-ray and examine the extent to which the caries lesion is present and then classify the type of caries present in the dental radiograph. Their software was based on object oriented concepts in which manual selection of threshold was required. Moreover, their database was limited to 5 images only. Hence, standardized method was not present to testify the pre diagnosis in a proper way. Ahmed et.al. [12] Have compared the original intra oral digital dental radiograph images with images that are enhanced using a combination of image processing algorithms. As these images are noisy, blur edges & lower in contrast. They have used three types of compound algorithms namely sharp adaptive histogram equalization (SAHE),

sharp adaptive median histogram equalization (SMAHE) & sharp adaptive contrast histogram equalization (SCLAHE). Detection of three pathological problems namely periapical radiolucency, widen periodontal ligament space and loss of lamina dura was being tried using above methods.

3.2 Review on Image Segmentation, Feature Extraction & Forensic Sciences in Dental X Ray Images

Eyad Haj et.al. [4] Presented an over view about an automated dental identification system for *Missing* and *Unidentified* persons. This dental identification system can be used by both law enforcement and security agencies in both forensic and biometric identification. The various techniques for dental segmentation of X-ray images to address the problem of identifying each individual tooth and how the contours of each tooth are extracted is presented. Their technique was not able to properly segment an X-ray by a single segmentation technique and it varied from image to image.

Dental biometric system have also been used in forensic science. In this system, as proposed by Shubhangi Dighe et.al. in 2012 [6] AM radiograph is matched with PM radiograph to identify unidentified individual. Dental biometrics consists of four steps as: pre-processing of dental radiograph, segmentation, feature extraction and matching of AM and PM radiograph. Segmentation is a method used for feature extraction like shape and size of tooth. These features are used in matching of two radiographs and based on this matching, individuals can be identified. In this paper segmentation is used to extract single tooth and also for the dental work extraction as shown in figure 5.
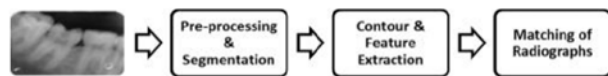

Figure 5: Block Diagram of Dental Identification System [6]

In [5] the authors present a match of X-ray teeth films using image processing based on special features of teeth. This method helps the dental doctors to match simply a pair of teeth using the special features of the teeth films. Teeth's pictures are scanned and adjusted by a

scanner and a computer, respectively, as well as then they are converted into binary code and decoded to the direction code (chain code). Chain code is a method for decoding a direction code from the binary images based on the special features of teeth. The chain code of each picture is compared with the statistical chain code. Therefore, the percentage of the same chain code is approximately 90% (i.e. matching same patterns) for the comparison of one root to one root (7 times) and two roots to two roots (7 times) while the percentage of the same chain code is reduced at relatively below 50% (i.e. matching different patterns) for comparison of one root to two roots (2 times). The percentage of the same chain code is approximately 90% (i.e. matching same patterns) for the comparison of one root to one root (7 times) and two roots to two roots (7 times) while the percentage of the same chain code is reduced at relatively below 50% (i.e. matching different patterns) for comparison of one root to two roots (2 times).

In [15], the degree of similarity/overlap between two radiographs is obtained by weighted sum of squared differences (SSD) cost function. This method was tested on a database of 571 radiographs belonging to 41 distinct individuals. Figure 6 shows an overview of this process. A total of 150 identification scenarios were taken then each single ROI was [identified/extracted] for comparing and matching with the dental x-ray images.
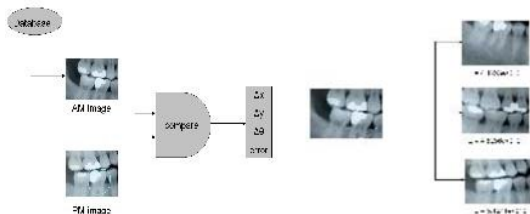

Figure 6 - Illustration of the identification test run & top three radiographs in the database ranked by the associated cost. [15]

The authors proposed a computer-aided framework for matching of dental radiographs based on a sum of squared differences cost criterion. In their framework, the operator would define the ROI by roughly circling the tooth of interest on a given post-mortem radiograph. Hence, even untrained staff able to participate in the identification efforts by roughly circles the tooth area. The system itself then matches the

selected region to radiographs found in the ante mortem database. For all possible shifts, the best brightness and contrast adjustment and rotation were computed, and the parameters that yielded the lowest cost are recorded along with the associated cost (match score). The radiographs in the database were then ranked according to the cost, with the lowest cost indicating the best match. This work was not tested on multiple ROI's as well as on different dental images.

Lailee Shaiaf et.al. [18] Investigated the fundamental problems in image segmentation using traditional segmentation techniques and proposed an improved technique for segmenting images captured under natural environment. Due to non-uniform illumination it is difficult to produce a significant threshold value along with lack of difference in reflection. Since different illumination may produce different colour intensity of the object surface and thus lead to inaccurate segmented images. The widely used traditional method for thresholding is ostu and fuzzy c-means respectively. In this method, the authors have added a step extra after thresholding with ostu method by converting the gray scale image into binary & then integrating the modified threshold algorithm with an inversion technique. The results were analyzed based on rand index function. By this the authors have concluded that the images after ostu method and thresholding which were not able to get separate and provide the required information are now being able to separate the interest area & background easily. The ability of this technique therefore has the potential to classify the poor images with inconsistent illumination condition.

Dental biometrics can be used in forensic science for human identification. It utilizes dental radiographs. This radiograph provides information related to teeth shape, teeth contour and relative position of neighboring teeth, also it gives shapes of dental work like crowns, filling & bridges etc. Different methods used for dental biometrics and related information are included in [16]. Dental biometrics requires ante mortem (AM) and post mortem (PM) radiographs for finding unidentified subject. Dental biometrics having three stages: Pre-processing and segmentation of radiographs, contour extraction or dental work extraction, atlas registration and matching. Segmentation can be done by various

methods. Contour or shape of teeth and dental work can be extracted. Method or code was developed by the authors to locate teeth this is known as dental atlas registration. Numbering to teeth from left to right of jaw and also differentiation between upper jaw and lower jaw was done, which help in the matching stage [16].

Omaima Nomir et.al. [17] Presents a system in which, given a dental image of a post-mortem (PM), the proposed system retrieves the best matches from an ante mortem (AM) database. The system automatically segments dental X-ray images into individual teeth and extracts the contour of each tooth. Features are extracted from each tooth and are used for retrieval. During retrieval, the AM radiographs that have signatures closer to the PM are found and presented to the user. Matching scores are generated based on the distance between the signature vectors of AM and PM teeth.
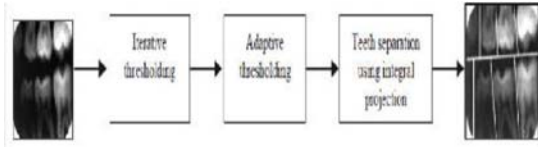

Figure 7 Block diagram of segmentation algorithm [17]

They introduced iterative and adaptive thresholding. Thereafter horizontal and vertical integral projection is used for separating the jaws as well as individual tooth. The block diagram of segmentation algorithm is as shown in Figure 7.This technique was not successful in matching images due to poor quality of images and shape of teeth could have changed with time as PM images were taken after a long time AM images were captured.

3.3 Review Based On Dental Software Programs

TM Lehmann et.al. [19] contributed greatly in a technical report regarding identifying and analyzing various methods for image processing provided by various commercial software programs used in digital dental imaging and to map them onto a standardized nomenclature. The features various software's like CDR, Clinicview,Dexis, Digora, Dimaxis, Emago Advanced, Friacom Dental, IOX Image Viewer, Multi X-ray, Proimage, Sidexis, Trophy, VixWin

2000 were discussed and compared in his work. The comparison of the software programs were analised based on following parameters:

Image Display: - Half of the programs mentioned above have only 1D line profiles. Trophy software offers 3D. Six out of thirteen software's (Dimaxis, Emago, IOX Image Viewer, Multi X-ray, Sidexis, and Proimage) provide interpolating images to various sizes rest do not. Friacom even do not allow the image to rotate.

Point processing: - More than 50% of the software's do not provide gamma correction & require image transforms for the purpose of diagnosis. Only Dexis and Emago provide direct thresholding out of 13 software's. Dexis do not provide contrast enhancement. Only 3 (CDR, Clinicview, Dimaxis) have histogram equalization facilities that to stretches or clips and does not actually equalize.

Spatial and frequency filtering: - Only Emago provides user defined masks up to 7*7 pixels rest do not. Only five (Dimaxis, Emago, Multi X-ray, Proimage, Sidexis) have spatial domain filter facility that to only non-linear median filter. They are able to remove salt & pepper noise rest doesn't. None incorporates frequency domain filtering.

Measurements and image analysis: - Dexis, IOX, Multi Xray, Proimage cannot determine angles from dental X-rays. Only 3(Sidexis, Emago & Vix Win 2000) provide area facility. None incorporates ROI selection, zooming, deblurring, denoising, morphological operations etc.

4. Discussion

The major researchers make use of thresholding and morphological operation for feature extraction and segmentation. However, in the existing software's used by doctors the option of adaptive or global threshold is not available. Hence, the benefits of these methods are not directly available. Much of the work have been done for human identification, but very few researchers have applied and realized the methods for diagnosis purpose. For the diagnosis of intra oral diseases specifically the region of interest selection, impacted 3rd molar using x ray

rendering of 3-D images and other related problems of gums and idiopathic resorption is still a missing feature in most of the software's. Interactive portions of X-ray selected for further processing specifically for the purpose of diagnosis is the need of the hour as it would help both doctor and patient to understand the problem and depth of disease. No software is using AI tools such as neural networking, fuzzy c-means, etc. for the better understanding and diagnosis purpose. Researchers up till now have been found concentrating on image enhancement or segmentation for extracting features for forensic sciences. No much research has effectively contributed for the diagnostic methods. Automated or semi-automated diagnosis of aforesaid objectives would be quiet useful for doctor as well as patient. It has been found through detail in depth discussion with selected dental experts that as radiographic imaging study in medical practice provides better clue for diagnosis. Image processing & enhancement functions are rarely incorporated in commercial software for direct digital imaging in dental radiology. Until now, comparison of software was limited by arbitrary naming used in each system. Standardized terminology and increased functionality of image processing should be offered to the dental profession.

Acknowledgement

REFERENCES

[1]   G.A.Kulkarni, A.S.Bhide, D.G. Patil, S.S.G.B.C.O.E. & T., Bhusawal, "Two Degree Greyscale Differential Method for Teeth Image Recognition", International Journal of computer Application, 2012

[2]   B. Yousefi , H. Hakim, N. Motahir, P. Yousefi1, M. M.Hosseini, "Visibility Enhancement of Digital Dental X-ray for RCT Application Using Bayesian classifier and Two Times Wavelet Image Fusion", Journal of American Science, pp 713, 2012

[3]   Ş. Oprea, C. Marinescu , I. Liţă, M. Jurianu, D. A. Vişan, I. B. Cioc, " Image Processing Techniques used for Dental Xray Image Analysis" , Electronics Technology, ISSE 2008, pp 125-129

[4]   E. H, said, G. Fahmy, D. nassar, H. Amar, "dental X-ray image segmentation" Biometric Technology for Human Identification, Proceedings of the SPIE, Vol. 5404, pp. 409417, 2004.

[5]   S. Kiattisin, A. Leelasantitham, K. Chamnongthai , K. Higuchi, " A Match of X-ray Teeth Films Using Image processing Based on Special Features of Teeth" , SICE Annual Conference 2008, pp 35-39

[6]   S. Dighe, R. Shriram, "Pre-processing, Segmentation and Matching of Dental Radiographs used in Dental Biometrics", International Journal of Science and Applied Information Technology,Volume 1, No.2, pp 52-56, May – June 2012

[7]   R. B. Tiwari, Prof. A. R. Yardi, "Dental X-ray image enhancement based on human visual system and local image statistics"., International Conference on Image Processing, Computer Vision and Pattern Recognition, 2006, pp 100-108

[8]   C. K. Modi , K. J. Pithadiya ,J. D.Chauhan, K. R. Jain, " Comparative study of Optimal edge detection algorithms for liquid level inspection in Bottles", International conference on Emerging Trends in Engineering and Technology , pp 447-452 , 2009 .

[9]   E. H. Said, D. E. M. Nassar, G. Fahmy, H. H. Ammar. "Teeth segmentation in digitized dental X-ray films using mathematical morphology," IEEE Transactions on information forensic and security, vol. 1, Issue. 2, pp. 178189, June. 2006.

[10]   White & Pharoah "Oral Radiology-Principles and Interpretation", Fifth Edition (2005), selected illustration by Dr. Donald O'Connor. ISBN 0-323-02001,published by MOSBY (An affiliate of Elsevier)

[11]   Shafer's Tb. "Textbook of Oral Pathology" sixth edition, 2006.

[12]   S.A.Ahmed, M.N.Taib, N.E.A.Khalid, R.Ahmad, H.Taib "Performance of compound

enhancement algorithms on dental radiograph images" WASET-2011 [13]Stefan Michel, Saskia M.Koller, Markus Ruh, Adrian Schwaninger, "Do "Image Enhancement" Functions Really Enhance X-ray Image Interpretation?" Cognitive Science Journal Archieve 2007

[14] Nirav P. Desai, D. B. Prajapati "A simple and novel CBIR technique for features extraction using AM dental radiographs" CSNT (IEEE) 2013, Gwalior, pp.198-202 , 2012 [15] Maja Omanovic, Jeff J. Orchard "Exhaustive Matching of Dental X-rays for Human Forensic Identification "Journal of the Canadian Society of Forensic Science, 2008 [16] S.Jadhav, R. Shriram "Dental biometrics used in forensic science" IJERS/Vol.III/ Issue I/January-March, 2012/26-29

[17] Omaima Nomir, M.A.Mottaleb "A system for human identification from X-ray dental radiographs" Pattern Recognition 38 (2005) 1295 - 1305.

[18] Sharifah Lailee, Nursuriati Jamil "Segmentation of Natural Images Using an Improved Thresholding-based Technique" IRIS 2012, Elsevier Procedia engg. Conference pp938-944.

[19] TM Lehmann, E.Troeltsch, K Spitzer" Image processing and enhancement provided by commercial dental software programs: A Technical Report" Dentomaxillofacial Radiology (2002) 31, 264-272.

[20] T. N. Cornsweet, Visual Perception, Academic Press, New York, 1970.

BRUSHLESS DC MOTOR SPEED CONTROL USING MICROCONTROLLER

[1]G.SanthoshKumar, S.Arockia Edwin Xavier
Thiagarajar College of Engineering ,Electrical and Electronic Engineering
Madurai,Tamil Nadu
Email: [1]Santhoshg92@gmail.com,[2]saexee@tce.edu

ABSTRACT

The hardware project is designed to control the speed of a BLDC motor using closed loop control technique. BLDC motor has various application used in industries like in drilling, lathes, spinning, electric bikes etc. The speed control of the DC motors is very essential. This proposed system provides a very precise and effective speed control system. The user can enter the desired speed and the motor will run at that exact speed.

KEYWORDS: Hall position sensors, Brushless DC motor, Microcontroller.

I. INTRODUCTION

Permanent-magnet excited brushless DC motors are becoming increasingly attractive in a large number of applications due to performance advantages such as reduced size and cost, reduced torque ripples, increased torque-current ratio, low noises, high efficiency, reduced maintenance and good control characteristics over a wide range in torque–speed plan.

In general, Brushless DC motors such as fans are smaller in size and weight than AC fans using shaded pole or Universal motors. Since these motors have the ability to work with the available low voltage sources such as 24-V or 12-V DC supply, it makes the brushless DC

motor fans convenient for use in electronic equipment, computers, mobile equipment, vehicles, and spindle drives for disk memory, because of its high reliability, efficiency, and ability to reverse rapidly. Brushless dc motors in the fractional horsepower range have been used in various types of actuators in advanced aircraft and satellite systems [1-4]. Most popular brushless DC motors are mainly three phases [5-7] which are controlled and driven by full bridge transistor circuits. Together with applying permanent magnet excitation, it is necessary to obtain additional torque components. These components can be obtained due to a difference in magnetic permeance in both quadrature and direct axis; therefore, reluctance torque is developed and torque null regions are reduced significantly [8, 11]. In this paper, a brushless DC motor with distributed winding and a special form of PM-rotor with special stator periphery are described. Which develop a speed control system for a BLDC motor by closed loop control technique.

The proposed system uses a microcontroller of the 8051 family and a rectified-power supply. A set of IR transmitter and photodiode are connected to the microcontroller for counting the number of rotations per minute of the DC motor as a

speed sensor. Optocoupler is connected to trigger the MOSFET for driving the BLDC motor which is duly interfaced to the microcontroller. A matrix keypad is interfaced to the microcontroller for controlling the speed of the motor.

The speed control of the BLDC motor is archived by varying the duty cycles (PWM Pulses) from the microcontroller according to the program. The microcontroller receives the percentage of duty cycles from the keypad and delivers the desired output to switch the motor driver so as to control the speed of the BLDC motor. The speed sensed by the IR sensor is given to the microcontroller to display it on the LCD display.

II. TYPES OF CONTROL TECHHIQUE OF BLDC MOTOR

Though various control techniques are discussed in [8] basically two methods are available for controlling BLDC motor. They are sensor control and sensor less control. To control the machine using sensors, the present position of the rotor is required to determine the next commutation interval. Motor can also be controlled by controlling the DC bus rail voltage or by PWM method. Some designs utilize both to provide high torque at high load and high efficiency at low load. Such hybrid design also allows the control of harmonic current [9]. In case of common DC motors, the brushes automatically come into contact with the communtator of a different coil causing the motor to continue its rotation. But in case of BLDC motors the commutation is done by electronic switches which need the rotor position. The appropriate stator windings have to be energized when rotor poles align with the stator winding. The BLDC motor can also be driven with predefined commutation interval. But to achieve precise speed control and maximum generated torque, brushless commutation should be done with the knowledge of rotor position. In control methods using sensors, mechanical position sensors, such as a hall sensor, shaft encoder or resolver have been utilized in order to provide rotor position information.

Hall Position sensors or simply Hall sensors are widely used and are popular. Whenever the magnetic poles pass near the sensors, they either give a high or low signal, indicating North or South Pole is passing the pole. The accurate rotor position information is used to generate precise firing commands for power converter. This ensures drive stability and fast dynamic response. The speed feedback is derived from the position sensor output signals. Between the two commutations signals the angle variation is constant as the Hall Effect Sensors are fixed relative to the motor, thus reducing speed sensing to a simple division. Usually speed and position of a permanent magnet brushless direct current motor rotor is controlled in a conventional cascade structure. The inner current control loops runs at a larger width than the outer speed loop to achieve an effective cascade control [10]. Various senseless methods for BLDC motors are analyzed in [11].Modeling of BLDC is given in [12].[11] Proposes a speed control of brushless drive employing PWM technique. The above literature does not deal with reduction of speed oscillations and also the motor can't runs at exact speed in BLDC drive. This paper deals with control method to reduce speed oscillations and to runs the motor at exact entered speed. This is achieve by using the microcontroller programming .

III. CONSTRUCTION AND OPERATING PRINCIPLE

Brushless DC motors were developed from conventional brushed DC motors with the availability of solid state power semiconductors. Brushless DC motors are similar to AC synchronous motors. The major difference is that synchronous motors develop a sinusoidal back EMF, as compared to a rectangular, or trapezoidal, back EMF for brushless DC motors. Both have stator created rotating magnetic fields producing torque in a magnetic rotor.
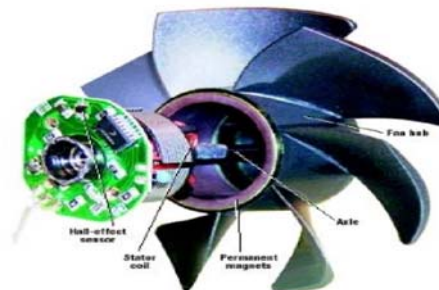

Fig.1 : Construction of BLDC motor

The basic construction of a brushless-dc consists of a fan blade attached to a permanent magnet rotor that surrounds the electromagnetic coils of the stator and associated control electronics.
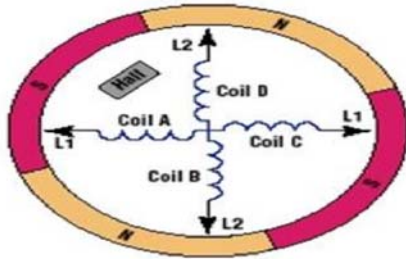

Fig.2 : DC Motor schematic diagram

A typical biphase brushless fan motor is made from a permanent magnet rotor assembly that surrounds four electromagnetic coils. The coils work in pairs, with coils A and C forming one phase and coils B and D the other phase. A Halleffect sensor monitors rotor position, providing feedback to the embedded MCU for commutation, speed regulation, and fault detection.
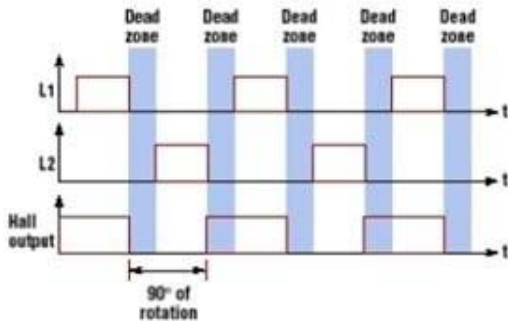

Fig . 3: Commutation Timeline Diagram

Commutation between the two phase windings in the dc fan takes place electronically by alternately applying power to L1 and L2. Dead zones between the power pulses limit current for speed control and helps minimize a cogging effect when the rotor magnets align with the stator coils. The on-and-off power of the commutation period resembles the output from a pulse-width modulator, or PWM.
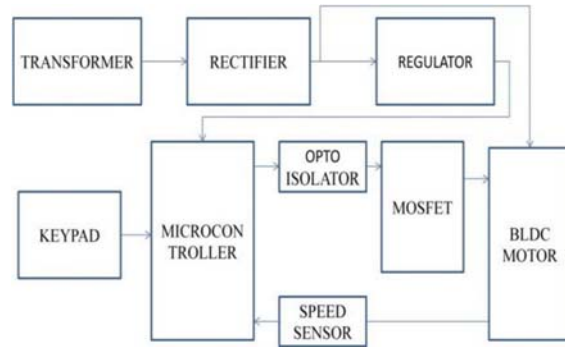

Fig .4 : Block Diagram

The Fig 4 describes the overall system design for the Closed loop control of BLDC motor. The MCU uses a PWM to control the period of the motor drivers and, thus set fan speed.

Feedback from the Hall sensor monitors actual fan rpm and indicate when communication should take place.
The MCU continuously monitors motor speed by measuring the output period of the Hall effect sensor.
A period that run shorter than the target length indicates motor speed is too fast. The schematic diagram of closed loop control 1 of BLDC motor is shown in fig. 5.
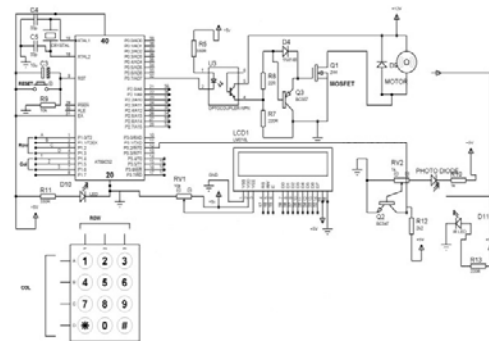

Fig 5. Schematic Diagram

IV. BLDC MOTOR SPEED CONTROL

Pulse-width modulation (PWM) is a commonly used technique for controlling power to an electrical device, made practical by modern electronic power switches. The average value of voltage (and current) fed to the load is controlled by turning the switch between supply and load on and off at a fast

pace. The longer the switch is on compared to the off periods, the higher the power supplied to the load is. The PWM switching frequency has to be much faster than what would affect the load, which is to say the device that uses the power. Typically switching's have to be done several times a minute in an electric stove, 120 Hz in a lamp dimmer, from few kilohertz (kHz) to tens of kHz for a motor drive and well into the tens or hundreds of kHz in audio amplifiers and computer power supplies

The term duty cycle describes the proportion of on time to the regular interval or period of time; a low duty cycle corresponds to low power, because the power is off for most of the time. Duty cycle is expressed in percent, 100% being fully on.

The main advantage of PWM is that power loss in the switching devices is very low. When a switch is off there is practically no current, and when it is on, there is almost no voltage drop across the switch. Power loss, being the product of voltage and current, is thus in both cases close to zero. PWM works also well with digital controls, which, because of their on/off nature, can easily set the needed duty cycle.

PWM has also been used in certain communication systems where its duty cycle has been used to convey information over a communications channel.
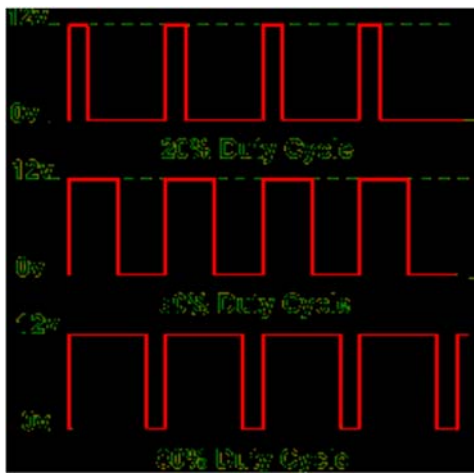

Fig.6 : PWM Pulses

The duly cycle determines the speed of the motor .

The desired speed can be obtained by changing the duty cycle. The PWM in microcontroller is used to control the duty cycle of DC motor.
Average Voltage=D * Vin

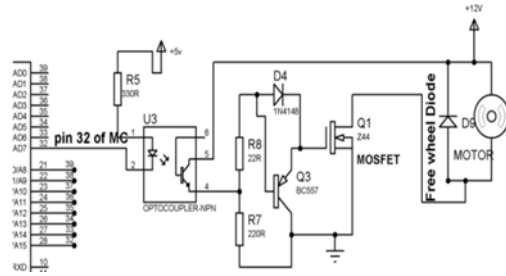## V. LOGICAL OPERATION OF BLDC MOTOR

Fig.7 : PWM Generating Circuit

While logic high during the on time duty cycle is delivered by the microcontroller to the input of the OPTO U3 , The opto led glows to bring the opto transistor pin no 5 and 6 to conduct . Now 12V supply is given at the junction point of R7 and R8 and reaches the gate of the MOSFET Q1 via D4 for Q1 to conduct thus enabling the motor to get supply to run. A freewheel diode is used across the motor to conduct the charge stored in the motor during off period. During off time of the duty cycle the opto transistor does not conduct and the charge which is stored in the gate of Q1 forces Q3 to conduct while the motor stops. This ON and OFF the motor reduces the speed . The DC power is available to the motor via the MOSFET as per the PWM generated by micro controller depending upon the input given to micro controller from a keypad. As well as the speed is displayed on a liquid crystal display. To sense the speed of BLDC motor an IR LED in photo diode arrangement is used. The value of speed is changed in percentage by using fuzzy logic. Fuzzy logic is something i.e. approximate but not accurate. So a program is written in to micro controller that uses fuzzy logic due to which we get the values almost equal to accurate values. A 230v -12v step down transformer is used to decrease AC supply voltage to 12v, now this ac voltage is rectified by using a full wave bridge rectifier, a blocking diode is used

before the filter capacitor to get the pulsating D.C. to get the fixed output D.C a 7805 voltage regulator is employed because micro controller fixed +5v pure DC. To filter pulsating D.C an electrolytic capacitor of value 470 micro farad's or 1000micro farad's is connected at the input of 7850. One more electrolytic capacitor is connected at the output of 7850 to remove complete ripple's if there any +5v D.C. A LED with a series resistor's is connected to indicate the power. 40 Micro controller has to generate PWM pulses as per error signal received from the speed sensing input to match the keyboard input in order to run the motor at the input RPM.

A push button is connected at the 9th pin of micro controller which is known as reset a 10 micro farad's electrolytic capacitor is connected across the button and a 10k resistor is used to pull down 9th pin of micro controller. When this reset pin is pressed during the operation , the program written in micro controller starts from beginning.

A crystal across oscillator of value 11.0592 MHz is connected across 18th & 19th pins of micro controller with the 33pico farad's ceramic capacitors are connected for stabilising it.
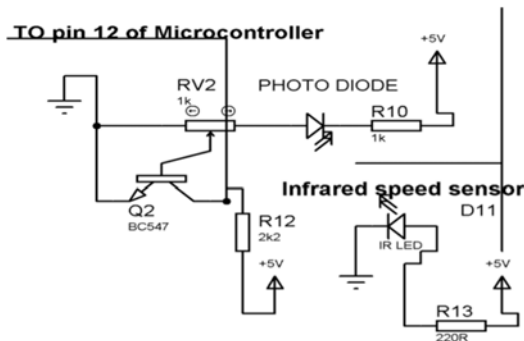

Fig.8 : Speed Sensing Circuit

To sense the speed of BLDC motor an infrared(IR) diode and photo diode are used. When light falls on photo diode the resistance across it decreases and vice versa. Hence photo diode is employed in a potential divider with a variable resistor. This potential divider supplies voltage to an N-P-N transistor whose collector is connected to micro controller input.

So, the IR LED and photo diode are placed near the shaft of BLDC motor and a white spot is made on the shaft infrared light gets reflected by white colour and the reflected light keeps falling on photo diode, due to which the voltage across it keeps changing thereafter the voltage at base of transistor also changes therefore at the collector of transistor a pulse is generated which is given to micro controller for counting the number of rotations per minute of D.C motor.

This sensed speed is displayed on LCD in rpm. To change the speed a keypad is used as an input to the micro controller. By using this we can enter how much percentage of speed would be required for the motor to run. Pressing '#' twice the maximum running speed is stored. After which pressing '*' the desired percentage of speed is entered. There after pressing # the desired speed is saved which are displayed on the LCD.There after the on time of the pulse width progressively goes on reducing to result the speed reduction. Speed sensors continuously send the error signal to pin 12 of the MC to lock the running speed of the motor at the desired speed.

VI. SIMULATION RESULTS FOR VARIOUS PWM PULSES.

The speed control technique employed here is pulse width modulation (PWM) technique The duty cycle determines the speed of the motor. The desired speed can be obtained by changing the duty cycle. The PWM in microcontroller is used to control the duty cycle of DC motor.

$$\text{Average voltage} = D * Vin$$

The average voltage obtained for various duty cycles is also mentioned and as the duty cycle percentage decreases average voltage also decreases from the supply voltage.
Duty cycle is defined as the percentage of time the
motor is ON. Therefore, the duty cycle is given as
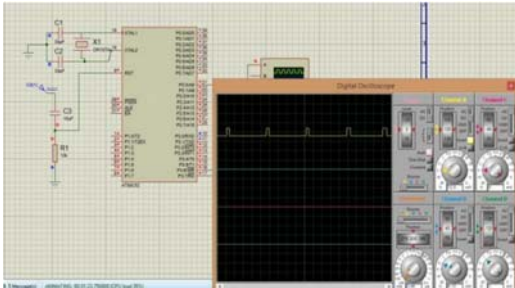
Duty Cycle = 100% x Pulse Width/Period
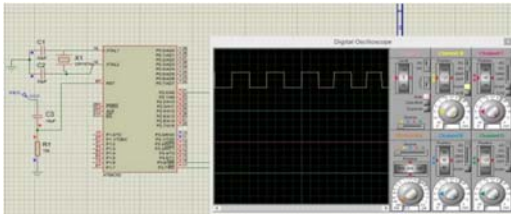Where,
Duty Cycle in (%)
Pulse Width = Time the signal is in the ON or high state (sec)

Period = Time of one cycle (sec).
The program for the closed loop control of BLDC motor operation is written in embedded C and executed in keil software. The PWM pulses generated from the microcontroller are viewed for various duty cycles,
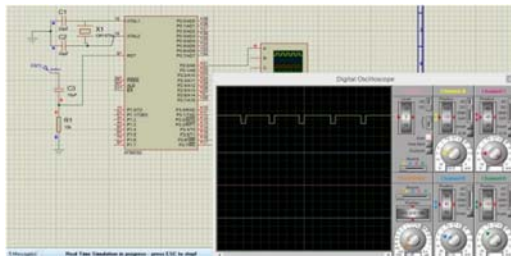
PWM Output for 20%

PWM Output for 50%

PWM Output for 80%

OUTPUT RESPONSE

INPUT DUTY CYCLE IN %	OUTPUT VOLTAGE	OUTPUT SPEED IN RPM
25%	3V	650
50%	6V	1300
75%	9V	1950
100%	12V	2600

HARDWARE SETUP

The hardware is designed and the operation has been done based upon the program written in the microcontroller for the Closed loop control of the BLDC motor and the speed is also controlled by using PWM technique. The hardware set up for the project is given below.
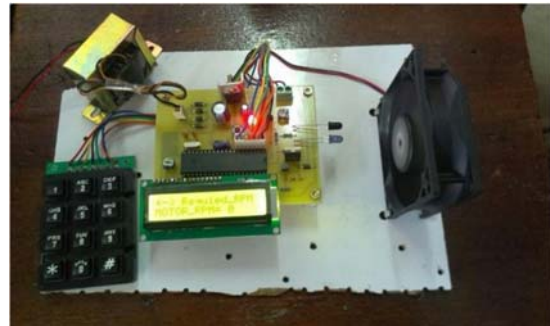
VII.   OPERATION PROCEDURE

1.   Press '#' once display shows the store Max RPM.

2.   Press '#' again to store Max.RPM.

3.   Press '*' to get the required RPM. Display shows % of Req_RPM:

4.   Enter the required percentage using Keypad. 5. Press '#' to save the required RPM.

CONCLUSION

The hardware for closed loop control of BLDC motor using microcontroller is designed. By using the PWM technique speed of the BLDC motor was controlled and it was made to run at exactly entered speed. In future this hardware will be implemented in dSPACE and the speed control will be observed.

REFERENCES

1. *Kusko, A. & Peeran, S. M. (1987) Brushless DC motor using asymmetrical field magnetization. IEEE Transactions on Industrial Applications, 23 (2):319*

2. *Bolton, H. R. & Ashen R.A. (1984) Influence of motor design and feed current waveform on torque ripples in brushless dc motor. IEE Proceeding, 131 (3): 82 – 90*

3. *Duane, H. (2002) Brushless Permanent Magnet Motor Design. University of Maine, Orno, USA, 2nd ed.*

4. *Khader, S. H. (2001) Implementation of an accurate mathematical method formodeling electromagnetic processes of brushless DC Motor. MESM, Amman, Jordan, 31-38*

5. *Miller, T. J. E. (1993) Switched Reluctance Motors and their Control, Oxford, UK, Magna Phys. Publication and Clarendon, 40-90*

6. *Faiz, J. & Finch, J.W. (1993) Aspects of design optimization for switched reluctance motors, IEEE transactions on Energy*

7. *Torrey, D.A., Niu, X. M. & Unkauf, E.J. (1995) Analytical modelling of variablereluctance machine magnetization characteristics. IEEE Proceedings, 142(1): 14-22*

8. *R.Krishnan, "Electric Motor Drives Modeling, Analysis, and Control, PrenticeHall InternationaInc., New Jersey, 2001*

9. *"New Approach to Rotor Position Detection and Precision Speed Control of the BLDC Motor "Yong-Ho Yoon Tae-Won Lee Sang-Hun ParkByoung-Kuk Lee Chung- 1-4244-0136-4/06/$20.00 '2006 IEEE*

10. *Ling KV, WU Bingfang HE Minghua and ZhangYu, "A Model predictive controller formultirate cascade system", Proc.of the American Control Conference, ACC 2004 USA, pp.1575-1579.2004.*

11. *G.Madhusudhanrao, B.V.SankerRam, B.SampathKumar, K.Vijay Kumar," Speed Control of BLDC Motor using DSP", International Journal ofEngineering Science and Technology Vol.2(3),2010*

12. *Nicola Bianchi, SilverioBolognani, Ji-HoonJang,Seung-Ki Sul," Comparison of PM Motor structures and sensor less Control Techniques for zero-speed Rotor position detection" IEEE transactions on power Electronics, Vol 22, No.6, Nov 2006*

13. *G.Madhusudhanrao, B.V.SankerRam, B.SampathKumar, K.Vijay Kumar," Speed Control of BLDC Motor using DSP", International Journal ofEngineering Science and Technology Vol.2(3),2010*

14. *Nicola Bianchi, SilverioBolognani, Ji-HoonJang,Seung-Ki Sul," Comparison of PM Motor structures and sensor less Control Techniques for zero-speed Rotor position detection" IEEE transactions on power Electronics, Vol 22, No.6, Nov 2006*

PERFORMANCE ANALYSIS OF UNICAST ROUTING PROTOCOL IN IEEE 802.11S WIRELESS MESH NETWORK

Aneri Fumtiwala[1], Himani Modi[2], Pinal Patel[3], Mrs.Payal T. Mahida[4]

[1,2,3,4]Department of Computer Science & Engineering

Shri S'ad Vidya Mandal Institute of Technology - SVMIT Bharuch,India.

annufumtiwala94@gmail.com[1], himani.modi93@gmail.com[2], pinalprem1988@gmail.com[3],

payal_mahida@yahoo.co.in[4]

Abstract— Wireless Mesh Network is a rising technology in the wireless network world to deliver last mile broadband access. It has amazing features such as low deployment cost, easy network maintenance, robustness, wide area coverage, self-healing, self-configuring and self-organizing which are responsible for growing rapid progress of wireless mesh networks and inspiring numerous applications. In order to take the advantage of this, wireless mesh networks need the new and improved routing protocols. This paper is the analysis of unicast routing protocol such as Ad-hoc On-demand Distance Vector Routing Protocol (Reactive Routing), Optimized Link State Routing Protocol (Proactive Routing), Hybrid Wireless Mesh Protocol (hybrid Routing) on the basis of performance metric like Packet Delivery Ratio, End-to-End Delay and Bit-rate in IEEE-802.11s Wireless Mesh Network using Network Simulator 3 (NS3).

Index Terms— **Wireless Mesh Network, IEEE 802.11s, Unicast Routing Protocol, AODV, OLSR, HWMP, NS3, PDR, Delay, Bit-rate**

I. INTRODUCTION

Wireless Mesh Networks (WMNs) can be considered as an integral part of Mobile Ad-hoc Networks (MANETs). MANET is a network that is composed of mobile client devices which represent fully dynamic topology whereas the WMN is a network that is composed of mobile client devices as well as routers which represents both dynamic and static topology. In order to understand mesh networking, first thing we need to understand is mesh topology. If we have n nodes which represent communication device in network, each node can communicate with other (n-1) nodes; this kind of structure is known as mesh topology. A wireless mesh network (WMN) is a promising technology composed of radio node connected through wire or wirelessly in mesh topology which provide high speed internet to end user.

WMNs have two types of nodes [1] [8]: mesh router and mesh client. A Mesh router is similar to conventional router in addition of having a capability of mesh networking. Mesh routers are a static node in mesh network which are connected to stable source of power and that is why they have less mobility. Mesh routers play the role of spine for mesh clients. Mesh Clients are devices which are dynamic in nature such as mobiles, PDAs or laptops. They have limited power compare to mesh router and basically they operate on batteries which have limited power capacity. Mesh clients can also be work as mesh router in WMN with fewer amounts of the hardware platform and software requirements and designs are much simpler than those of mesh routers. Although mesh networking consists of

mesh routers and mesh clients, mesh router are also having capability of the gateway/bridge gateways are one type of router that has direct access to the wired infrastructure or Internet. As the mesh gateways can connect to wired or wireless network through multiple interfaces, so for this reason they are expensive. Therefore, a less number of Mesh gateways are used in wireless mesh network. Wireless mesh networks can be accepted with a variety of wireless technologies. The main intention at the back of the development of wireless mesh networks are to beat the restrictions of single hop communication, and consequently data packets have to navigate over multiple wireless hops. Since 2004 Task Group S has been raising an amendment to the 802.11 standard to precisely give attention to the aforementioned necessitate for multi hop communication. The IEEE 802.11 TGs has continuing to effort in developing a

functionalities which help in the incorporation of WMNs with various other networks. Mesh mesh standard for local area wireless networks. [2]

[2][3]Any IEEE 802.11 based components which are either access point (AP) or station (STA) having mesh functionality or we can say carry a mesh relay function to form IEEE 802.11s mesh network. IEEE 802.11s mesh network contain: mesh station (MSTA), mesh access point (MAP), and mesh point portal (MPP). A mesh point (MP) is an either AP or STA which partially or completely bring a mesh-relay function in IEEE 802.11s mesh network. The MP performs few operations which comprise neighbor finding, channel association, and structure a relationship with neighbors. MPs have a capability of directly communicating with their neighbors and by using bidirectional wireless mesh link forward traffic on behalf of other MPS
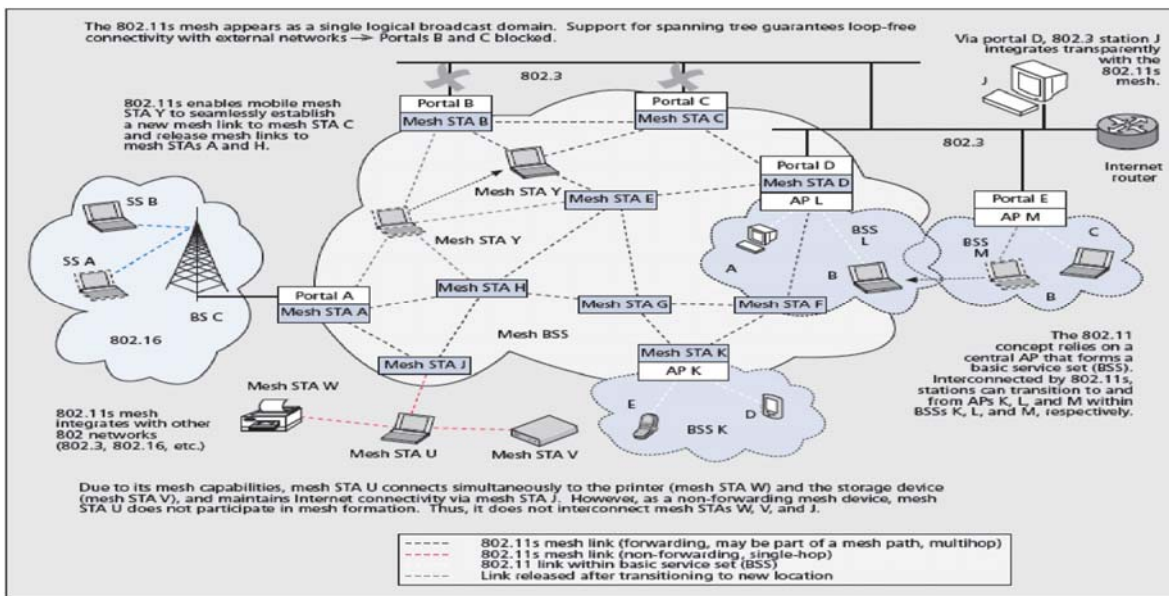

Fig. 1. IEEE 802.11s Mesh Network [2]

The BSS in traditional IEEE 802.11 is differentiated by a set of MPs and the mesh links which represents Wireless distributed system (WDS) in IEEE 802.11s mesh network. A mesh access point in IEEE 802.11s is a mesh point having functionality of access point (AP). A mesh point portal is an entity in Mesh network which allow numerous WLAN meshes to communicate with each other. An MPP can also

act as the IEEE 802.11 point portal and operate as a bridge/gateway between the WLAN mesh and other type of networks in the DS.

II. ROUTING PROTOCOL

Routing is an elementary attribute of Wireless Mesh Network (WMN). The performance of WMNs is directly affected by the strengths and weakness of routing protocols. The competing

technologies can take the several advantages of WMNs by enabling the routing protocols.

Wireless Mesh Networks are the part of mobile ad-hoc networks. So routing protocol used in MANET can easily used for WMN. Still there are some differences between them. First is, most of the time all the traffic starts from gateway and trimmings ups on gateway in WMNs. Second one is nodes are clearly separated from each other either in the form of stagnant nodes or mobile nodes.

A. Ad-hoc On-demand Distance Vector Routing Protocol (AODV)

[11] The Ad hoc On Demand Distance Vector (AODV) (Huhtonen 2004) is a reactive type routing protocol or on-demand protocol. In on-demand routing protocol, routes are creates and maintains only when nodes in network want to communicate with the other node in network. A node in network maintain the routing table which stores information regarding to the next hop to the preferred destination and a sequence number received from the destination, which is use for preserving the freshness of the information stored.

Algorithm: AODV routing protocol use three type of messages: Route REQuests (RREQ), Route REPlies (RREP) and Route ERRors (RERR). This protocol works in two phases: route discovery and route maintains. In a route discovery, route is initiated between two nodes only when they want to communicate. It is made by broadcasting a route request message with the destination and sequence number to the neighbors. When every node in network receives the route request message, they increase their hop metric and revised its own routing table. Upon receiving the route request message, the destination node throws a route reply message back to the source node. Route maintained is responsible for repairing a broken route or finding a new one when a route failure occurs. AODV have capability to notify the affected set of nodes when links fails. A route error message is propagated to transmitting node, so that they are able to cancel the routes using the lost link. AODV algorithm facilitates dynamic, self-configuring, self-healing, loop free, multi-hop routing between nodes which is suitable for WMN's characteristic.

B. Optimized Link State Routing Protocol (OLSR)

[12][13] The Optimized Link State Routing is a table driven proactive link state protocol. OLSR contain various optimizations that aim to drop the price of forward information in the network. In particular, for each node there is a subset of neighbors which is called the multipoint relays and is used to reduce the duplicate retransmission in the same region.

Algorithm: In order to wrap all two hop neighbor nodes, each node chooses its multipoint relay set among its one-hop neighbors. A bidirectional link is provided to each of those neighbors by OLSR. The MPR is used to occasionally broadcast information about its one-hop neighbors in the network. Each node calculates or updates its routes on the basis of this MPR selectors list. The route is made up of sequence of hops through MPRs. Each node periodically broadcasts HELLO messages containing a neighbor list and their link status in order to detect bidirectional links with neighbors. The HELLO messages permits every node to recognize the existence of neighbors up to two-hops. It also allows the selection of its MPRs. By using that information each node can construct its MPR selector table.

In routing table each node broadcasts specific control messages called Topology Control (TC), which is used to build the routing table for forwarding purposes. TC messages are sent from time to time by nodes to declare its MPR selector set. TC messages are used to maintain topology tables for each node. Because of that there is no route discovery delay and even if we do not increase the number of routes, routing overhead is still larger than a reactive protocol. If hello messages have been received freshly, OLSR assumes that a link never fails but is not always true in WMNs.

C. Hybrid Wireless Mesh Protocol (HWMP)

[5][14] The 802.11s specifies the Hybrid Wireless Mesh Protocol (HWMP) which operates on the MAC layer. HWMP is a Hybrid type of routing protocol which incorporates both proactive and reactive components. HWMP use routing metric or combination of routing metric. HWMP inherit advantage of both the routing

scheme that is the reactive routing provides great flexibility in dynamic environments and proactive tree based routing which is more efficient for static mesh networks. HWMP by default uses airtime metric and can be combined with other metrics to achieve better performance.

Algorithm: The reactive mode of HWMP is based on

AODV, which works at MAC layer. AODV routing protocol use three type of messages: Route REQuests (RREQ), Route REPlies (RREP) and Route ERRors (RERR). This protocol works in two phases: route discovery and route maintains. In a route discovery, route is initiated between two nodes only when they want to communicate. It is made by broadcasting a route request message with the destination and sequence number to the neighbors. When every node in network receives the route request message, they increase hop metric of its own and revised its own routing table. Upon receiving the route request message, the destination node throws a route reply message back to the source node. Route maintained is responsible for repairing a broken route or finding a new one when a route failure

occurs. In the Proactive mode of HWMP, one of the nodes in network plays the role of ROOT node. This ROOT node periodically broadcasts proactive type PREQs. PREQs contains address field of broadcast address. After receiving such message, every node sends PREP back to ROOT node. Through this process, a tree is build and ROOT node maintains the routing table which stores all possible destinations within the network. HWMP protocol contain following elements,

1. Root Announcement (broadcast) which informs mesh points about the existence and distance of Root Mesh Point.
2. Root Request (Broadcast/Unicast) which requests the destination mesh points to structure a reverse route to the source.
3. Route Reply (Unicast) which organized a forward route to source and validates the reverse route.
4. Route Error (Broadcast) which notify about the source which no longer supports certain route for receiving mesh points.

HWMP operate in two phase:

1. Route Discovery: In HWMP, Route discovery is done by on-demand routing. Route Request packet from the source node forms the forward paths and Route Reply Packet sends from destination node forms the reverse paths.
2. Route Maintenance: In active routes, the link state of nest hops is supervised by other nodes. In the case of link fails, a Route Error message which is a broadcast message is used to notify other nodes.

III. SIMULATION ENVIRONMENT

A. Performance Metric

The comparison is made between aforementioned routing protocols on the basis of following performance metric.

1) Packet Delivery Ratio

Packet delivery ratio is a very important factor to compute the performance of routing protocol in any network. The packet delivery ratio can be defined as ratio of the total number of data packets received at destinations and the total number of data packets sent from sources. High PDR indicate superior performance of network. Mathematically it can be shown as:

$$PDR = \frac{\Sigma \,(\text{Number of RECEIVED packets}) * 100}{\Sigma \,(\text{Number of SEND packets})}$$

2) End-to End Delay

Average End-to-end delay defines the time taken by a data packet to reach from source to destination through the network. The average end-to-end delay can be obtained by calculating the average of delay of successfully delivered messages. So, it is clear that end–to-end delay in some measure depends on the PDR. The probability of packet drop is depends on the distance between source and destination which is increased when distance is more between source node and destination node.

Mathematically it can be shown as:

$$Delay = \frac{\Sigma \,(\text{arrive time} - \text{send time})}{\Sigma \,\text{Number of connections}}$$

3) Bit Rate

The bit rate is defining as the number of bits which bypass all the way through the network from a source to destination in an agreed quantity of time, generally a second.

B. Simulation Parameter

The network simulator NS3 version 3.20 is used to establish 802.11s mesh network. IEEE802.11s draft3.0 was preconfigured in NS3. We have used grid topology and the result is taken by varying the number of nodes. The traffic application used is of type constant bit rate, with a maximum data rate of 50packet/sec.

TABLE I. SIMULATION PARAMETER

Parameter	Values
Wifi Model	Yans WiFi Helper
Topology	Grid Topology
Routing Protocol	AODV,OLSR,HWMP
Agent	UDP
No. of Packets	50
Packet Size	1024
Speed	Random
No. of Nodes	10,20,30,40,50
MAC	802.11s
Simulation Time	240 sec

IV. PERFORMANCE ANALYSIS

A. Packet Delivery Ratio

The fig 2 shows that performance of OLSR is better than AODV and HWMP. But when we increase the node density, performance of AODV constantly decreased. AODV gives very poor result when numbers of nodes are increased. Initially a performance of AODV is better than HWMP but after when we have increased numbers of nodes HWMP gives better performance than AODV. When there are large numbers of nodes HWMP is more preferable compare to AODV. Among these three routing protocols, performance of OLSR is the best in context of PDR.
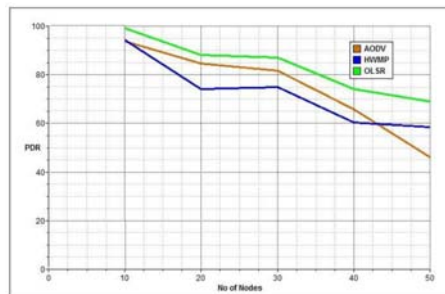

Fig. 2. No of Nodes verses Packet Delivery Ratio

B. End-to-End Delay

The Fig 3 demonstrates the performance of mentioned routing protocol on the basis of End-to-End Delay. It can be clearly seen from the figure that the delay of AODV is extremely high because it is an on demand protocol, it starts route discovery whenever two nodes want to communicate. While OLSR is a table driven protocol so it updates their routing table at certain time intervals so their delays are lesser compared to AODV. OLSR has less delay than that of AODV and HWMP which remains constant even after increasing number of nodes.
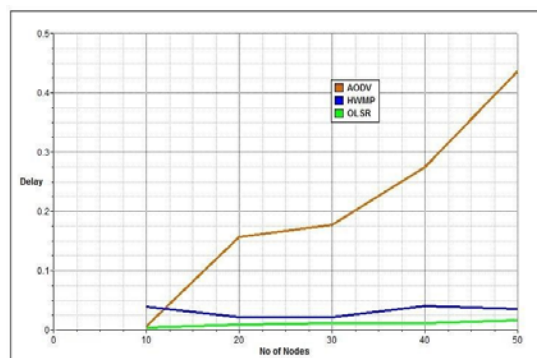

Fig. 3. No of Nodes verses End-to-End Delay

C. Bit Rate

The graph of bit-rate illustrates that initially OLSR is a superior in terms of data transfer speed than AODV and HWMP. But after increasing the numbers of nodes its performance is affected. Even after increasing the numbers of nodes, its bit rate remains constant. The performance of AODV is also decreased after some time when numbers of nodes are increased to some extent.
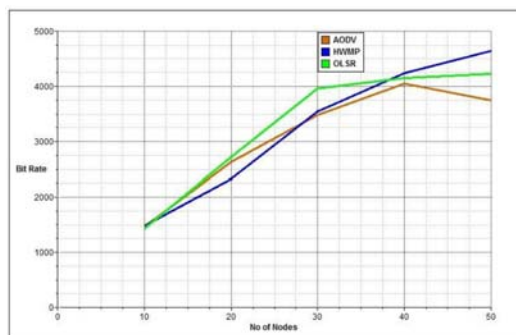
Fig. 4. No of Nodes verses Bit Rate

V. CONCLUSION

We have evaluated performance of unicast routing protocols named as AODV, OLSR and HWMP on the basis of some metrics. First metric is a PDR which shows the reliability of protocol. In terms of PDR, performance of OLSR is better than AODV and HWMP. AODV gives very poor result when numbers of nodes are increased. Second is End-to –End Delay, AODV having extremely high delay in compare to OLSR and HWMP. OLSR has less delay than that of AODV and HWMP which remains constant even after increasing number of nodes. Third one is bit rate; initially OLSR is a superior in terms of data transfer speed than AODV and HWMP. But after increasing the numbers of nodes its performance is affected. The performance of AODV is decreased after some time when numbers of nodes are increased to some extent.

We conclude that In WMN, OLSR is superior to HWMP and AODV in terms of PDR and End-to-End delay. If we want more data transfer speed than we can also go for HWMP instead of OLSR. But the performance of HWMP is not as better than OLSR in terms of PDR. The delay rate of HWMP is tolerated if we want more data transfer speed. The performance of AODV is very poor than HWMP and OLSR.

REFERENCES

[1] Ian F. Akyildiz, Xudong Wang, and Weilin Wang, "Wireless Mesh Networks: A Survey", Computer Networks, March 2005.

[2] Guido R. Hiertz, Sebastian Max, Rakesh Taori,Javier Cardona, Lars Berlemann and Bernhard Walke, "IEEE 802.11s: The WLAN Mesh Network", IEEE Wireless Communications, February 2010

[3] Myung J. Lee And Jianliang Zheng, Young-Bae Ko And Deepesh Man Shrestha "Emerging Standards For Wireless Mesh Technology", IEEE Wireless Communications, April 2006

[4] Camp, J.D., Knightly, E.W., "The IEEE 802.11s Extended Service Set Mesh Networking Standard", IEEE Communications Magazine, August 2008

[5] Xudong Wang and Azman O. Lim, "IEEE 802.11s wireless mesh networks: Framework and challenges", Ad Hoc Networks, August 2008

[6] S. M. Faccin et al., "Mesh WLAN Networks: Concept and System Design", IEEE Wireless Communication, April. 2006.

[7] S. Waharte, B. Ishibashi, R. Boutaba, "Performance Study of Wireless Mesh Networks Routing Metrics", Computer Systems and Applications, April 2008.

[8] Er.Pushpender Sarao , Dr. Sohan Garg, Prof. (Dr.) YashPal Singh "Wireless Mesh Networks: WMN Architecture, Issues and Challenges", International Journal of IT, Engineering and Applied Sciences Research (IJIEASR), September 2013.

[9] NS-3, http://www.nsnam.org

[10] Venkat Mohan.S, Dr. Kasiviswanath.N, "Routing Protocols for Wireless Mesh Networks", International Journal of Scientific & Engineering Research, August-2011

[11] C. Perkins, E. Belding-Royer, and S. Das, "Ad Hoc on-Demand Distance Vector (AODV) Routing", IETF RFC 3561, July 2003.

[12] Thomas Clausen and Philippe Jacquet, "Optimized Link State Routing Protocol (OLSR)", IETF RFC 3626, October 2003

[13] Christopher Dearlove, ThomasClausen and Philippe Jacquet, The Optimized Link State Routing Protocol version-2, IETF draft, September 2009

[14] Md.Shariful Islam, Md. Abdul Hamid, Choong Seon Hong, "A Secure Hybrid Wireless Mesh Protocol for IEEE802.11s Wireless Mesh Networks", December 2009

OPTIMAL EDGE DETECTION TECHNIQUE FOR DIAGNOSIS & TREATMENT OF LEUKOPLAKIA IN ORAL MUCOSA

K R Jain[1], N P Desai[2], E A Patel[3]
[1,2]Asst. Prof., [3] PG Student.
G. H. Patel College of Engg., and Technology, V V Nagar
Email: kavindrajain@gcet.ac.in, niravdesai@gcet.ac.in,
ektapatel460@gmail.com

Abstract: Tongue inspection plays a very important role to monitor the health of patient and it is commonly used in Traditional Chinese Medicine (TCM). Texture analysis of Tongue Contours is an important issue in development of disease diagnostic expert system using analysis of tongue images. In this paper we present an approach of medical biometrics to detect and diagnose Leukoplakia. The aim of this paper will be to enhance the extracted part of the tongue, finding the severity of affected part and decide the proper treatment of the same. In this proposed system we not only extract the affected area but also calculate the same using geometrical and textural features of image.

physiological and pathological changes and get a patient physical condition. Traditional tongue diagnosis mainly depends on the doctor's experience and knowledge, this can't cause the diagnosis of subjectivity and difficult to repeatability. It is required to combine TCM expert's clinical experience with modern information technology. In order to analyze tongue image, the important premise is to accurately segment tongue from original tongue image. Because of the various shapes and colors, and lots of noise information from the mouth, nose and face, segmenting the tongue effectively becomes a difficult problem. And the segmentation result will directly affect the accuracy of image analysis. So we need to improve the efficiency of the technique used to segment the tongue image.

M. Dhanalakshmi et al. [1] had introduced a sequential image processing technique for automated tongue segmentation in which a gradual, step by step sequential process for extraction of the shape feature, color feature and so on for the tongue analysis. The aim of this method was to reduce the complexity in tongue segmentation. Lam

*Keywords-***Tongue Image, Leukoplakia,**

ISEF, TCM, Tongue Extraction.

I.   INTRODUCTION

A tongue is an organ that reflects the physiological and clinic pathological condition of the body. Tongue diagnosis is one of the most widely used diagnostic methods in Traditional Chinese Medicine (TCM). Through the observation of tongue, the doctors can understand the body's ia Jaafar Belaidet al. [2] presented a new method for image segmentation based on the watershed

transformation using mathematical morphology.

In which topological gradient approach is used to avoid an over segmentation. Yian-Leng Chang et al. [3] propose a simple, yet general and powerful, region growing framework for image segmentation in which no parameter tuning or a priori knowledge about the image is required.

M. Kasset al. [4] firstly introduced the basic model of snake or active contours in 1987, which are curves defined within an image domain that can move under the influence of internal forces coming from within the curve itself and external forces computed from the image data. The defects of traditional dynamic contour are: (1) Smaller convergence domain, (2) Exist re-entrant corner in the target cannot be convergence. Therefore this method is less automatically, can't be completely out of people's participation, not suitable for large sample and clinical applications. Therefore Zhai Xue-Ming et al. [5] presents a new segmentation method called dual snake method, namely the use of two Snakes on both sides from inside and outside the body to locate the outline of the tongue, and then the exact division of the tongue part. Experiments show that the accuracy of the single-Snake is 81.63%, and the accuracy of the double Snake is 92.89%. So compared with the traditional segmentation, double Snakes have a lower request on the initialization of outline, and more accurate results of the segmentation.

The paper has been fragmented into six parts. Section 2 discusses the tongue anatomical precancerous diseases and its related problems. Section 3 comprises of the basic concepts of leukoplakia, extraction, its detection and further details. In section 4 we propose an approach for detection of leukoplakia. Section 5 concludes the paper. Acknowledgments are being provided to specialized dental doctors, without their massive support nothing would have been possible in section 6.

II. PROBLEM DEFINITION

In oral mucosa apart from all diseases related to tongue, we are particularly interested in Leukoplakia. The presence of white or gray colored patches on the tongue, gums, roof of your mouth, or the inside of the cheeks of your mouth may be a sign of leukoplakia. The patch may have developed slowly over weeks to months and be thick, slightly raised, and may eventually take on a hardened and rough texture. It usually is painless, but may be sensitive to touch, heat, spicy foods, or other irritation.

In the Traditional Chinese Medicine, patient physical condition was checked by the doctor through the observation of tongue but it mainly depends on auto biopsy done by doctor, later by his knowledge and experience to diagnose that part of tongue. Therefore it is very important to use computer technology to achieve the quality tongue diagnosis for a better treatment.

III. BASIC CONCEPTS OF LEUKOPLAKIA

Leukoplakia is a white or gray patch that develops on the tongue, the inside of the cheek, or on the floor of the mouth. It is more frequently found in men, can occur on any mucosal surface, and infrequently causes discomfort or pain. Leukoplakia usually occurs in adults older than 50 years of age. The presence of leukoplakia does not necessarily mean cancer, but this precancerous condition has the highest risk of developing into cancer.

For this diagnosis we suggest a technique as briefed in Table-I. The detail description of the same is explained below it.

TABLE I: PROPOSED ALGORITHM

Sr.No.	Steps
1	Acquire tongue anatomical images.
2	Select the Region of Interest (ROI).
3	Convert RGB image into YCbCr plane.
4	Apply pre-processing technique to remove noise and enhance the image.
5	Extraction of leukoplakia from image.

| 6 | Edge detection using optimal edge detection technique. |
| 7 | Measurement of severity geometrical and textural analysis. |

A. *Image Enhancement*

The original tongue image was captured by digital camera under standard light source situation. It usually contained tongue body, upper lip, partial lower lip and face. In which we require only the area of tongue body. So we extract the part in which we are interested from the original image. After that image is converted to YCbCr. Separating the three different planes of Y, Cb, Cr. Out of three planes Y plane has more information than Cb and Cr as can be seen in fig. 1. So here we select Y plane for further enhancement. Now for image enhancement we apply thresholding to separate out foreground and background region from the image.
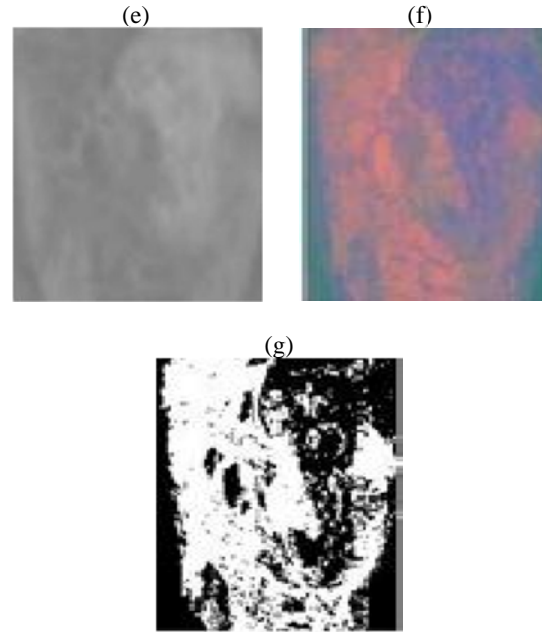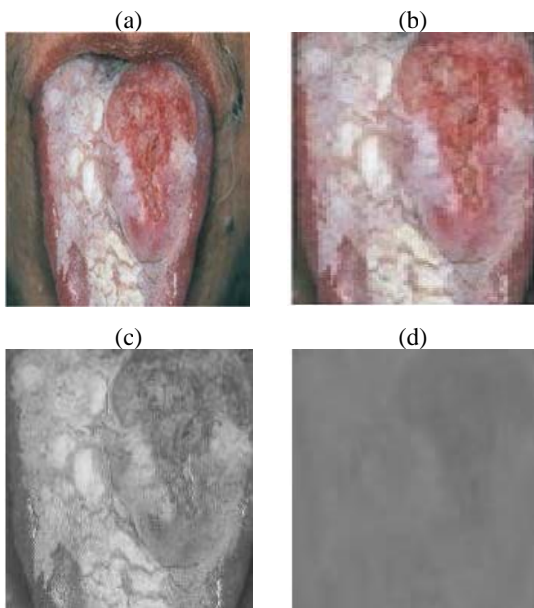
(e) (f)

(g)

Figure 1: (a) Original Image (b) ROI (c) Y plane (d) Cb plane (e) Cr plane (f) YCbCr (g) Threshold

(a) (b)

(c) (d)

B. *Edge Detection using ISEF*

In our proposed system edge detection of leukoplakia is done by ISEF (Infinite Symmetric Exponential Filter). The steps for ISEF algorithm are shown in Table II.

TABLE II: ISEF ALGORITHM

Sr.No.	Steps
1	Apply ISEF Filter in X direction
2	Apply ISEF Filter in Y direction
3	Apply Binary Laplacian Technique
4	Apply Non Maxima Suppression
5	Find the Gradient

Shen Castan Infinite Symmetric Exponential Filter is an optimal edge detector. In which first of all the whole image will be filtered by the recursive ISEF filter in X and Y direction respectively which can be implemented by using following equations:

Recursion in x direction:

$$Y_1[i,j]=(1-b)/(1+b)\ I[i,j] + b\ Y_1[i,j-1],$$
$$j= 1….N, i= 1…M \quad (1)$$

$$Y_2[i,j]=b\ (1-b)/(1+b)\ I[i,j] + b\ Y_1[i,j+1],$$
$$j= 1….N, i= 1…M \quad (2)$$

$$r[i,j]= Y_1[i,j]+ Y_2[i,j+1] \quad (3)$$

Recursion in y direction:

$$Y_1[i,j]=(1-b)/(1+b)\ I[i,j] + b\ Y_1[i-1,j],$$
$$i= 1…M , j= 1….N \quad (1)$$

$$Y_2[i,j]=b\ (1-b)/(1+b)\ I[i,j] + b\ Y_1[i+1,j],$$
$$i= 1…M , j= 1….N \quad (2)$$

$$Y[i,j]= Y_1[i,j]+ Y_2[i+1,j] \quad (3)$$

$$b=\text{thinning factor } (0<b<1)$$

Subtract the filtered image from the original image to obtain the Laplacian image. In the filtered image, there will be zero crossing in the second derivative at the location of an edge pixel because the first derivative of the image function should have an extreme at the position corresponding to the edge in image. Non maxima suppression is used for thinning purpose for false zero crossing. The gradient is either a maximum or a minimum at the edge pixel. If the second derivative changes sign from positive to negative, it is known as positive zero crossing and if it changes sign from negative to positive, it is known as negative zero crossing. We will permit positive zero crossing to have positive gradient and negative zero crossing to have negative gradient. We considered all other zero crossing as false zero crossing. Thresholding is applied on gradient image. One cutoff is used in simple thresholding but ShenCastan suggests for Hysteresis thresholding in which two cut offs are used. Thresholding is applied on the output of an edge detector to decide significant edges. Noise will create spurious response to the single edge that will create a streaking problem. Streaking is defined by breaking up of the edge contour caused by the operator fluctuating above and below the threshold.

Hysteresis thresholding is used to eliminate streaking problem. Individual weak responses usually correspond to noise, but if these points are connected to any of the pixels with strong responses, they are more likely to be actual edge in the image. Such connected pixels are treated as edge pixels if their response is above a low threshold. The ISEF algorithm is given in table II. Output is shown in fig. 2.

Figure 2: Leukoplakia extracted using ISEF

For the output shown in fig. 2 the thresholding value is kept constant for all the acquired samples.

C. Leukoplakia Extraction

We extract the leukoplakia from the resultant threshold image, so that leukoplakia affected area can be visible more properly as shown in fig. 3. The need of thresholded image was not only to see the affected area but also to measure the geometrical and textural features of the image. Based on the geometrical and textural features one could easily identify the affected part as well the next step for diagnosis.

Figure 3: Extracted Leukoplakia from thresholded image

IV. RESULTS AND DISCUSSION

As discussed above the leukoplakia affected areas of tongue were analyzed from the given set of database from Dr. Dhrumin Patel. It is to be noted here that the results so obtained after the geometrical and textural based feature extraction are quite satisfactory and approved even by the doctor. Moreover the results are satisfying as compared to clinical laboratory diagnosis. In case of clinical laboratory data destructive analysis is to be done where the sample of the affected area of patients tongue is taken and being analyzed. Whereas in this particular approach the technique so used is not only quick, but even it is nondestructive in nature. The information so gathered can be used for further treatment of the patient. The threshold so taken for the rest samples of tongue were same and hence the results too were satisfactory as per the doctor's approval. The images shown below clear depict the above said approach for the purpose of further diagnosis and treatment.
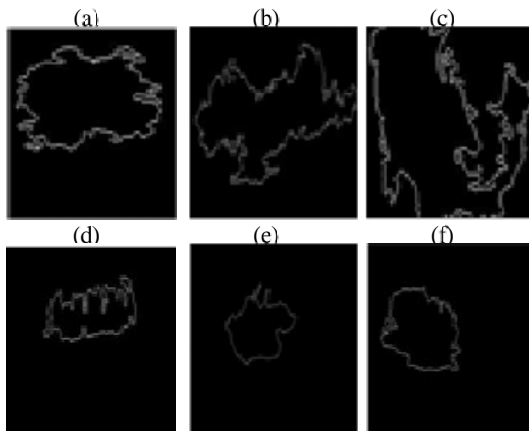

Figure 4 Results of various tongue image of various patients for detection of leukoplakia

V. GEOMETRICAL AND TEXTURAL FEATURES

For severity measurement, geometrical and textural features must be analyzed. As these two things are the basic fundamental component of analysis for further treatment and medication in case of tongue. In case of such measurements the two things required is the area being affected and the other is its severity. For geometrical features,

as shown in fig. 2 the edges are being detected which help in first of all finding the area which can done by finding out length of the horizontal and vertical level of white pixel from top to bottom. In case of textural analysis the region bounded boxes would be clearly depicting the area more and less affected as based on the white patches intensity such rectangular shapes would be produced to understand the severity in the affected area of tongue as shown in fig. 5. As shown in the fig. 4 (a)-(f) are 6, 5.9161, 7.1414, 5.7446, 6.7082, 7.4833 and 7.8740 respectively are the diagonal length of the pixels in the affected area. Similarly for the case of textural features the fig. 6 as shown below clearly indicates the boxes where the white patches are growing presently and the left over areas are the most affected part of the image having strong white patches. Even based on those boxes one can calculate the area being affected.

VI. CONCLUSION

At present, to realize the recognition and diagnosis of tongue image is very important to the development of tongue diagnosis in **TCM**. We suggest a new approach for automatic tongue area extraction in the system of tongue inspection.

The figures shown in 4 & 5 clearly depict its effect on tongue and the various approaches

through which one can find the extracted and affected part of tongue.

VII. ACKNOWLEDGMENT

REFERENCES

[1] M. Dhanalakshmi, P. Premchand, and A. Govardhan "An Approach For Tongue Diagnosing With Sequential Image Processing Method" International Journal Of Computer Theory And Engineering, Vol. 4, No. 3, June 2011.

[2] Lamia JaafarBelaid and Walid Mourou "Image Segmentation: A Watershed Transformation Algorithm" Image Anal Stereol 2009; 28:93-102. [3] Yian-Leng Chang And Xiaobo Li "Adaptive Image Region-Growing" IEEE Transactions On Image Processing, Vol. 3, No. 6, November 1994. [4] Kass M, Witkin A, Terzopoulos D. "Snakes: Active Contour Models", International Journal of Computer Vision, 1988, 1(4):321-331.

[5] ZhaiXue-Ming, Lu Hang-Dong, Zhang Li-Zhong "Application of Image Segmentation Technique in Tongue Diagnosis" 2000 International forum on Information Technology and Applications.

[6] John Canny. A Computational Approach to Edge Detection. Pattern Analysis And Machine Intelligence, IEEE Transactions On, Pami8(6):679–698, Nov. 1986.

[7] X. Yu, Y. Tan, Z Zhu, Z. Suo, G. Jin, W. Weng, X. Xu, W. Ge, "Study On Method Of Automatic Diagnosis Of Tongue Feature In Traditional Chinese Medicine", Chinese Journal Of Biomedical Engineering, 1994, 13(4): 336-344.

[8] Chiu Chuang-Chien, "A Novel Approach Based On Computerized Image Analysis for Traditional Chinese Medical Diagnosis of the Tongue" [J]. Computer Methods and Programs in Biomedicine 2000, 61(2) 77—89.

[9] Saleh Al-Amri, Salem; Kalyankar, N. V.; Khamitkar S., D. "Image Segmentation By Using Threshold Techniques" Journal Of Computing, Volume 2, Issue 5, May 2010.

[10] Y.W.Jiang, "Computerization of Traditional Tongue Diagnosis System" [J]. Chinese Journal of Integrated Tradition and Western Medicine 2000, 20(2) 145—147.

[11] S. Shen, B. G. Wei, "Image Analysis for Tongue Characterization", Acta Electronica Sinica, 2001, Pp.1762-1765.

[12] Y.W.Jiang, "Computerization of Traditional Tongue Diagnosis System" [J]. Chinese Journal of Integrated Tradition and Western Medicine, 2000, 20 (2):145-147.

[13] Jia Wu, Yonghong Zhang, Jing Bai, "Tongue Area Extraction in Tongue Diagnosis of Traditional Chinese Medicine," Iengineering in Medicine And Biology Society, IEEE-EMBS 2005. 27th Annual International Conference of the Volume, Issue, 2005 Pp. 4955 – 4957.

[14] Y. Jiang, J. Chen, H. Zhang, "Computerized System of Diagnosis of Tongue in Traditional Chinese Medicine", Chinese Journal of Integrated Traditional and Western Medicine, 2000, 20(2): 145-147.

[15] L. Shen, B. Wei, Y. Cai, X. Zhang And Y. Wang, "Image Analysis For Tongue Characterization", Chinese Journals Of Electronics, 2003, 12(3):317-323.

[16] B. Pang, D. Zhang, And K. Wang, "Tongue Image Analysis For appendicitis Diagnosis," Transactions on Information Sciences, Vol. 175, No. 3, Pp: 169-176, 2005.

[17] Zhou Yue, Shen Li, Yang Jie, "Feature Analysis Method of Tongue Image by Chinese Medical Siagnosis Based On Image Processing", Infrared and Laser Engineering, 2002, Vol. 31 No. 6, 490-494.

NUMERICAL STUDIES ON HIGH PRESSURE RATIO AIRFOILS FOR AXIAL FLOW COMPRESSORS

Aravind G P[1], Nilesh P Salunke[2], Salim A. Channiwala[3]
[1, 2, 3,] Sardar Vallabhbhai National Institute of Technology,
Email: [1]anu.aravind007@gmail.com, [2]sainilesh1@gmail.com, [3]sac@med.svnit.ac.in

Abstract— The gas turbine engine manufacturers are looking for the efficient engines which can produce higher thrust, and having higher thrust to weight ratio. To achieve these goals, improvement in compressor blade design is essential. Therefore, the goal of the blade design is to achieve the desired flow turning with minimum losses, within the constraint of the blade rows. The new airfoil design include various parameterization, meshing, solving N-S computation and optimization techniques. A CDA airfoil section has been used as base airfoil and then parameterized by Bezier Parsec parameterization method. The optimization of parametric CDA cascade model is carried out by Genetic algorithm coupled with CFD. Parameterization and generation of new airfoil coordinates are made using the programme code prepared in Matlab. Numerical simulation have been carried out by CFD software GAMBIT and FLUENT. Matlab evaluates the airfoil and optimizes the airfoil using Genetic algorithms and checks the objective function in each iteration. The main objective is to get lower value of total pressure loss coefficient at higher pressure ratio without any flow separation.

This would indicates that the airfoil section is capable of producing that pressure ratio without flow separation. This process is repeated till an optimum solution reached. The maximum pressure ratio attained by base airfoil was found out to be 1.4. The process was carried out for finding solutions for higher pressure ratios. The optimal solutions are obtained for higher pressure ratios up to 3.0.

Index Terms— Numerical Simulation, High Pressure Ratio Airfoils.

NOMENCLATURES

b	Bezier Parameter
c	Chord
y	Camber/Thickness
k	Curvature
p	Static Pressure
T	Static Temperature
P_o	Stagnation Pressure
T_o	Stagnation Temperature
V	Velocity
U	Peripheral Velocity
C_D	Coefficient of Drag
ΔP_o	Total Pressure Loss

r	Radius	
β	Blade angle	
θ	Camber angle	
ω		Total Pressure Loss Coefficient
X_{cg} ,Y_{cg}		Center of Gravity of airfoil
Cp		Coefficient of Pressure
γ		Stagger angle

I. INTRODUCTION

The study of turbomachinery has gone through several historical stages from the 1940s till now. The study in this period has moved from one-dimensional to two-dimensional and three-dimensional flows, from inviscid to viscous flows, and from steady to unsteady flows [1]. The principal type of compressor being used nowadays, in majority of the gas turbine and power plants and especially in aircraft applications, is the axial flow compressor. This dominance is mainly due to the ability of the axial flow compressor to satisfy the basic requirements of the aircraft gas turbine. Transonic axial flow compressors are today widely used in aircraft engines to obtain maximum pressure ratios per single stage. High stage pressure ratios are important because they make it possible to reduce the engine weight and size and, therefore investment and operational costs. Performance of transonic compressors has today reached a high level but engine manufacturers are oriented towards increasing it further [2]. A small increment in efficiency, for instance, can result in huge savings in fuel costs. The increase in gas turbine efficiency mainly dependent on Increase in Pressure Ratio. So in the present work CDA airfoil is parameterized and optimized for higher pressure ratios up to 3.0 with reduction of overall total pressure loss.

II. LITERATURE REVIEW

One of the challenging topics in optimization is the selection of the mathematical representation of airfoil design variables that provides a wide variety of possible airfoil shapes. A new method for airfoil shape parameterization is presented which takes into consideration the characteristics of viscous transonic flow particularly around the trailing edge. Typical practice is to resort to using a series of curves, such as polynomials and Bezier curves, to describe the profile. This typically reduces the number of degrees of freedom to a much smaller, manageable number. The method is then applied to airfoil shape optimization at high Reynolds number turbulent flow conditions using a Genetic Algorithm [3]. The influence of the selection of the parameterization on the optimization has received relatively little consideration to date. A new airfoil parameterization, Bezier-PARSEC, that was developed to extend and improve the typical Bezier parameterization found in use. This parameterization was found to fit the known shape of a wide range of existing airfoil profiles as well as resulting in accelerated convergence. [4], [5]. Another innovative method for airfoil geometry optimization is based on the coupling of a PARSEC parameterization for airfoil shape and a genetic algorithms (GA) optimization method to find Nash equilibria (NE). While the PARSEC airfoil parameterization method has the capability to faithfully describe an airfoil geometry using typical engineering parameters, on the other hand the Nash game theoretical approach allows each player to decide, with a more physical correspondence between geometric parameters and objective function, in which direction the airfoil shape should be modified[6]. Lars Sommer [7] introduces a new curvature based design parameterization of two-dimensional high pressure compressor blade sections to be used in a multi-criteria aerodynamic design optimization process. The suction side of the airfoil section is represented by its curvature distribution which is described by a B-spline curve. The coordinates are then derived by numerical integration. The camber line as well as pressure side are obtained by adding a thickness distribution perpendicularly to the camber line. Yongsheng Lian [8] reviewed the recent progress in design optimization using evolutionary algorithms to solve real-world aerodynamic problems. Evolutionary algorithms (EAs) are useful tools in design optimization. Due to their simplicity, ease of use, and

suitability for multi-objective design optimization problems, EAs have been applied to design optimization problems from various areas. Sergey Peigin [9] suggested a new approach to the constrained design of aerodynamic shapes. The approach employs Genetic Algorithms (GAs) as an optimization tool in combination with a Reduced-Order Models (ROM) method based on linked local data bases obtained by full Navier–Stokes computations. Naixing Chen [10] describes an optimization methodology for aerodynamic design of turbomachinery combined with a rapid 3D blade and grid generator (RAPID3DGRID), a N.S. solver, a blade parameterization method (BPM), a gradient-based parameterization-analyzing method (GPAM), a response surface method (RSM) with zooming algorithm and a simple gradient method. Syam [11] suggested the Bezier-PARSEC method for camber and thickness distribution of CDA airfoil and Genetic Algorithm for optimization. T Sonoda [12] introduced two different numerical optimization methods; the evolution strategy (ES) and the multi-objective genetic algorithm (MOGA), which were adopted for the design process to minimize the total pressure loss and the deviation angle at the design point at low Reynolds number condition. Akira Oyama [13] developed a reliable and efficient aerodynamic design optimization tool using evolutionary algorithm for transonic compressor blades.

III. PARAMETERIZATION AND OPTIMIZATION

Here we are introducing the method used for the parameterization of CD Airfoil and the MATLAB Genetic Algorithm (GA) toolbox used for Optimization. The mainly used parameterization methods are briefly presented herein.

A. Bezier Curves [3]

One of the most popular methods for airfoil shape representation is the Bezier curve method that introduces control points around the geometry. These points are then used to define the airfoil shape. A Bezier curve of degree n is uniquely defined by n +1 vertex points of a polygon. These vertices are called the control points of the nth order Bezier curve. The general expression for an nth order Bezier curve is given below:

$$P(u) = \sum_{t=0}^{n} P_i \left(\frac{n!}{i!(n-1)!}\right) u^i (1u)^{n-i} \tag{1}$$

Where Pi = i^{th} control point. The parameter u goes from 0 to 1; with 0 at the zeroth control point and unity at the nth control point. The Bezier parameterization is determined by its control points which are physical points in the plane. However the other control points need not be on the curve even though they determine the shape of the curve. The number of design variables is often so high that the computational time of the whole process becomes unaffordable. Fainekos and Giannakoglou [14] used the Bezier curve to define the airfoil shape in inverse design of turbomachinery blade airfoils. In their research, Fainekos and Giannakoglou [14] fixed the leading edge and trailing edge control points and also abscissas of the rest of the control points. Song and Keane [15] compared the Bezier curve method with original basis functions in generating airfoils and concluded that the Bezier curve produces better shapes in terms of accuracy but at a higher computational time. In addition, special curvature distributions that are required to achieve a desirable pressure distribution are not evident in this method.

B. PARSEC method [3]

Another common method for airfoil shape parameterization is PARSEC which has been successfully applied to many airfoil design problems. This technique has been developed to control important aerodynamic features by using the finite number of design parameters. In this method there are basic eleven parameters that are used in PARSEC method including leading edge radius (r_{LE}), upper and lower crest locations (X_{UP} , Z_{UP} , X_{LO} , Z_{LO}) and curvatures (Z_{xxUP} Z_{xxLO}), trailing edge coordinate(Z_{TE}) and direction(α_{TE}), trailing edge wedge angle(β_{TE}) and thickness(ΔZ_{TE}). A

linear combination of shape functions is used to present the airfoil shape in this method.

$$Z_K = \sum_{n=1}^{6} a_{n,k} X_K^{(n-1)/2} \qquad (2)$$

The coefficients a_n are determined from defined geometric parameters. The airfoil is divided into upper and lower surfaces and the coefficients a_n are determined using the information of the points in each section. The subscript k changes from 1 to 2 in order to consider the length of the upper and lower surfaces, respectively.

C. Bezier PARSEC Parameterization [4]

Derksen and Rogalsky [4] have introduced the Bezier–PARSEC parameterization. This approach will use the advantages of both the Bezier and PARSEC parameterization and avoid the disadvantages of both to represent the airfoil and provide enough flexibility over geometrical and aerodynamic parameters. Their approach is further subdivided into two parameterization methods viz. BP3333 and BP3434. In both the methods, Bezier control points are determined in terms of the PARSEC parameters of an airfoil. The camber-thickness formulation of the Bezier curves is more directly related to the flow than is the upper curve-lower curve formulation for PARSEC, while the PARSEC parameters are more aerodynamically oriented than the Bezier parameters. The BP parameterization uses the PARSEC variables as parameters, which in turn define four separate Bezier curves. These curves describe the leading and trailing portions of the camber line, and the leading and trailing portion of the thickness distributions. While the Bezier parameterization joins the leading and trailing curves with first-order continuity.

The BP parameterization uses second-order continuity. The parameters are:

Leading edge radius – rle,
Trailing camber line angle – ate,
Trailing wedge angle – bte,
Trailing edge vertical displacement – zte,
Leading edge direction -gle,
Location of the camber crest –xc, yc,
Curvature of the camber crest – kc,
Position of the thickness crest – xt, yt,
Curvature of the thickness crest –kt ,

the half thickness of the trailing edge –dzte, and several Bezier variables, b0, b2,b8, b15 and b17. This type of parameterization improves the robustness and convergence speed for aerodynamic optimization, which makes it more suitable for optimization using Genetic algorithms.

D. Optimization of Base CDA using GA [11]

Total pressure loss as objective function for optimization since it is more significant in the compressor blade efficiency. And the optimization is carried out for compressor cascade at high subsonic velocities. The optimization is meant for finding a profile section with minimal loss for the compressor blade. In this investigation we selected a CDA cascade, third stage of a compressor for the optimization. Before starting the optimization process we used to analyze the base cascade to predict the performance. The analysis is carried out numerically in CFD softwares, Gambit for modeling and meshing and Fluent for analysis. The optimization of cascade has mainly five steps as shown on the optimization flow chart. All the process is carried out using Matlab code. The design parameters are selected from the parameters obtained from the BP334. This new parameters are generated at each iteration by the GA based on the constraints and the objective function. We selected 15 parameters of BP3434 for optimizing the cascade. The first step is terminated with the generation of the new parameters by GA. The next step is to generate the airfoil section from these parameters. In the third step CFD software Gambit is called in Matlab in batch mode for the cascade modeling and meshing using reading the Gambit journal file in Matlab. After the completion and generation of the mesh file as a fourth step Fluent is called in Matlab using the system command and reads the Fluent journal file, which includes all the commands for the analysis. By the execution of the Fluent we will get all the inlet and outlet parameters such as total pressures, total temperatures, static pressures, Mach numbers, etc. Also we will get the flow parameters over the cascade i.e. Mach number, static pressure, etc. The objective function is selected as total pressure loss

coefficient for this optimization which calculated from the results of Fluent analysis. At each iteration GA checks the value of the loss coefficient for the next generation of next population of parameters. The process ends when the loss coefficient is minimized. Genetic Algorithm (GA) is used as an optimization algorithm because of its global optimization nature and speed of convergence. The objective function used for GA is total pressure loss coefficient. We selected the constraint as Chord length of the Cascade and is fixed as 46.46 mm and set the number of generation as 100 with a crossover fraction of 0.8. After calculating and checking the value of loss coefficient GA generates the new population based on the crossover, selection and mutation with a constraint fixed chord length.

After the convergence of the optimization algorithm for a generation of 100 we obtained the airfoil section which has minimized the objective function. The table 1 shows the newly generated profile has optimal total pressure loss coefficient compared to the base profile.

Table 1: Comparison of Base and Optimized Airfoil [11]

Airfoil Sections	Total pressure		Pressure loss coefficient
	Inlet	Outlet	
Base Airfoil	33800	335150	0.0427
Optimized Airfoil	33800	335370	0.0394

This process was repeated for various pressure ratios ranging from 1.1 to higher pressure ratios and it was found that there was a drag reversal after a pressure ratio of 1.4. The negative drag indicates the reversal of flow hence we derived a conclusion that a pressure ratio greater than 1.4 cannot be achieved from the above airfoil for the given set of conditions and there is a need to optimize the airfoil further to gain higher pressure ratios.

E. Optimization of CDA for Higher Pressure Ratios up to 2.4 [16] [17]

The following boundary conditions were applied:

Solver: Green Gauss node based, 2d, steady, implicit, density based

Model: Spalart-Allmarus

Convergence Criteria: 0.001

Fluid: Air with ideal gas density and Sutherland viscosity

Discretization: Flow: Second order upwind

Modified turbulent viscosity: Second order upwind

Inlet Total Pressure P_{O1} = 338000 Pa

Inlet Total Temperature T_{O1} = 426K

Boundary conditions:

Pressure Ratio	Inlet Mach No.	P_1 (Pa)	T_{02} (K)	P_2 (Pa)
1.5	0.75	232737.6	478.3231	349106.5
1.6	0.75	232737.6	487.225	372380.2
1.7	0.75	232737.6	495.7379	395654
1.8	0.75	232737.6	503.9003	418927.8
1.9	0.75	232737.6	511.7449	442201.5
2.0	0.75	232737.6	519.2998	465475.3
2.2	1.2	139383.4	533.6354	306643.62
2.4	1.4	106213.4	547.0681	254912.62

Table 2: Boundary Conditions for Higher PR [16] [17]

The table 3 shows the total pressure loss coefficient obtained up to 2.4 pressure ratios

Table 3: Pressure loss coefficient comparison up to 2.4 PR [17]

Pressure Ratio	CDA Base Airfoil	Optimized Airfoils
	Pressure Loss Coefficient	Pressure Loss Coefficient
1.5	----	0.007903
1.6	----	0.006527
1.7	----	0.009531
1.8	----	0.005681
1.9	----	0.004332
2.0	----	0.017324
2.2	----	0.008038
2.4	----	0.015610

IV. SIMULATION RESULTS OF HIGHER PRESSURE RATIOS MORE THAN 2.4

Further optimization of the airfoil and up to how much pressure ratio will be possible is found out in this work. We obtained a pressure ratio of 3.0 without any flow separation for a Mach number of 1.4. Beyond that further optimization is not possible with this method.

Table 4: Boundary conditions for Higher PR up to 3.1

Pressure Ratio	Inlet Mach No	P_1 (Pa)	T_{02} (K)	P_2 (Pa)
2.6	1.4	106213.4	559.7233	276154.9
2.8	1.4	106213.4	571.7011	297397.6
3.0	1.4	106213.4	583.0824	318640.2

The boundary conditions for pressure ratios up to 3.0 is as shown in table 4.

Distribution of Mach number of Optimized airfoils are given below.
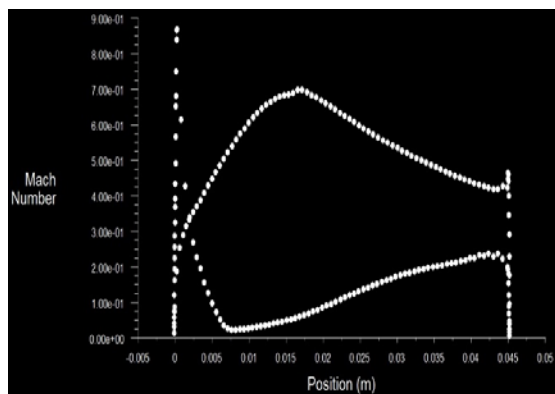
Figure 1: Mach number plot for optimized 2.6 PR airfoil
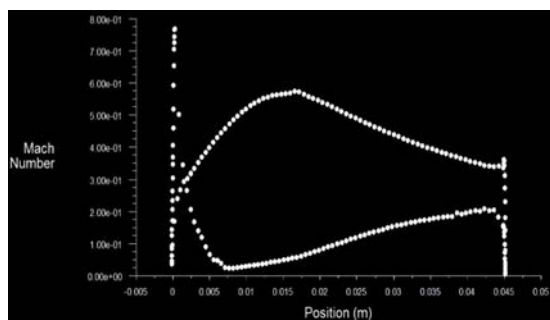
Figure 2: Mach number plot for optimized 2.8 PR airfoil
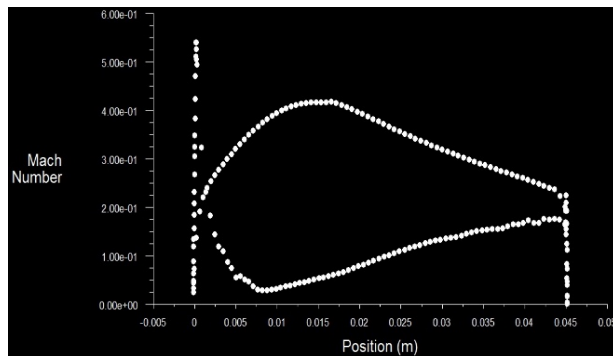
Figure 3: Mach number pot for optimized 3.0 PR airfoil

The newly optimized airfoils can perform better at higher pressure ratios up to 3.0. The optimized blades have shown perfect velocity and pressure distribution as of CDA. In the above plots we can see the exit Mach number is reducing as the pressure ratio increases.

Table 5: Pressure Loss Coefficient Comparison for PR up to 3.0

Pressure Ratio	CDA Base Airfoil	Optimized Airfoils
	Pressure Loss Coefficient	Pressure Loss Coefficient
2.6	----	0.006009
2.8	----	0.001717
3.0	----	0.007102

V. VALIDATION OF SIMULATION RESULTS

The optimized airfoil showed close CDA characteristics which confirm its good behaviour at higher pressure ratios. The suction peak is low at higher pressure ratios as expected and uniform diffusion is there till the trailing edge. The pressure on the lower surface increases uniformly till trailing edge. It is also observed that as the pressure ratio increases the peak Mach number decreases. For given pressure ratios, on upper surface, the Mach number first increases to a value of peak Mach number and thereafter it reduces continuously. On lower surface, Mach number first reduces and then increases gradually. It signifies that over upper surface, fluid is accelerated first and then it

decelerates constantly to match the flow conditions at the trailing edge. These all are the typical characteristics of a controlled diffusion airfoil. Hence our optimized airfoils exhibit the characteristics of a CDA airfoil.

VI. CONCLUSION

- The parameterization and GA optimization method is capable of finding efficient and optimum airfoils in fewer number of generations.
- The development of a combined Bezier-PARSEC (BP) parameterization utilize the advantages of both the Bezier and PARSEC parameterizations.
- Coupling of Bezier-PARSEC parameterization with GA and CFD together, offers an optimal cascade profile with a reasonable total pressure loss co efficient reduction with efficient flow pattern over the cascade.
- The base CDA airfoil can offer maximum pressure ratio of 1.4, beyond which a converged solution is not obtained indicating that it cannot gain pressure ratios higher than 1.4.
- The blade optimization with Bezier PARSEC Parameterization has offered most optimized results. The newly optimized blades can perform better at higher pressure ratios up to 3.0. The optimized blades have shown perfect velocity and pressure distribution as of CDA. Up to 3.0 PR and Mach 1.4 we can use these optimized airfoils without any flow separation.

REFERENCES

1. Naixing Chen., Aerothermodynamics of Turbomachinery Analysis and Design, 1st Edition, John Wiley & Sons,Singapore,2010,chap.14.
2. Saravanamuttoo H.I.H, Rogers G. F. C, Henry Cohen., Gas Turbine Theory, 6th Edition, Prentice Hall, USA, 2008.chap.5
3. Ava Shahrokhi, Alireza Jahangirian, "Airfoil shape parameterization for optimum Navier–Stokes design with genetic algorithm", Aerospace science and technology, 11(2007) 443-450
4. R.W. Derksen, Tim Rogalsky, "Bezier-PARSEC: An optimized aerofoil parameterization for design", Advances in Engineering Software 41 (2010) 923–930.
5. Athar Kharal, Ayman Saleem, "Neural networks based airfoil generation for a given Cp using Bezier–PARSEC Parameterization", Aerospace Science and Technology 23 (2012) 330–344.
6. Pierluigi Della Vecchia, Elia Daniele, Egidio D'Amato, "An airfoil shape optimization technique coupling PARSEC parameterization and evolutionary algorithm", Aerospace Science and Technology 32 (2014) 103–110.
7. Lars Sommer, Dieter Bestle, "Curvature driven two-dimensional multi-objective optimization of compressor blade sections", Aerospace Science and Technology 15 (2011) 334–342.
8. Yongsheng Lian, Akira Oyama, Meng-Sing Liou, "Progress in design optimization using evolutionary algorithms for aerodynamic problems", Progress in Aerospace Sciences 46 (2010) 199–223
9. Sergey Peigin, Boris Epstein, "Robust optimization of 2D airfoils driven by full Navier–Stokes computations", Computers & Fluids 33 (2004) 1175–1200.
10. Naixing Chen, Hongwu Zhang, Yanji Xu, Weiguang Huang, "Blade Parameterization and Aerodynamic Design Optimization for a 3D Transonic Compressor Rotor", Proceedings of the 8th International Symposium on Experimental and Computational Aerothermodynamics of Internal Flows Lyon, July 2007, Paper reference: ISAIF8-0021
11. Syam, Channiwala S A, "Optimization of CDA cascade using Parameterization and Genetic Algorithm coupled with CFD", 2nd International Conference on Mechanical, Automotive and Aerospace Engineering, ICMAAE 2013.

12. T Sonoda, Y Yamaguchi, T Arima, M Olhofer, B Senghoff and H A Schreiber, "Advanced High Turning Compressor Airfoils for Low Reynolds Number Conditions, Part 1: Design and Optimization", Proceedings of ASME Turbo Expo 2003, GT 2003-38458.

13. Akira Oyama, Meng sing Liou, Shigeru Obayashi, "Transonic Axial Flow Blade Shape Optimization using Evolutionary Algorithm and 3D Navier Stokes Solver", AIAA Journal of Propulsion and power, 2002-5642.

14. Fainekos and Giannakoglou, Inverse Problems in Science and Engineering, 4th Edition, Taylor & Francis, UK, 2004 chap 4.

15. Song W, Keane A, A Study of Shape Parameterization Methods for Airfoil Optimisation, 10th AIAA/ISSMO Multidisciplinary Analysis and Optimization Conference, 2004-4482.

16. Vilash Rajendra Shingare, A study on High Pressure Ratio Airfoils for Axial Flow compressors, Mtech Thesis, S. V. National Institute of Technology, Surat, 2012.

17. Rajesh N, High Pressure Ratio Blade Design by Parameterization and Optimization, MTech Thesis S. V. National Institute of Technology, (2014).

18. MATLAB User Guide Genetic Algorithm and Direct Search Toolbox User's Guide Copyright, Mathworks, 2004.

DIGITAL SIMULATION OF PRODUCER GAS FIRED SI ENGINE

Rahul P. Nagpure[1], Parth D. Shah[2], Salim A. Channiwala[3]

[1, 2, 3]Sardar Vallabhbhai National Institute of Technology

Email:[1]rahulpnagpure@gmail.com, [2]shahparth2525@gmail.com, [3]sac@med.svnit.ac.in

Abstract—Engine emissions becoming stringent, gaseous fuels are gaining prominence as cleaner fuels like LPG and CNG both for stationary and automotive applications. But scarcity of those fuels arises big question for future. Producer gas obtained from biomass gasification can be good alternative for non-renewable fuels especially in developing country like India, where biomass is available in huge quantity. In the present study simulation based on actual thermodynamic cycle analysis is performed to assess the performance of 118 cc S.I. engine. All the four basic processes taking place in an S.I. engine are analyzed and the values of pressure and temperature at every 2° of crank rotation are found out with the aid of certain assumptions. The model involves good deal of calculations and iterations and hence, it is coded in 'c'. The simulation result is validated with the technical specifications provided in the technical manual of the engine. Digital simulation shows with producer gas as a fuel power and thermal efficiency relatively de-rated by 11.54 % and 5.72 % respectively, compared to gasoline.

Index Terms— Digital Simulation, Producer Gas Fuel.

NOMENCLATURES

ATDC After Top Dead Centre

BTDC Before Top Dead Centre

BMt Billion Metric tones

CA Crank Angle

cc Cubic Centimeters

C_h Convection Heat-Transfer

C_h Convective Heat-Transfer Co-Efficient

C_k Thermal Conductivity

C_m Mean Piston Velocity

CNG Compressed Natural Gas

CPG Compressed Producer Gas

CR Compression Ratio

D Cylinder Bore

GHG Greenhouse Gases

h Steady Turbulent Heat-Transfer

HC Hydro-Carbons

IA Ignition Advance

L Cylinder Stroke Length

LNG Liquefied Natural Gas

Mtoe Million Tons of Oil Equivalent

NO_X Nitruc Oxides

Nu Nusselt Number

Re Reynolds Number

S.I. Spark Ignition

V_s Displacement/Swept Volume

W_{mv} Mean Gas Velocity

μ_{cy} Viscosity of Cylinder Gas

I. INTRODUCTION

In the year 2013, India's net imports are nearly 144.3 million tons of crude oil, 16 Mtoe of LNG and 95 Mtoe coal totaling to 255.3 Mtoe of primary energy which is equal to 42.9% of total primary energy consumption [1]. India imports nearly 75% of its 4.3 million barrels per day crude oil needs but exports nearly 1.25 million barrels per day of refined petroleum products which is nearly 30% of its total production of refined products [2]. The growth of electricity generation in India has been hindered by domestic coal shortages and as a consequence, India's coal imports for electricity generation increased by 18 % in 2010. The electricity sector in India had an installed capacity of 249.488 GW as of end June 2014 [3]. World CO_2 (GHG) emission will grow from 31 BMt in 2010 to 45 BMt in 2040, which is mainly responsible for global warming. This data shows there is desperate need of new renewable energy resource. India has biomass capacity of 66000 MW [2] in form of resources such as rice husk, crop stalks, small wood chips, and other agro-residues. Biomass can be gasified in gasifiers and used as alternative fuel for current depleting fuels.

II. LITERATURE REVIEW

Gasoline has the fastest flame propagation development followed by LPG and CNG, CPG. CPG burns with blue flame compared to violent combustion of gasoline. Presence of H_2 causes fast burning rates initially, which slows down due to low burning speed of CO after H_2 has burnt [4]. CNG having higher efficiency and lower CO, CO_2, HC emission compared to gasoline and LPG but produces more NOx emission [5], [6]. But these fuels are on the verge of depletion. Shashikantha [7] reported that Producer gas with low energy density (5 MJ/kg) but reasonably high mixture energy density (2.12 MJ/kg) can replace these gases with almost same thermal efficiency of 28–32 %. but power derating of up to 30 %. Presence of Hydrogen does not give any pre-ignition problem due to gas being dilute. Producer Gas

efficiency increases with increase in CR 30.7 % at CR of 17 and reduces to 27.4 % at CR of 10 [8]. Ignition advance should be retarded for increase in CR. Producer gas can be used up to CR of 17 without formation of knock [8], [9]. It reduces CO emissions considerably but NO_X and CO_2 will be increased. Hydrogen content in gas increases thermal efficiency but it is limited by process of gasification.

Dual-fuel mode operation requires less modifications giving good performance with diesel as pilot fuel used to generate spark. Supercharging in dual fuel mode improves performance of engine. Brake Thermal efficiency with supercharged producer gas-diesel is 15 % more than premixed producer gas-diesel engine [10]. Diesel can be replaced by biofuels like Honge-Oil making the fuel complete renewable. This dual fuel mode operation in CI engine shows maximum efficiency 20 % with reduction in all emissions. Tri-generation can be best option to utilize maximum part of biomass energy in higher generation systems [11].

III. SIMULATION OF ACTUAL CYCLE

The various models and equations used in simulation are briefly presented herein.

A. Model for Heat Transfer

Woschni's equation was used which is based on the similarity law of steady turbulent heat transfer [13], [14].

$$h = 0.820 *D^{-0.2}*p^{0.8}*W_{mv}^{0.8}*T^{-0.53} \text{ (kW/m}^2\text{.K)} \tag{1}$$

The reference velocity W_{mv} in the above formula represent the mean gas velocity affecting heat transfer and is given for each process. D is the cylinder bore taken as the characteristic length,

$$W_{mv} = \left[C_1 * C_m + C_2 * \left(\frac{V_s * T_1}{p * v_1}\right) * (p - p_0)\right] \tag{2}$$

For the gas exchange processes, $C_1 = 6.18$ & C_2

= 0,

For the compression processes, C_1 = 2.28 & C_2 = 0,

For the combustion & expansion processes,

C_1 = 2.28 & C_2 = 3.24*10-3

Here p_0 is the pressure in the MPa obtained for motoring and V_s is the displacement volume in m^3 and the coefficient C_m is the mean piston speed. The subscript 1 denotes a specified time when the pressure and the temperature are known.

In the Suction and Exhaust process Woschni's heat-transfer model was used during the simulation.

Anand [15], separates out the convection and radiations terms. Typical approach to the heat transfer theory proposed by Anand is his expression for the Nusselt number 'Nu' leading to a conventional derivation of the convection heat transfer coefficient C_h.

Anand recommends the following expression to connect the Reynolds and Nusselt number:

$Nu = b*Re^{0.7}$

(3)

Where, b = 0.26, for the two stroke engines and

b = 0.49, for the four stroke engines.

The Reynolds number is calculated as,

$Re = \dfrac{\rho_{cylinder}*C_m*D}{\mu_{cylinder}}$

(4)

The viscosity should be that of the cylinder gas,

$\mu_{cy} = 7.457*10^{-6} + 4.1547*10^{-8}*T - 7.4793*10^{-12}*T^2$ (5)

The mean piston velocity C_m is found from the dimensions of the cylinder stroke, L and the engine speed, N in rev/min.

$C_m = \dfrac{2*L*N}{60}$

(6)

The convectional heat transfer coefficient can be extracted from the Nusselt number, as

$C_h = \dfrac{C_k*Nu}{D}$

(7)

The parameter C_k is the thermal conductivity of the cylinder gas and can be assumed to be identical with that of air at the instantaneous cylinder temperature.

$C_k = 6.1944*10^{-3} + 7.3814*10^{-5}*T - 1.2491*10^{-8}*T^2$ (8)

In the compression and expansion process this heat-transfer model is adopted.

B. Model for Combustion [13]

Wiebe function was used to find out the mass fraction burnt during the combustion process.

$X_b = 1 - \exp\left[-a * \left(\dfrac{\theta - \theta_s}{\Delta\theta_c}\right)^{m+1}\right]$

(9)

Where, X_b is the mass fraction burned, "a" is an efficiency parameter and "m" is a slope parameter.

C. Input Data [16]

For the simulation purpose Honda GX-120 engine had been selected. Its specifications are as follows:

Engine Type   : Air Cooled 4-s petrol engine
Bore * Stroke   : 60 * 42 mm
Swept Volume   : 118 cc
Comp. Ratio   : 8.5:1
Max. Net Torque : 7.3 Nm@2500 rpm
Net Power   : 2.6 kW@3600 rpm
No. of Cylinders : 1

Producer gas composition on volume basis: CO=24.6 %, H_2=21.9 %, CO_2=8.17 %, H_2O^g=7.75 %, N_2=37.53 %.

IV. SIMULATION RESULTS

1. Suction Stroke:

Fig. 1 shows during suction stroke pressure falls rapidly (from initial 0.93 bar) after start of piston downward acceleration up to 50^0

CA, because of low valve lift and lower curtain area allowing less air-fuel mixture coming in cylinder. The cylinder pressure falls to 0.58 bar at 50° CA. However, thereafter a gradual pressure building is observed due to increased availability of mass flow with higher range due to valve lift and curtain area is sufficiently high to allow gases to pass inside and increase the inner pressure. Peak mass inflow found at 90^0 CA. Suction happens till final pressure reaches atmospheric pressure (1.013 bar). As shown in fig 2 temperature obviously will reduce with increased availability of mass flow with increasing crank angle. The mass-θ curve in fig. 3 clearly shows gradual rise in mass flow during initial valve lift and thereby explain the trend of P-θ curve too. Thus, the basic results of suction process are as per logical trend observed in actual I.C. engines and this validates the model used in present case.

Fig.3 Mass-θ Curve for Suction Stroke
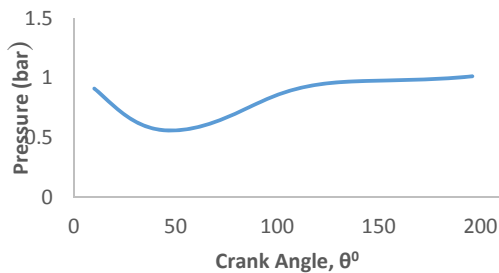
Fig.1 P-θ Curve for Suction Stroke

Fig.2 T-θ Curve for Suction Stroke

2. Compression stroke:

After suction charge is sealed and compressed with gradual rise of pressure up to 290^0 CA and stiff rise in pressure after 290^0 CA till the final pressure of 14.7 bar as shown in fig.4 and temperature 657 K as shown in fig. 5 at 336^0 CA. Specific heats found to be increasing and compression index gamma reducing at higher temperature. More heat loss occurs as inside temperature increases.
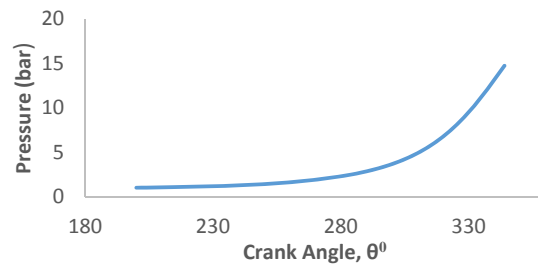
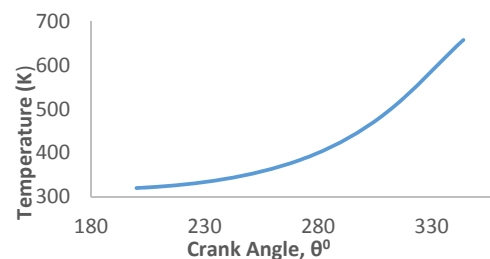**Fig**.4 P-θ Curve for Compression Stroke

Fig.5 T-θ Curve for Compression Stroke

3. Combustion Process:

Ignition occurs after end of compression 16^0 BTDC causing release of heat from combustion of charge produces peak pressure 38 bar at 372^0 CA as shown in fig.6. The rate of heat addition

under these circumstances is more than the heat losses. As a result the temperature continues to rise and reaches to its peak value 1809 K at 379^0 CA as shown in fig.7. Mass burning curve in fig.8 shows higher mass burning rate found during high pressure and temperature formation. At 370^0 CA, 75% of mass has been burnt releasing huge amount of heat to produce peak pressure and temperature. Heat losses found more in this process.
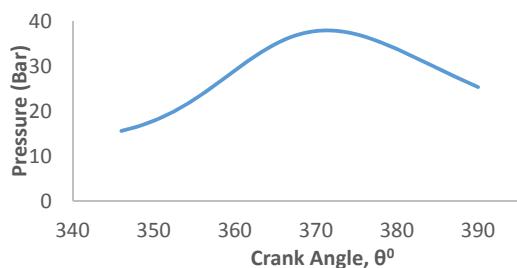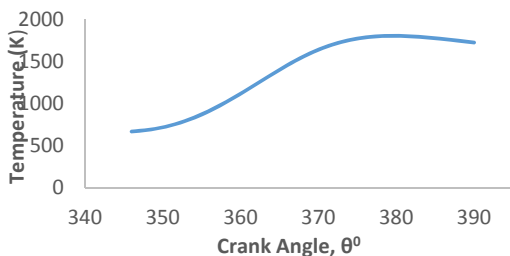

Fig.6 **P-θ Curve for Combustion Process**

Fig.7 **T-θ Curve for Combustion Process**
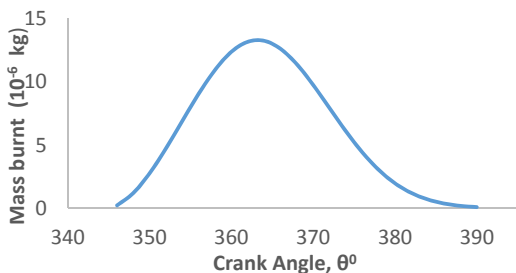
Fig.8 Mass burnt-θ Curve for Combustion Process

4. Expansion Stroke:

Combustion products with very high temperature get expanded due to increase in cylinder volume, which in turn reduce the pressure inside the cylinder drastically. At the end of combustion process the pressure inside the cylinder is 25.42 bar as shown in fig.9. This gives higher energy extraction. At the end of expansion process, pressure reduces to 3.5 bar at 510° CA, whereas temperature reaches to 990 K as shown in fig.10. P-θ Curve for expansion stroke shows initial stiff curve of pressure reduction up to 440^0 CA and then gradual expansion i.e. most of power will be transmitted before 440^0 CA.
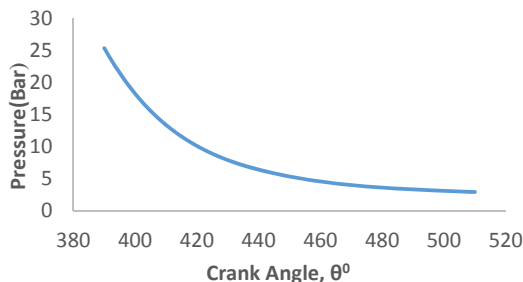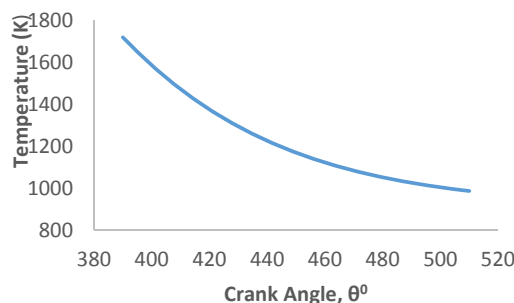

Fig.9 P-θ Curve for Expansion Stroke

Fig.10 T-θ Curve for Expansion Stroke

5. Exhaust Stroke:

During exhaust stroke, pressure falls to 1.02 bar at 610° CA and then rises up to 1.8 bar at the end of exhaust process shown in fig. 11. After 640° CA slow pressure building inside the cylinder is observed due to throttling effect. The temperature obviously will reduce with high temperature burnt mass leaving to the atmosphere with increasing crank angle as shown in fig. 12. It is observed from the T-θ curve that, like pressure, there is not any rise of temperature during the later stage of exhaust process.
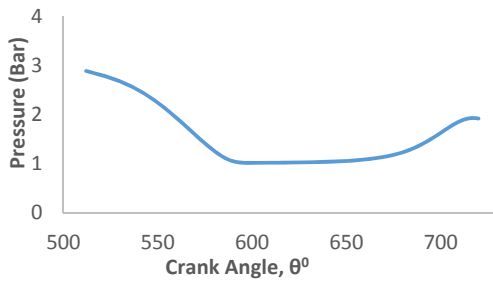
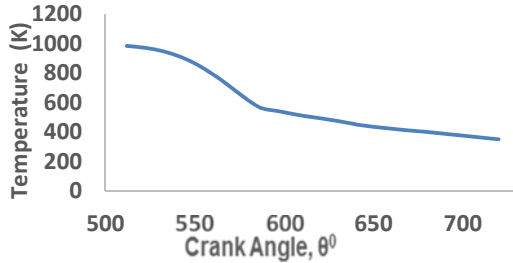**Fig.11 P-θ Curve for Exhaust Stroke**

Fig.12 T-θ Curve for Exhaust Stroke

6.   Full Cycle

 Fig. 13 shows the variation of pressure with volume for the full cycle. Area under the curve gives the work done and thereby power output of engine. The indicated power calculated by data obtained from the simulation is 2.3 kW @3600 rpm for the Producer gas as a fuel. Thermal efficiency found to be 28.19 % with Specific fuel consumption   2.62 kg/kWh and mean effective pressure found to be   6.7 bar. Fig. 14 T-θ in fig. 14 shows high temperature region where heat loss from cylinder will be more.
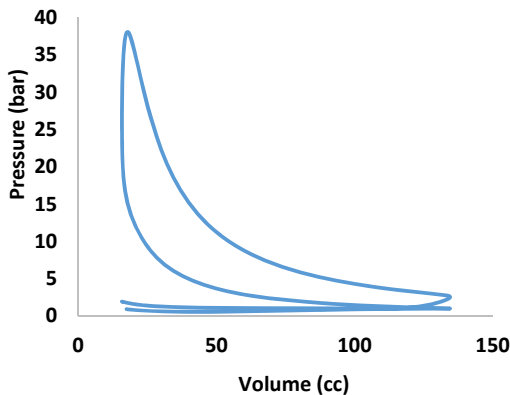

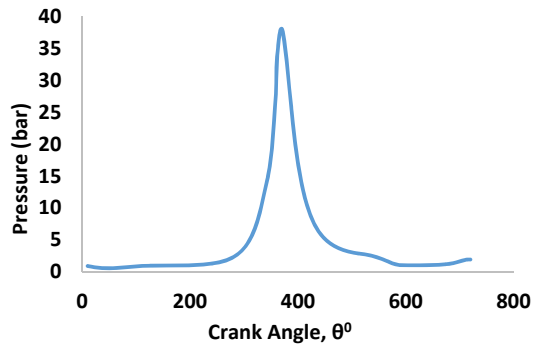**Fig.13 P-θ Curve for full Cycle**

Fig.14 T-θ Curve for full Cycle
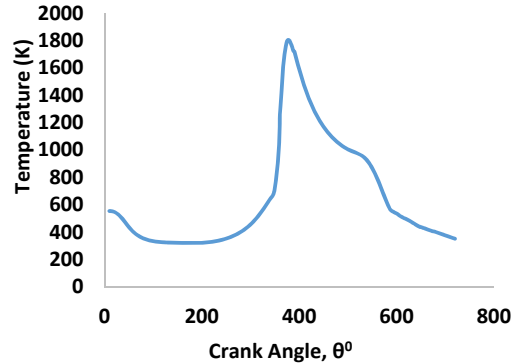

Fig.15 P-V Curve for full Cycle

V.   VALIDATION OF SIMULATION RESULTS

As per the specifications given in the manual of Honda   GX-120 engine the net power is 2.6 kW @3600 rpm for the gasoline. The indicated power calculated by data obtained from the simulation is 2.3 kW @3600 rpm with thermal efficiency 28.19 % for the Producer gas as a fuel, which shows the relatively reduction in power and thermal efficiency 11.538 % and 5.71 % respectively as compared to gasoline. The literature clearly indicates that the engine offers 15-30 % power de-rating and 3-10 % reduction in thermal efficiency as that of gasoline [7], [9] and thus looking to this fact present simulation may be treated as adequately validated.

VI.   CONCLUSION

- Peak pressure and temperature produced in combustion is 38 bar and 1809 K.
- The indicated power calculated by data obtained from the simulation is 2.3 kW @ 3600 rpm. These simulation results are quite in tune with Honda GX-120 engine power output   considering the fact that there exist

the relative de-rating of engine by 15-30 % with Producer gas as a fuel.

- Thermal efficiency found to be 28.19 % which is relatively de-rated by 5.7 % compared to gasoline as fuel.

REFERENCES

1. http://en.wikipedia.org/wiki/Electricity_sector_in_India.
2. www.mospi.gov.in
3. http://www.mnre.gov.in/
4. S. N. Soid, Z. A. Zainal, "Combustion characteristics and optimization of CPG (compressed producer gas) in a constant volume combustion chamber," Energy, 73, pp. 59-69, May 2014.
5. E. Ramjee, K. Vijaya, Kumar Reddy, "Performance analysis of a 4-stroke SI engine using CNG as an alternative fuel,"Indian Journal of Science and Technology, vol. 4, No-7, pp. 0974-6846, Jully 2011.
6. Munde Gopal G., Dr. Dalu Rajendra S., "Review of Compressed Natural Gas as an Alternative Fuel for Spark Ignition Engine," IJEIT, vol. 2(6), pp. 2277-3754, Dec 2012.
7. Shashikantha *et al.,* "Development and Performance Analysis of a 15 kWe Producer Gas Operated SI Engine," Renewable Energy, Vol. 5, Part-II, pp. 835-837, 1994.
8. S. Dasappa, G, Sridhar, H. V. Sridhar, N. K. S. Rajan, P. J. Paul, A. Apasani, "Producer gas engine- Proponent of clean energy technology," 15th European Biomass Conference & Exihibition, 7-11, May 2007.
9. G. Sridhar, P. J. Paul and H. S. Mukunda,"Biomass derived producer gas as a reciprocating engine fuel-an experimental analysis," Biomass & Bioenergy, 21 pp. 61-72, 2001.
10. S. Hassan, F. Mohd Nor, Z. A. Zainal, M A Miskam, "Performance and emission characteristics of Supercharged Producer Gas -Diesel Dual Fuel engine,"

Journal of Applied Sciences 11(9), pp. 1606-1611, 2011.
11. N.R. Banapurmath , P. G. Tewari, V. S. Yaliwal, Satish Kambalimath, " Combustion characteristics of a 4-stroke CI engine operated on Honge oil, Neem and Rice Bran oils when directly injected and dual fuelled with producer gas induction," Renewable Energy, 33, pp. 2077-2083, Dec 2007**.**
12. P. D. Shah, "Optimisation of Design and performance Parameters of CNG Fuelled S.I. Engine," M.Tech Thesis, Sardar Vallabhbhai National Institute of Technology, Surat, 2014.
13. Heywood J. B.," Internal Combustion Engine Fundamentals," 1st Edition, Tata McGraw Hill Book Company, USA, 1988.
14. Shashikantha, Klose W. and Parikh P. P., "Producer-gas engine and dedicated Natural gas engine-Computer simulation for performance optimization," SAE, 1998.
15. Anand W. J. D., "Heat transfer in the cylinders of reciprocating Internal combustion engines," Proc. I. Mech. E., 177 (1963).
16. Junior Quarter Midgets Australia (JQMA) – Honda GX-120 Technical Manual.